

NORTHWESTERN UNIVERSITY

Pdlim7 Regulates Nuclear/Cytoplasmic Localization and Activity of Tbx5 During Cardiac
Development

A DISSERTATION

SUBMITTED TO THE GRADUATE SCHOOL
IN PARTIAL FULFILLMENT OF THE REQUIREMENTS

for the degree

DOCTOR OF PHILOSOPHY

Field of Developmental Biology
Integrated Graduate Program in the Life Sciences

By

Troy Camarata

EVANSTON, ILLINOIS

December 2008

© Copyright by Troy Camarata 2008

All Rights Reserved

Abstract

Pdlim7 regulates nuclear/cytoplasmic localization and activity of Tbx5 during cardiac development

Troy Camarata

The T-box transcription factor, Tbx5, is involved in heart development and congenital disease. For example mutations in human TBX5 lead to Holt-Oram syndrome, a disease characterized by a range of heart and arm malformations. Tbx5 gene activity has been perturbed in several animal models including the chicken, mouse, and zebrafish. In zebrafish, the *tbx5 heartstrings (hst)* mutation results in embryos that fail to develop pectoral fins (forelimbs) and form a non-looped, string-like heart. Despite the importance of Tbx5 in heart formation, little is known about its function and regulation. To gain insight into Tbx5 regulation, the Simon laboratory performed a yeast two-hybrid screen to identify interacting proteins. One candidate isolated from the screen was Pdlim7, a member of the PDZ-LIM protein family. I hypothesized that the binding of Tbx5 to Pdlim7 modifies its transcriptional activity and explored the consequences of Tbx5/Pdlim7 complex formation *in vitro* employing appropriate cultured cells and *in vivo* using the zebrafish embryo.

Evidence from others in the laboratory using *in vitro* binding studies and *in vivo* protein localization in the chicken limb and heart suggested an interaction between Tbx5 and Pdlim7. However, what is the mechanistic action of the Tbx5/Pdlim7 complex on a cellular level? Using co-immunoprecipitations and confocal imaging I demonstrated that Tbx5 and Pdlim7 bind in the cell. In the presence of Pdlim7, employing FRAP, I was able to show that Tbx5 shuttles dynamically between the nucleus and cytoplasm and, in a complex with Pdlim7, localizes to the actin cytoskeleton. To test whether the relocalization from nuclear to cytoplasmic sites

interfered with downstream gene expression, I used luciferase reporters and demonstrated that *Pdlim7* acts as a repressor of *Tbx5* activity.

Several studies had shown the importance of *Tbx5* in heart formation, however, nothing was known about *Pdlim7* function *in vivo*. Therefore I asked, what is the role of *Pdlim7* during development, specifically does it relate to heart formation and *Tbx5* regulation? I performed functional studies to perturb *Pdlim7* function in zebrafish embryos. First, I demonstrated overlapping expression domains for both *tbx5* and *pdlim7* in the developing heart. Next, inhibition of *Pdlim7* function by injection of antisense morpholino (MO) oligonucleotides which resulted in a failure of cardiac looping, reminiscent of *tbx5 hst* mutants. Interestingly, *tbx5* and *pdlim7* also appeared to genetically interact, suggesting that *Pdlim7* and *Tbx5* operate in a common pathway during cardiac development. Loss of *Pdlim7* function in zebrafish embryos did not affect early cardiac patterning or gene expression. However, changes in gene expression were observed at the atrioventricular boundary (AV). Loss of *Pdlim7* resulted in a loss of gene expression at the AV boundary and in some cases blood regurgitation, suggesting valve defects. Using the AV boundary *Tbx5* target gene *tbx2b* as a readout, I was able to show that *Pdlim7* regulates *Tbx5* *in vivo*. Misregulation of *Pdlim7* in wild-type and *hst/+* compromised embryos resulted in inappropriate *tbx2b* expression due to improper subcellular localization of *Tbx5*. Therefore, it appears that *Tbx5* and *Pdlim7* work together to regulate gene expression and cardiac shape at the AV boundary through a mechanism of modifying *Tbx5* subcellular localization.

Acknowledgements

This journey has been, at times, challenging and difficult, yet enjoyable and fulfilling. It is a journey that I have not taken alone and I have many people to thank for their support, both personally and professionally. First, I need to thank Laurence von Kalm for taking in a lost undergraduate and preparing him for the perils of graduate school. Without you, I never would have gotten my feet off the ground. I would also like to thank my thesis committee for helping me shape this work into something I am very proud of.

I would like to thank my fellow graduate students at CMRC (CMIER) for understanding the hazards that come with being a student 'off campus' and for making the long days in lab a little less lonely. I need to thank all of the labs and their members in the Developmental Biology core for their support and useful discussions about science and the world around us.

I especially need to thank all of the members, past and present, of the Simon laboratory. Ange, Will, Pauli, Jenny, David, Jeff, Ben, Andre, Christine, Sarah, little Jenny, and Claudia. Thank you for making the past 6 years enjoyable and an overall fun experience. I am amazed that all of you put up with my craziness for so long.

I need to give a great deal of credit to Hans-Georg Simon. You have been an excellent mentor. I thank you for creating a supportive environment and giving me the freedom to explore. I believe that I am a better scientist as well as a person for it. If I can do half the job of advising others that you have done for me, then I will consider myself a success.

I would like to thank my parents, who may not always understand what I am doing, but have always been interested in my work. Mostly, I need to thank you for letting me follow my instincts and for putting me in a position to succeed. Your love, support, and help has meant a

great deal. I also need to thank Dan and Ann for always providing help and as I usually do not show it; your love has always been greatly appreciated.

Finally, I cannot say enough about the most important people in my life. The sacrifices that have been forced upon you are more than I can make up for. But you have made every moment worthwhile by providing a home and a place where I do not have to fret over the mostly meaningless issues of work. Thank you Brenden and Ann for your unconditional love and for always running for a hug every time I come home. Most importantly, thank you Rebecca for taking my hand for this journey and never letting go. You have not always liked the time I have had to devote to this accomplishment, but you have always understood and in many cases helped push me farther. This degree belongs to you as much as it does to me. I thank you and love you with all my heart.

Table of Contents

Abstract	3
Acknowledgements.....	5
Table of Contents	7
List of Figures.....	10
Chapter 1: Introduction.....	11
<i>Vertebrate cardiac development</i>	11
<u>Overview of avian and mammalian cardiac morphogenesis</u>	11
<u>Cardiac development in zebrafish</u>	14
<i>T-box transcription factors in vertebrate development</i>	16
<u>Tbx5 and Tbx4 encode tissue-specific transcription factors</u>	19
<u>Common Pathways in Heart and Limb Development</u>	22
<i>PDZ-LIM family of proteins</i>	23
<u>PDZ-LIM proteins act as cellular regulators</u>	24
<u>An emerging role for PDZ-LIM genes during embryonic development</u>	26
<u>Pdlim7: a potential signal transduction mediator</u>	27
<i>Hypothesis: Pdlim7 regulates the T-box transcription factors Tbx5 and Tbx4</i>	27
Chapter 2: Pdlim7 regulates Tbx5 protein subcellular localization and activity	29
<i>Introduction</i>	29
<i>Results</i>	32
<u>Polyclonal antibodies specifically recognize Pdlim7</u>	32
<u>Individual expression of Tbx4, Tbx5, or Pdlim7 results in localization to separate cellular compartments</u>	34
<u>Co-expression of Tbx4 or -5 and Pdlim7 leads to Tbx/Pdlim7 interactions at cytoplasmic sites</u>	37
<u>Pdlim7 LIM domain 3 is required for interaction with Tbx5</u>	41
<u>Actin destabilization does not change Tbx5/Pdlim7 binding or co-localization</u>	42
<u>Pdlim7 represses Tbx5 transcriptional activity</u>	45
<u>In the presence of Pdlim7, Tbx5 shuttles dynamically between the nucleus and cytoplasm</u> 47	47
<i>Discussion</i>	51
<u>Tbx5 sub-cellular localization is dynamic and related to cell differentiation</u>	51
<u>An emerging role for Pdlim7 as a signal mediator in Tbx5 regulation</u>	52
<u>Nuclear versus cytoplasmic Tbx5 localization and its relation to development and disease</u> 54	54

Chapter 3: Pdlim7 regulation of Tbx5 specifies zebrafish atrio-ventricular boundary formation	56
<i>Introduction</i>	56
<i>Results</i>	59
<u>Identification of zebrafish pdlim7</u>	59
<u>pdlim7 is coexpressed with tbx5 in the heart and pectoral fins</u>	59
<u>Pdlim7 is critical for embryonic development</u>	61
<u>pdlim7 and tbx5 functionally interact during heart development</u>	69
<u>Cardiac differentiation and chamber identity is not altered after loss of Pdlim7</u>	72
<u>Pdlim7 and Tbx5 are required for atrio-ventricular boundary formation</u>	77
<u>Tbx5 and Pdlim7 regulate tbx2b atrio-ventricular expression</u>	79
<i>Discussion</i>	85
<u>Pdlim7 is required for cardiac morphogenesis</u>	85
<u>Tbx5 and Pdlim7 specify atrio-ventricular identity</u>	86
<u>TBX5 regulation in congenital heart disease</u>	87
Chapter 4: Conclusions	90
<i>Model of Pdim7/Tbx5 interactions</i>	90
<u>Tbx5 nuclear/cytoplasmic localization is dynamic</u>	90
<u>Regulation of Tbx5 shuttling and Pdlim7 interaction</u>	91
<i>T-box proteins are nuclear/cytoplasmic shuttling proteins</i>	96
<i>PDZ-LIM proteins facilitate cytoplasmic retention of nuclear factors</i>	97
References	101
Appendix A: Materials and Methods	115
<i>Pdlim7 antibody design</i>	115
<i>Cell culture, transfection and reporter assays</i>	115
<i>Immunofluorescence and imaging</i>	116
<i>FRAP</i>	117
<i>Co-immunoprecipitation</i>	117
<i>Actin disruption</i>	118
<i>Expression constructs</i>	118
<i>Zebrafish</i>	119
<i>Identification of zebrafish pdlim7</i>	119
<i>In situ hybridization</i>	120
<i>Morpholino and RNA injection</i>	120
<i>Genotyping</i>	121

	9
<i>Online supplemental material</i>	121
Appendix B: Pdlim7 interacts with the Insulin receptor	122
Appendix C: Pdlim7 ΔLIM3 behaves as a dominant-negative	125

List of Figures

Figure 1.1	12
Figure 1.2	13
Figure 1.3	15
Figure 1.4	18
Figure 1.5	20
Figure 1.6	25
Figure 2.1	33
Figure 2.2	36
Figure 2.3	38
Figure 2.4	40
Figure 2.5	43
Figure 2.6	44
Figure 2.7	46
Figure 2.8	49
Figure 2.9	50
Figure 3.1	60
Figure 3.2	62
Figure 3.3	64
Figure 3.4	65
Figure 3.5	66
Figure 3.6	67
Figure 3.7	68
Figure 3.8	70
Figure 3.9	73
Figure 3.10	75
Figure 3.11	78
Figure 3.12	82
Table 3.1	84
Figure 4.1	95
Table 4.1	98
Figure Appendix B.1	123
Figure Appendix B.2	124
Figure Appendix C.1	126
Figure Appendix C.2	127

Chapter 1: Introduction

Vertebrate cardiac development

The functioning heart is the first organ to develop in the vertebrate embryo. The heart is the centerpiece of the circulatory system that is required to supply oxygen and nutrients throughout the body. Blood flow is established by coordinated contraction of two-, three- or four-cardiac chambers, depending on the species. Birds and mammals have a four-chambered heart allowing two parallel circulatory systems while fish have a simplified single circulation with two chambers (Fig. 1.1). Interestingly, despite the difference in structural complexity, early cardiac morphogenesis in the avian or mammalian heart is highly conserved in fish.

Overview of avian and mammalian cardiac morphogenesis

In higher vertebrates, such as birds and mammals, the earliest cardiac precursors are located in two bilateral fields in the splanchnic mesoderm of the anterior lateral plate mesoderm (ALPM) (for review see Harvey, 2002; Kirby, 2007). These early heart progenitors arise during gastrulation where they migrate through the node and organizer, and primitive streak. The cells then take their position by E7.75 in the mouse (stage 5, (HH) Hamburger-Hamilton 1951, in the chick) in the ALMP, where they will then migrate laterally, fuse, and give rise to the cardiac crescent (Fig. 1.2) (Kirby, 2007). Two of the three major cell layers of the heart can be distinguished in the cardiac crescent, the outer myocardium and inner endocardium. It is at the crescent stage that the heart field begins to express cardiac genes such as *Nkx2-5*, *Gata4*, and *Tbx5* (Franco et al. 1998; Bruneau et al. 1999; Harvey, 2002). Caudal growth of the head folds then causes the cardiac cells of the crescent to move ventrally forming the heart tube, which then

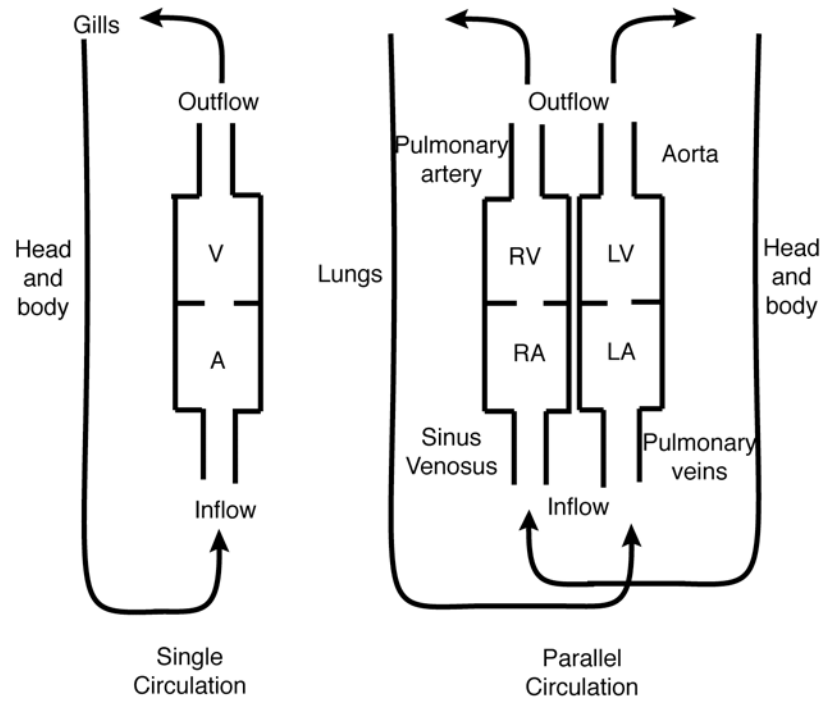


Figure 1.1: Schematic comparing single circulation, such as that found in zebrafish, to parallel circulations systems which are found in avians and mammals. Adapted from Kirby, 2007.

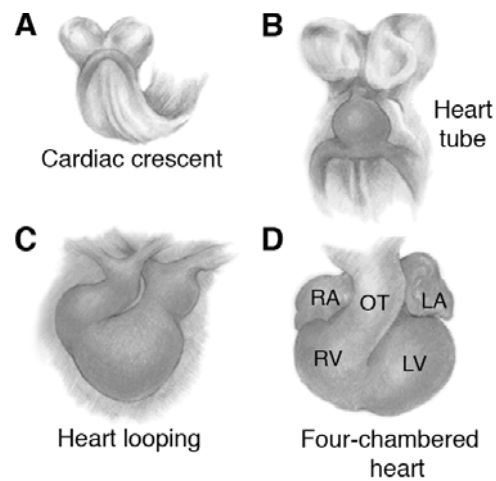


Figure 1.2: Development of the mouse heart. (A) Cardiac crescent stage of heart development composed of an inner endocardial layer and outer myocardial layer. Cardiac progenitors are present in the shaded curved region below the head folds. (B) The heart tube forms after the cardiac progenitor cells move ventrally and caudally as a result of growth of the head folds. (C) The heart tube loops bringing the infow and outflow tracts into proximity of each other. (D) After the heart loops, significant heart remodeling occurs to distinguish the major cardiac chambers and various cells types within the heart. Adapted from Stennard and Harvey, 2005.

elongates between E8.25 and E10.5 (10-17HH). As the heart tube elongates it loops toward the right side of the embryo, influenced by the left/right patterning pathway (Levin, 2005). Looping brings the inflow and outflow ends of the tube into approximation (Fig. 1.2). By the end of cardiac looping (E12.5; 24HH), the heart begins to remodel, establishing the cardiac chambers and other specialized cells within the heart. By this developmental stage the heart contains all of the myocardium necessary to form the chambers and the trabeculations within the chambers. In addition, endocardial cells located in the atrioventricular canal of the heart tube go through epithelial-to-mesenchyme transition (EMT) to produce cardiac cushions in the outflow tract and between the atria and ventricles (AVC). The endocardial cushions will give rise to the valves and contribute to the septa. All morphogenesis during and after the linear heart tube stage occurs while the organ is beating. Therefore, heart morphogenesis occurs in parallel with functional development.

Cardiac development in zebrafish

Similar to higher vertebrates, the development of the two-chambered zebrafish heart begins with the migration of cardiac precursor cells from the ALPM to the dorsal midline (reviewed in Glickman and Yelon, 2002; Stainier, 2001). This process begins around 12 hours post-fertilization (hpf) (6 somites) and the migrating precursor cells reach the midline by 15.5 hpf (13 somites). The cells then fuse to create a transient structure called the cardiac cone, which at this point consists of both inner endocardial and outer myocardial cells. The cardiac cone begins to elongate and jog to the left side of the embryo by 22 hpf to form a heart tube which then begins to beat at 24 hpf. Cardiac looping begins at 36 hpf and is completed by 48 hpf. The looped heart resembles an S-shape bringing the ventricle to the right of the atrium (Figure 1.3).

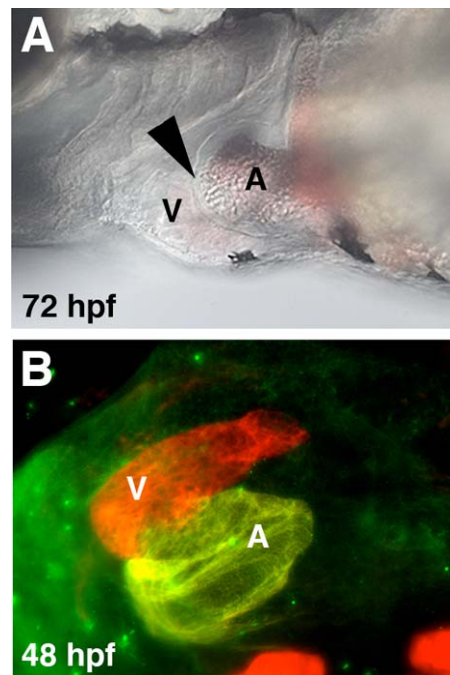


Figure 1.3: Zebrafish cardiac morphology. (A) Lateral view of a zebrafish heart at 72 hours post-fertilization (hpf). Due to proper heart looping the ventricle is out of focus within the plane of the image. Arrow denotes the position of cardiac looping. Head is to the left. (B) Ventral view of a looped zebrafish heart at 48 hpf. Embryo has been stained with antibodies against a cardiac myosin (MF20) to stain the entire heart (red) and an atrial specific myosin (S46) to label the atrium (green). The ventricle is visualized in red and the atrium in yellow. Head is positioned at the top. V, ventricle. A, atrium.

As in the mouse and chicken, *nkx2.5* and *tbx5* are among the earliest determinants of the early zebrafish cardiac field (Lints et. al. 1993; Schultheiss et. al. 1995; Chen and Fishman, 1996; Bruneau et. al. 1999; Begemann and Ingham, 1999). Several other genes that play critical roles in vertebrate heart development, such as *gata5* (thought to be the equivalent to *Gata4* in the chick and mouse), are also conserved in the zebrafish (Reiter et. al. 1999; Glickman and Yelon, 2002; Stainier, 2002).

To go along with the homologous morphogenesis and gene expression of heart development, the zebrafish model also provides a number of experimental advantages. The zebrafish embryo is transparent which greatly aids in the visualization of developmental defects, especially heart defects. Furthermore, embryonic development is relatively rapid and large numbers of embryos, typically 200-300 embryos per clutch, can be obtained for experimental manipulation. The zebrafish also provides a key advantage as compared to other vertebrate systems, especially mammals. The zebrafish embryo is able to survive for several days without a functioning cardiac system due to oxygen uptake by passive diffusion. Therefore, severe heart defects can still be studied without disrupting other aspects of development, a feature not present in mouse embryogenesis.

T-box transcription factors in vertebrate development

One class of genes essential for vertebrate development, especially heart morphogenesis, is the family of T-box transcription factors. T-box transcription factors share a conserved N-terminal DNA binding domain called the T-domain and possess a more variable C-terminal transactivation domain. The T-domain was originally identified in the founding member of the T-box protein family, T, also named Brachyury (Kispert and Herrmann, 1993). There have been

17 members identified in the mouse genome which can be divided into five subfamilies based upon amino acid alignments (Fig. 1.4) (Naiche et al. 2005). T-box proteins play important roles in a variety of developmental processes such as the development of extraembryonic tissues, mesoderm specification as well as in craniofacial, limb, pituitary, and cardiac development (Naiche et al. 2005).

A subset of T-box genes have found to be expressed in the heart and they appear to be important for heart development and disease. This subset includes *Tbx1-5*, *Tbx18*, and *Tbx20* (Isphording et al. 2004; Stennard and Harvey, 2005). Mouse knock-out models have shown a critical requirement for several of the cardiac expressed T-box genes in the development of a variety of heart tissues such as the outflow tract (*Tbx1*, Lindsay et al. 2001; *Tbx2*, Harrelson et al. 2004), myocardium (*Tbx5*, Bruneau et al. 2001), and differentiation of the cardiac chambers (*Tbx20*, Cai et al. 2005). Evidence for the role of T-box family members during heart formation also comes from clinical cases where specific human syndromes are associated with mutations in T-box genes. DiGeorge syndrome is associated with mutations in *TBX1* (Gong et al. 2001; Merscher et al. 2001) and is characterized by abnormalities in the outflow tract, facial dysmorphogenesis, cleft palate and hypoplasia of the thymus (DiGeorge and Harley, 1965; Shprintzen et al. 1978; Goldberg et al. 1993). Mutations in *TBX5* leads to Holt-Oram syndrome with affected patients having atrial and ventricular septal defects, conduction disturbances, atrial hypoplasia, and upper arm malformations (Basson et al. 1997; Li et al. 1997). Despite the large amount of experimental and clinical data showing the requirement for T-box genes in cardiac morphogenesis, the precise function of each encoded protein in heart formation is unclear.

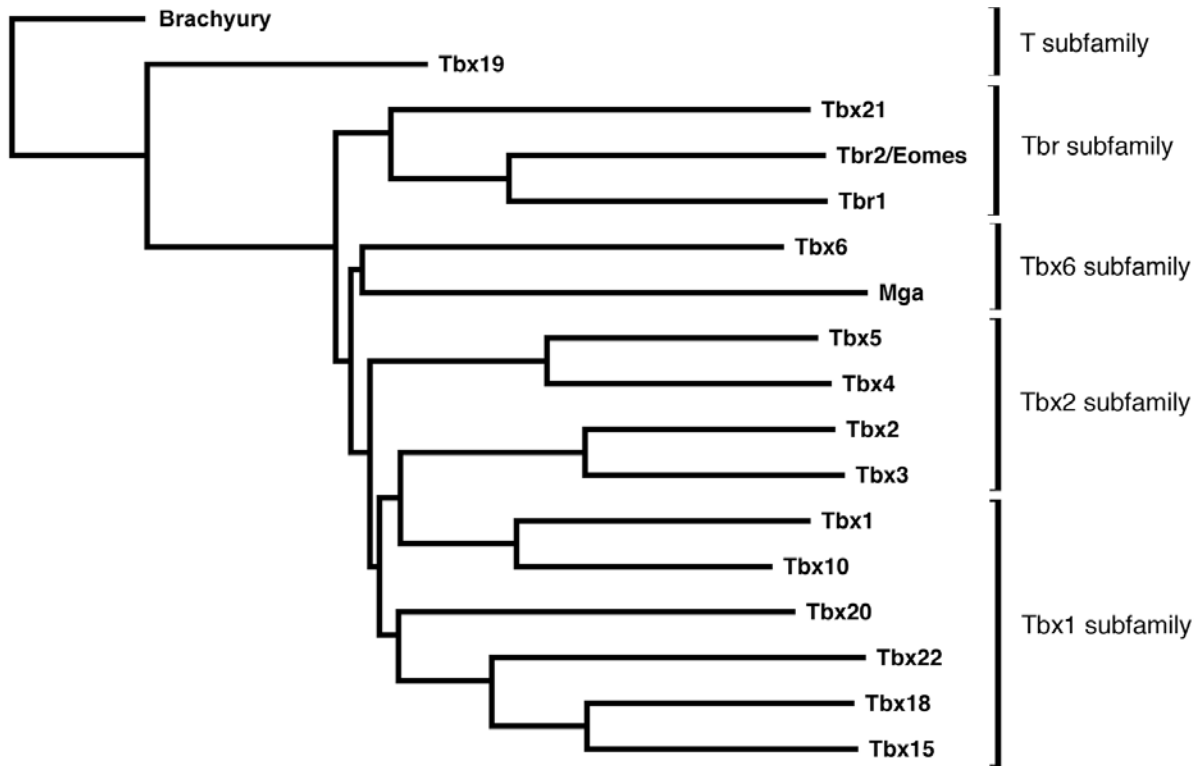


Figure 1.4: Phylogenetic tree of T-box transcription factors from mouse. Analysis of amino acid sequences of murine T-box proteins reveals five subfamilies. The division of the T-box family is a result of the evolutionary history of the T-box genes which arose through successive rounds of duplication and modification (Simon 1999; Naiche et al. 2005). T-box gene accession numbers used to derive amino acid sequences for phylogenetic tree: Brachyury, NM_009309; Tbx1, NM_011532; Tbx2, NM_009324; Tbx3, NM_011535; Tbx4, NM_011536; Tbx5, NM_011537; Tbx6, NM_011538; Mga, NM_013720; Tbx10, NM_001001320; Tbx15, NM_009323; Tbx18, NM_023814; Tbx19, NM_032005; Tbx20, NM_194263; Tbx21, NM_019507; Tbx22, NM_145224; Tbr1, NM_009322; Tbr2, NM_010136.

Tbx5 and Tbx4 encode tissue-specific transcription factors

As discussed, many of the T-box proteins have been found to play important roles in development and disease. Two T-box transcription factors in particular seem to be essential for both heart and limb development. *Tbx5* and *Tbx4* belong to the *Tbx2/3/4/5* subfamily of T-box genes (Simon, 1999) and are expressed in both the developing heart and limbs (Fig. 1.5) (Bruneau et al. 1999; Gibson-Brown et al. 1996; Krause et al. 2004). Interestingly, *Tbx5* and *Tbx4* have complementary expression profiles. In chick and mouse embryos *Tbx5* is expressed in the forelimbs, and posterior parts of the heart, such as the inflow region, atria, and left ventricle (Logan et al. 1998; Bruneau et al. 1999). *Tbx4* on the other hand, is expressed in the hindlimbs and anterior parts of the heart such as the right ventricle and outflow tract (Gibson-Brown et al. 1996; Chapman et al. 1996; Krause et al. 2004).

Data showing the importance of *Tbx5* and *Tbx4* during development has come from a variety of studies, for example mouse knock-out models (Bruneau et al. 2001; Naiche and Papaioannou, 2003). Mouse knock-out experiments showed that *Tbx5* and *Tbx4* gene expression relates directly to limb induction. Loss of *Tbx5* in the presumptive forelimb field or *Tbx4* in the hindlimb progenitor cells results in loss of limb induction and outgrowth. In addition to the early role in limb initiation, it was thought that *Tbx5* and *Tbx4* function in limb identity and outgrowth due to their limb specific expression (Gibson-Brown et al. 1998; Logan et al. 1998; Bruneau et al. 1999). However, ectopic expression of *Tbx4* in the mouse forelimb field that has had *Tbx5* genetically deleted results in a normal forelimb (Minguillon et al. 2005). Further experimentation has shown that *Tbx5* and *Tbx4* are not required for limb outgrowth either, as genetic removal of either T-box gene after limb induction does not perturb limb development (Hasson et al. 2007; Naiche and Papaioannou, 2007). Therefore, *Tbx5* and *Tbx4* may not be

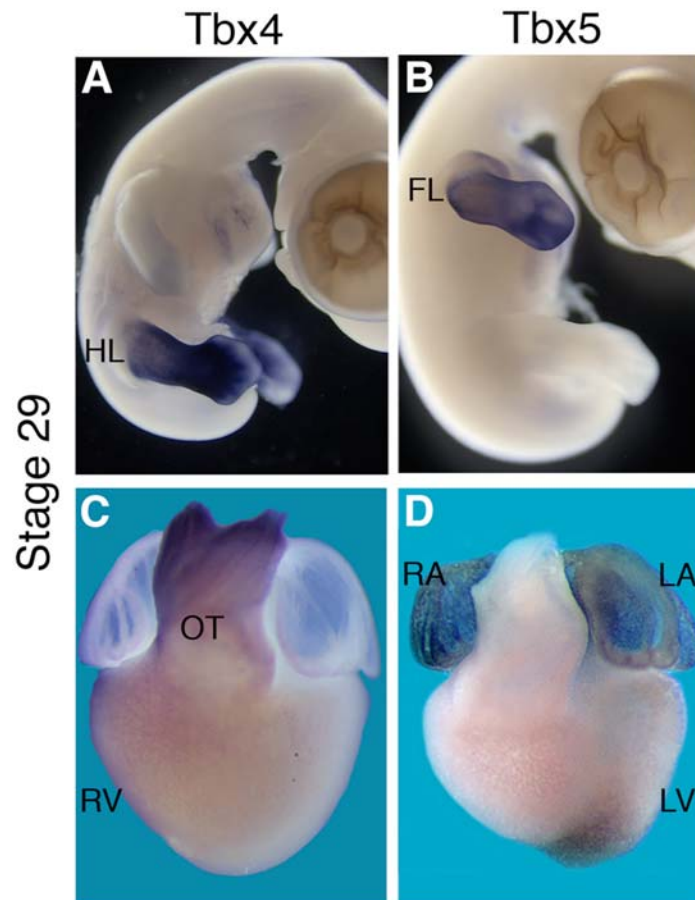


Figure 1.5: Complementary expression of *Tbx4* and *Tbx5* in the developing chicken embryo. (A) *Tbx4* expression in the hindlimb (HL) of a stage 29 HH (Hamburger and Hamilton 1951) chicken embryo. (B) *Tbx5* expression in the forelimb (FL). (C) Expression of *Tbx4* in the chicken heart. *Tbx4* is detected in the right ventricle (RV) and outflow tract (OT). (D) *Tbx5* expression is detected in both atria (RA and LA) and the left ventricle (LV). Taken from Ispording et al. 2004.

required to specify limb identity or control outgrowth, however, the T-box genes are essential at the earliest step of limb induction.

Similar to its role in the limbs, *Tbx5* appears to be the earliest determinant of vertebrate heart growth and has been implicated in the regulation of cardiomyocyte proliferation (Hatcher et al. 2001). In the mouse, *Tbx5* is expressed initially at E8.0 in a broad region of the LPM that corresponds to the cardiac crescent (Bruneau et al. 1999). By E8.5, *Tbx5* expression is still confined to the developing heart but shortly after robust expression is observed in a discrete region of the LPM that corresponds to the forelimb field. In the developing heart, *Tbx5* is expressed in the posterior segments that give rise to both atria and the left ventricle. In zebrafish, *tbx5* expression is observed in two bilateral stripes, comparable to the cardiac crescent expression in mice (Ahn et al. 2002). The more anterior *tbx5* expressing cells of the bilateral stripes will give rise to the heart primordium. *Tbx5^{del/del}* mice display normal anterior/posterior (AP) patterning of the developing heart while growth of the atria and left ventricle are severely impaired (Bruneau et al. 2001). Based on this genetic evidence, AP patterning of the heart is not dependent on *Tbx5*, however, early differentiation and growth of specific segments require *Tbx5* function. Mutant analysis in zebrafish also revealed that *tbx5* expression is crucial for normal heart development (Garrity et al. 2002; Ahn et al. 2002). Morpholino (MO) antisense oligonucleotide knock-down of *tbx5* expression leads to severe heart septation and growth defects. In both mice and zebrafish where *Tbx5* expression has been genetically removed or reduced by MOs, severe heart phenotypes are observed along with limb/fin phenotypes. This suggests a common relationship between heart and limb development with *Tbx5* as a central player.

Common Pathways in Heart and Limb Development

As indicated above, several studies have shown that *Tbx5* is vital for the development of the vertebrate heart and forelimb/pectoral fin in mouse (Bruneau et al. 1999; Rallis et al. 2003; Agarwal et al. 2003), chicken (Gibson-Brown et al. 1998; Isaac et al. 1998; Logan et al. 1998; Ohuchi et al. 1998; Takeuchi et al. 2003), and zebrafish (Ahn et al. 2002; Garrity et al. 2002; Ng et al. 2002). *Tbx5* loss-of-function studies in both mouse and zebrafish have shown severe heart and limb phenotypes. Homozygous knock-out mice, for instance, form heart tubes but they fail to loop and no forelimbs are present (Bruneau et al. 2001; Rallis et al. 2003). In contrast, heterozygous *Tbx5* deficient mice display heart and limb malformations that are very similar to the human Holt-Oram syndrome (HOS; Bruneau et al. 2001). *Tbx5*^{del/+} mice have septal defects as well as subtle paw and wrist defects. Genetic and morpholino antisense knock-down studies in zebrafish revealed that *tbx5* is essential for heart and pectoral fin formation as well. Reduced *tbx5* expression leads to severe heart defects and loss of pectoral fins (Ahn et al. 2002; Garrity et al. 2002; Ng et al. 2002). An additional important piece of evidence connecting heart and limb development comes from zebrafish where it appears that heart and limb precursor cells are derived from a common pool (Ahn et al. 2002). At the 10-somite-stage (14 hours-post-fertilization; hpf) *tbx5* expressing cells are found in two bilateral stripes at the midline. Approximately five hours later the contiguous stripe is broken up into an anterior group of cells and a more posterior group of cells, giving rise to the heart primordia and prospective pectoral fin bud respectively. MO-knockdown interference of *tbx5* expression causes failure of these cells to migrate resulting in loss of pectoral fins (Ahn et al. 2002).

Clinical manifestations along with the developmental studies indicate the existence of common genes and pathways in heart and limb development. Mutations in the human *TBX5*

gene are responsible for Holt-Oram syndrome (HOS; Basson et al. 1997; Li et al. 1997). HOS results in a range of heart defects that include atrial septal defects and ventricular septal defects. The heart defects in HOS are commonly accompanied by defects in the upper arms. These defects range from subtle bone abnormalities, to missing digits to long bone reductions. The heart and limb malformations in HOS coincide with the developmental expression profile of *Tbx5* in animal models and in those where *Tbx5* expression and/or function has been experimentally compromised.

Furthermore, mutations in the human *TBX4* gene have been found to be responsible for small patellar syndrome (SPS; Bongers et al. 2004). The clinical manifestations of SPS are mild compared to HOS. Some of the reported phenotypes include patellar hypoplasia and foot anomalies such as wide spacing between the first and second toes. There is a lack of *Tbx4* mutations observed in congenital heart syndromes, however, this is most likely due to that fact that the heart expression of *Tbx4* has only recently been described and researchers have yet to look for *Tbx4* mutations in diseased hearts (Krause et al. 2004). Alternatively, it is conceivable that strong heart phenotypes are not viable and therefore not observed in the human population. Also, it is possible that other *T-box* genes expressed in the heart have redundant functions and can supplement for loss of *Tbx4* activity.

PDZ-LIM family of proteins

PDZ-LIM proteins are a class of molecules with an emerging role in a variety of fundamental biological processes, such as cytoskeletal organization, cell migration, signal transduction, and organ development (Dawid et al. 1998; Fanning and Anderson, 1999; Bach, 2000; Kadmas and Beckerle, 2004). Members of the PDZ-LIM family contain an amino-terminal PDZ domain and

either a single (Alp subfamily) or three (Enigma subfamily) carboxy-terminal LIM domains (Fig. 1.6), which act as sites for protein-protein interactions (Schmeichel and Beckerle, 1994; Ponting et al. 1997). The PDZ-LIM domain structural organization is found throughout evolution from invertebrates such as *Drosophila* and *C. elegans* to vertebrates such as humans (McKeown et al. 2006). Interestingly, *C. elegans* may provide a snapshot of how the different family members evolved in higher vertebrates. The nematode, as well as the fruitfly, contains a single PDZ-LIM encoding gene, with a single N-terminal PDZ domain and four C-terminal LIM domains (McKeown et al. 2006). It appears *C. elegans* utilizes alternative splicing to create isoforms that contain either a single or four LIM domains. Analysis of the human genome has shown that in many cases an Alp subfamily member (single LIM domain) is paired on the same chromosome with a member of the Enigma subfamily (three LIM domains). Therefore it is likely that the current complexity of the PDZ-LIM protein family in vertebrates arose by gene duplication and mobilization from a more ancestral gene such as the one found in *C. elegans* (McKeown et al. 2006).

PDZ-LIM proteins act as cellular regulators

PDZ-LIM proteins are thought to have diverse roles as regulators of cytoarchitecture (Kadmas and Beckerle, 2004). Several members of the PDZ-LIM family are localized within a cell to sites of actin anchorage. The PDZ domains of Pdlim1, Pdlim3, and Pdlim5 bind to α -actinin and localize the proteins to actin filaments (Vallienius et al. 2000; Xia et al. 1997; Pomies et al. 1999; Nakagawa et al. 2000). The interaction between Pdlim3 and α -actinin has been detected in the intercalated discs of cardiac muscle cells and enhances the ability of α -actinin to crosslink actin fibers (Pashmforoush et al. 2001). The PDZ-LIM protein Ldb3, which also binds to α -actinin, is

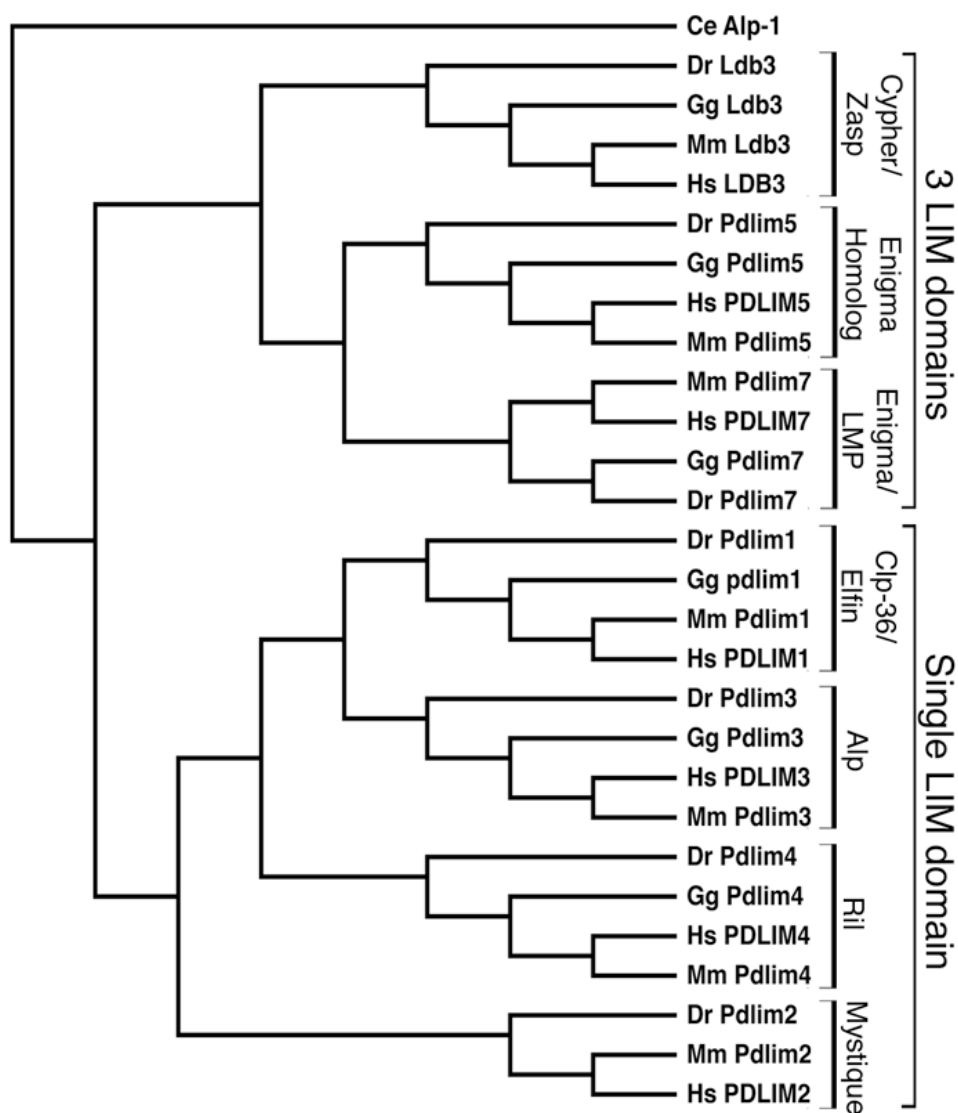


Figure 1.6: Phylogenetic analysis of Pdlim7 proteins. Amino acid alignments of PDZ-LIM proteins containing single or three LIM domains were compiled to create the phylogenetic tree using MacVector. *C. elegans* Alp-1 PDZ-LIM protein was included as the out-group. Both published and GenBank nomenclature is given. Genbank accession numbers for all nucleotide sequences used to derive amino acid sequence are as follows: *C. elegans* alp-1, CAE52903. Ldb3: *Homo sapien*, NM_007078; *Mus Musculus*, NM_011918; *Gallus gallus*, XM_421495; *Danio rerio*, DQ012157. Pdlim5: *Homo sapien*, NM_006457; *Mus Musculus*, NM_019808; *Gallus gallus*, AJ851689; *Danio rerio*, BC045922. Pdlim7: *Homo sapien*, NM_005451, *Mus musculus*, NM_026131; *Gallus gallus*, NM_001005345; *Danio rerio*, NM_200840. Pdlim1: *Homo sapien*, NM_020992; *Mus musculus*, NM_016861; *Gallus gallus*, XM_426503; *Danio rerio*, BC092978. Pdlim3: *Homo sapien*, NM_014476; *Mus musculus*, NM_016798; *Gallus gallus*, NM_001001764; *Danio rerio*, NM_001042718. Pdlim4: *Homo sapien*, NM_003687; *Mus musculus*, NM_019417; *Gallus gallus*, NM_204839; *Danio rerio*, NM_001042696. Pdlim2: *Homo sapien*, NM_176871; *Mus musculus*, NM_145978; *Danio rerio*, NM_001042766. Pdlim2 sequence could not be identified in the *Gallus gallus* genome.

localized to the Z-lines in muscle cells (Faulkner et al. 1999; Zhou et al. 1999; Passier et al. 2000). Loss of *Ldb3* results in defects of striated muscle, further supporting the role for PDZ-LIM proteins in actin function and cellular architecture (Zhou et al. 2001).

At the opposite end from the PDZ domain are the C-terminal LIM domains, whose function is less understood. Only a handful of proteins have been shown to bind to the LIM domains, which appear to be specific for their target protein despite the overall similarity between family members. For example, the LIM domain of *Pdlim1* binds to the kinase *Clik1* and targets it to actin stress fibers (Vallénus and Makela, 2002). The LIM domains of *Pdlim5* and *Pdlim7* have been shown to interact with different isoforms of protein kinase C (PKC) (Kuroda et al. 1996) and LIM1 of *Pdlim5* also binds to the basic helix-loop-helix inhibitor *Id2* (Lasorella and Lavarone, 2006). Receptor tyrosine kinases interact with the LIM2 (Ret receptor) and LIM3 (Insulin receptor) domains of human PDLIM7 (Wu and Gill, 1994; Wu et al. 1996). However, the function of the interactions between the LIM domains of PDZ-LIM proteins and receptor tyrosine kinases, as well as other kinases, is poorly understood.

An emerging role for PDZ-LIM genes during embryonic development

Even less is known about the roles PDZ-LIM proteins play during embryonic development. What little information is available suggests members of this protein family are critical for skeletal and cardiac muscle formation (Pashmforoush et al. 2001; Zhou et al. 2001; van der Meer et al. 2006). Genetic deletion of *Pdlim3* in the mouse results in cardiomyopathy (Pashmforoush et al. 2001). Similar cardiac defects are also observed after genetic deletion of *Ldb3* in the mouse or by respective morpholino antisense oligonucleotide knock-down in the zebrafish (Zhou et al. 2001; van der Meer et al. 2006). Loss of *Ldb3* function also results in disorganization of

striated muscle architecture, a tissue where Ldb3 normally localizes to the Z-line. Furthermore, mutations have been identified in human *LDB3* from patients with dilated cardiomyopathy (Vatta et al. 2003). The function of other PDZ-LIM family members during vertebrate embryonic development has not been examined and the specific roles of *Pdlim3* and *Ldb3* in skeletal and cardiac muscle development remain to be investigated.

Pdlim7: a potential signal transduction mediator

Pdlim7 was the initial PDZ-LIM family member identified in a yeast two-hybrid screen that used the endocytic code peptide of the human insulin receptor (Insr) as bait (Wu and Gill, 1994). Follow-up *in vitro* studies have shown that the LIM3 domain of Pdlim7 is sufficient to interact with the endocytic code of the Insr (Wu and Gill, 1994) and this interaction may play a role in glucose transport in adipose tissue (Barres et al. 2006). Additionally, Pdlim7 interacts with the Ret receptor via the LIM2 domain and this interaction is required for normal mitogenic signaling of the Ret receptor in cultured cells (Durick et al. 1996; Durick et al. 1998). In osteoblast cultures, overexpression of Pdlim7 induces bone formation mediated through BMP-6 signaling presumably by an interaction with Smurf1 (Boden et al. 1998; Sangadala et al. 2006). However, the function of Pdlim7 beyond the limited *in vitro* studies, especially during embryonic development, is completely unknown.

Hypothesis: Pdlim7 regulates the T-box transcription factors Tbx5 and Tbx4

Biochemical studies of the N-terminus, including the DNA binding domain, of Tbx5 have shown critical interactions with the transcription factors Nkx2-5 and Gata4 (Hiroi et al. 2001; Garg et al. 2003). Binding of Tbx5 with either Nkx2-5 or Gata4 in the heart allows for synergistic

activation of target genes. No work, however, had been performed using the C-terminal transactivation domain of Tbx5 and little was understood how this region of the protein may contribute to the transcription factor's function.

In an effort to gain insight into how Tbx5 functions, the Simon laboratory performed a yeast-two hybrid screen using the C-terminus of chicken Tbx5 as bait (Krause et al. 2004). Using a chicken limb bud cDNA library as prey, several putative Tbx5 interactors were isolated, one of which was Pdlim7. *In vitro* GST binding assays confirmed the interaction between Tbx5 and Pdlim7 as well as an interaction between Pdlim7 and Tbx4, however, not with the related Tbx3 or Tbx2. Interestingly, Pdlim7 binds the C-terminus of Tbx5 and Tbx4 via separate LIM domains, LIM3 and LIM2, respectively (Krause et al. 2004). Coexpression of *Pdlim7* with both *Tbx5* and *Tbx4* in the developing chicken limbs and heart validated the *in vitro* binding studies.

Based upon coexpression and *in vitro* interactions, I hypothesized that Pdlim7 regulates Tbx5 and Tbx4 function. I tested this hypothesis by 1) elucidating the cellular mechanism of Pdlim7/Tbx interactions and 2) by determining the role of Pdlim7 during vertebrate embryonic development with a focus on Tbx5 function during cardiac morphogenesis. The outcomes from this work will aid in the understanding of how T-box proteins function and are regulated, and additionally, provide more detailed evidence for the importance of PDZ-LIM proteins during cardiac formation.

Chapter 2: Pdlim7 regulates Tbx5 protein subcellular localization and activity

Introduction

Tbx5 and Tbx4 belong to the family of T-box transcription factors that share a homologous DNA-binding domain (T-domain) first described in the mouse *brachyury* (or *T*) gene product (Herrmann et al. 1990; Kispert and Herrmann, 1993). Studies in chicken (Logan and Tabin 1998; Rodriguez-Esteban et al. 1999; Takeuchi et al. 1999), zebrafish (Ahn et al. 2002; Garrity et al. 2002), and mouse (Agarwal et al. 2003; Naiche and Papaioannou 2003; Rallis et al. 2003) revealed that both Tbx5 and Tbx4 play critical roles in the outgrowth and specification of vertebrate forelimbs and hindlimbs, respectively. In addition to the limbs, Tbx5 has been shown to be required for proper heart development in zebrafish (Garrity et al. 2002) and mouse (Bruneau et al. 2001). In the chicken, Tbx4 expression has also been described in the heart, complementing the asymmetrical Tbx5 expression in this organ and suggesting parallel pathways for these transcription factors in the limbs and heart (Krause et al. 2004). While there is strong evidence that Tbx5 and Tbx4 are critical for embryonic development, little is known about how the transcription factors are regulated and function at the cellular level.

In a protein-protein interaction screen from chicken, the Simon laboratory has identified a new protein called Pdlim7, by its ability to interact with the C-terminal transactivation domain of the Tbx5 and Tbx4 transcription factors (Krause et al. 2004). In chicken embryos, Pdlim7 is expressed in the developing eye, heart, forelimbs, and hindlimbs; all organs that express either Tbx5 or Tbx4 (Bruneau et al. 1999; Krause et al. 2004; Logan et al. 1998). Pdlim7 is a member of an emerging class of scaffolding proteins, denoted PDZ-LIM proteins, which appear to function in fundamental biological processes including cytoskeletal organization, cell lineage

specification, and organ development (Dawid et al. 1998; Fanning and Anderson 1999, Kadrmas and Beckerle 2004). PDZ-LIM proteins contain cassettes of two different types of protein-protein interaction domains: a single N-terminal PDZ domain and one or three C-terminal LIM domains. The PDZ domain is an 85 amino acid β -barrel protein interaction motif that binds to both C-terminal peptides as well as internal sequences of target proteins (Harris and Lim 2001). The PDZ domains of the PDZ-LIM proteins Pdlim5 and Pdlim1 both bind to α -actinin and this interaction localizes the proteins to actin filaments (Nakagawa et al. 2000; Vallenius et al. 2000). The LIM domain is a 55 amino acid sequence that contains two zinc-finger-like motifs with conserved cysteine residues (Kadrmas and Beckerle 2004). The LIM domains of PDZ-LIM proteins have been found to interact with protein kinases, such as Clik1 (Vallenius and Makela 2002), PKC (Kuroda et al. 1996), and receptor tyrosine kinases (Wu et al. 1996; Wu and Gill 1994). All of the described binding partners for PDZ-LIM proteins suggest a role for this protein family as mediators, regulating protein function and/or signaling.

PDZ-LIM family proteins can be subdivided into two subclasses depending on the number of LIM domains present. For example, Pdlim1 contains a single C-terminal LIM domain while Pdlim5 and Pdlim7 contain three. The Pdlim5 and Pdlim7 proteins share significant sequence homology between their PDZ and LIM domains. However, there still appears to be specificity within the binding motifs. The PDZ domains of rat Pdlim5 and human Pdlim7 bind to α -actinin (Nakagawa et al. 2000) and β -tropomyosin (Guy et al. 1999), respectively; while the LIM domains of each protein bind different isoforms of PKC (Kuroda et al. 1996).

We have proposed that Pdlim7 interacts with Tbx5 and Tbx4 and regulates their activities by localizing the transcription factors out of the nucleus (Krause et al. 2004). Building upon our previous developmental studies, here I focus on Tbx5 and use it as a model to understand the

mechanism of Pdlim7/Tbx interactions. I have conducted a detailed cellular investigation utilizing cell biology and biochemical techniques to test the working hypothesis and uncover a novel mechanism that regulates Tbx protein sub-cellular localization and transcriptional activity.

Results

Polyclonal antibodies specifically recognize Pdlim7

In order to better understand the function of Pdlim7 binding to Tbx5, we generated Pdlim7-specific antibodies. To avoid cross-reactivity, we compared protein sequences of the closely related members of the PDZ-LIM protein family, and identified a 17-amino acid peptide from the proline-rich (P-rich) region, between the PDZ and LIM domains, to be highly conserved among the Pdlim7 protein orthologs from different species but not to the related Pdlim5 proteins (Fig. 2.1A). The respective chicken Pdlim7 peptide was used for the generation of specific antisera in rabbits followed by affinity purification using the peptide and then tested for specificity against Pdlim7 proteins expressed in both *E. coli* and COS-7 cells (Fig. 2.1B-F). On Western blots the antibodies recognized a recombinant form of Pdlim7 containing the PDZ and P-rich domains, but did not interact with the LIM domains or the GST tag (Fig. 2.1B). Furthermore, the Pdlim7 PDZ/P-rich protein band was absent after pre-incubation of the serum with the peptide used for immunization, demonstrating exclusive specificity for this antigen (Fig. 2.1B, lane 6). The Pdlim7 antibodies also recognized full-length Pdlim7 proteins expressed from chicken and zebrafish cDNAs transfected into COS-7 cells (Fig. 2.1C, lanes 1 and 2). As an additional test of specificity, COS-7 cells were transfected with an HcRed-Pdlim7 fusion expression construct and processed for confocal immunohistochemistry with the Pdlim7-specific antisera (Fig. 2.1D-F). HcRed-Pdlim7 localized to cortical actin in transfected COS-7 cells (Fig. 2.1D) overlapping with the localization detected by the Pdlim7-specific antibodies (Fig. 2.1E-F). The specific antisera displayed no significant background on untransfected COS-7 cells in either the red 546 nm (Fig. 2.1G) or green 488 nm (Fig. 2.1H) channels. Based on our Western blot

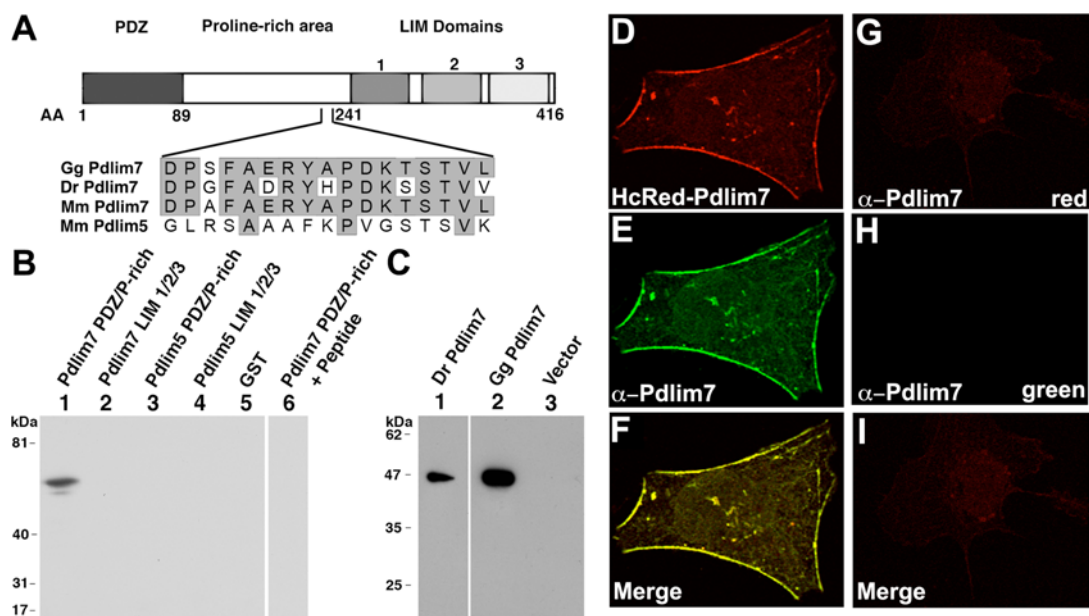


Figure 2.1: Specificity of polyclonal Pdlim7 antibodies. (A) Sequence comparison of 17 amino acid peptide in proline-rich (P-rich) region of mouse, chicken, and zebrafish Pdlim7 and mouse Pdlim5. (B) Western blot analysis of *E. coli* lysates including GST fusion proteins, Pdlim7, and Pdlim5. The Pdlim7 antiserum recognized the antigen containing PDZ/P-rich form of Pdlim7 but not the LIM domains, any form of recombinant Pdlim5, or the GST tag. Preincubation of the Pdlim7 serum with the peptide antigen effectively blocked specific recognition of the Pdlim7 PDZ/P-rich recombinant protein. (C) Western blot analysis of COS-7 cell lysates after transfection of chicken or zebrafish Pdlim7 expression constructs. After probing with Pdlim7 antiserum, single protein bands of the expected size of 45 kDa were observed for chicken and zebrafish Pdlim7. Vector control lysates did not reveal any antibody reaction. Equal protein loading was determined by probing for GST (B) or by BCA protein assay (C) (data not shown). (D-F) COS-7 cell transfected with HcRed-Pdlim7. (D) HcRed-Pdlim7. (E) HcRed-Pdlim7 transfected cell stained with Pdlim7 antiserum. (F) Merge of D and E. (G-I) Nontransfected COS-7 cell control stained with Pdlim7 antiserum and imaged in three red channel (G) and green channel (H). (I) Merge of G and H. *Gg*, *Gallus gallus*; *Dr*, *Danio rerio*; *Mm*, *Mus musculus*.

and immunohistochemical data with recombinant Pdlim7 proteins expressed in prokaryotic and eukaryotic cells, the generated antiserum appeared to be specific for its Pdlim7 target.

Pdlim7 is a member of a larger family of PDZ-LIM proteins, and we wished to ensure that the serum would not interact with a related family member. For this reason, recombinant protein from the evolutionarily closest PDZ-LIM protein, mouse Pdlim5 (Nakagawa et al. 2000), was produced in *E. coli*. Similar to Pdlim7, Pdlim5 contains conserved N-terminal PDZ and three C-terminal LIM domains. However, the proline-rich regions of mouse Pdlim5 and chicken Pdlim7 vary significantly in sequence (Fig. S1A). In Western blot analyses the Pdlim7 antiserum did not cross-react with any portion of mouse Pdlim5 (Fig. S1B). Additionally, pre-immune serum did not react with the *E. coli* or COS-7 cell lysates (data not shown). Equal protein loading was determined by either probing for GST or by BCA assay (data not shown). Thus, the polyclonal antibody specifically recognizes Pdlim7 and does not cross-react with the highly related PDZ-LIM protein family member Pdlim5.

Individual expression of Tbx4, Tbx5, or Pdlim7 results in localization to separate cellular compartments

Previously, we have shown co-expression of *Tbx4* and *Tbx5* with *Pdlim7* mRNA in chicken embryos during heart and forelimb development. Additionally, Tbx4, and -5 protein binding with Pdlim7 was shown by *in vitro* GST pull-down experiments (Krause et al. 2004). However, Tbx proteins have been shown to localize to the nucleus while PDZ-LIM proteins have been shown to be associated with actin filaments (Collavoli et al. 2003; Zaragoza et al. 2004; Nakagawa et al. 2000; Vallenius et al. 2000; Krause et al. 2004). To further elucidate the mechanism of Tbx4, -5/Pdlim7 interactions and where within a cell they occur, we utilized COS-

7 cells. COS-7 cells do not express either Tbx4, -5 or Pdlim7 (data not shown) and therefore allowed us to dissect the localization and function of each protein separately, as well as in combination.

Our group, as well as others, has shown nuclear localization of Tbx4 and -5 in transfected cells (Collavoli et al. 2003; Krause et al. 2004; Zaragoza et al. 2004). However, many of these experiments used large fusion proteins such as EGFP for detection, which we have found to cause Tbx5 to function at suboptimal levels (Fig. 2.7). To reduce the risk for functional interference, we have constructed non-tagged and small C-terminal epitope-tagged Tbx4 and -5 expression plasmids. A Tbx5-HA expression construct was transfected into COS-7 cells and protein localization was detected by indirect fluorescence using anti-HA antibodies (Fig. 2.2A-D). Using confocal immunofluorescence detection, Tbx5-HA displayed a clear nuclear localization in COS-7 cells. The nuclear localization of Tbx5-HA was confirmed using cellular fractionation (Camarata et al. 2006). Tbx5-HA protein was only detected by Western blot analysis in the nuclear lysate of transfected COS-7 cells. Additionally, COS-7 cells were transfected with a Tbx4-HA expression construct and protein localization was detected by immunofluorescence (Fig. 2.2E-H). Tbx4-HA displayed a strictly nuclear localization, similar to Tbx5-HA. Empty vector controls displayed no specific localization by immunofluorescence (data not shown).

Previously, we have shown that Pdlim7 localizes to cytoplasmic sites using an HcRed-Pdlim7 fusion expression construct (Krause et al. 2004). To verify our earlier findings, similar to Tbx5, we employed expression plasmids containing Pdlim7 with a small C-terminal myc-epitope tag for transfections. Pdlim7-myc was transfected into COS-7 cells and detected by indirect fluorescence using the Pdlim7-specific antiserum (Fig. 2.2I-L). Pdlim7 protein displayed a

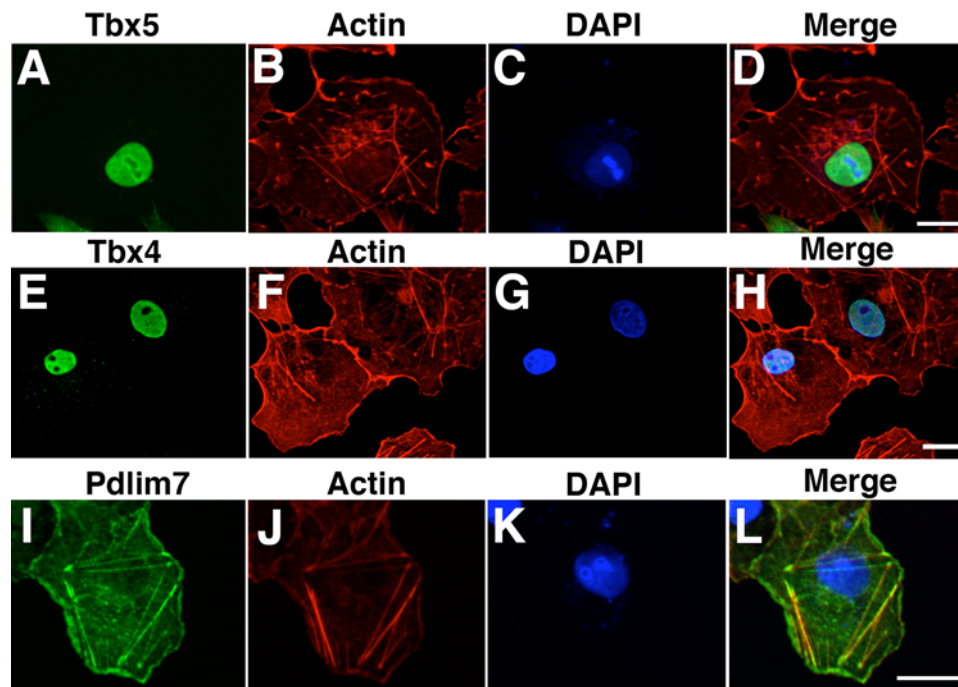


Figure 2.2: In single transfections chicken Tbx5, Tbx4 and Pdlim7 localize to separate cellular compartments. (A-D) COS-7 cells transfected with Tbx5-HA and its expression detected using anti-Tbx5 antibodies (A). (B) Cells were counterstained for actin using Alexa Fluor 633 phalloidin and the nucleus using DAPI (C). (D) The merged image shows Tbx5 exclusively localized to the nucleus. (E-F) COS-7 cells transfected with Tbx4-HA and detected using anti-HA antibodies. (E) Tbx4 localizes strictly to the nucleus. Cells were counterstained for actin (F) and the nucleus (G). (H) Merge of E-G. (I-L) COS-7 cells transfected with Pdlim7-myc and its expression detected using Pdlim7 antibodies (I). Cells were counterstained for actin (J) and the nucleus (K). The merged image (L) shows co-localization of Pdlim7 to actin stress fibers with no obvious nuclear localization. Scale bar= 20 μ m.

filamentous distribution that overlapped with phalloidin stained actin. This pattern is comparable to our previous data with HcRed-Pdlim7 and those obtained using an anti-myc antibody for detection (Krause et al. 2004). Cellular fractionation also confirmed the presence of Pdlim7 protein in the cytoplasmic fraction and not the nuclear fraction of transfected cells (Camarata et al. 2006). We note that we could not detect conclusive nuclear localization for Pdlim7 in these single transfection experiments. Empty vector controls displayed no specific localization by immunofluorescence (data not shown). Thus, using cell biology and biochemical methods, individually expressed Tbx4, -5, and Pdlim7 localize to separate sub-cellular compartments in COS-7 cells: the nucleus and actin cytoskeleton, respectively.

Co-expression of Tbx4 or -5 and Pdlim7 leads to Tbx/Pdlim7 interactions at cytoplasmic sites

We next co-transfected COS-7 cells with Pdlim7-myc and Tbx5-HA or Tbx4-HA and protein localization was determined by indirect fluorescence. Cells cotransfected with Pdlim7-myc and Tbx5-HA were stained with anti-myc and anti-HA specific antibodies. The anti-HA antibody detected Tbx5-HA within the nucleus but also at cytoplasmic structures (Fig. 2.3A). Pdlim7-myc, as detected by anti-myc, produced a localization pattern comparable to single transfections indicating association with actin filaments (Fig. 2.3B). However, we also observed a higher level of non-filamentous cytoplasmic staining for this protein. Comparing Tbx5 and Pdlim7 localization in the merged image revealed co-localization of Tbx5 and Pdlim7 within the cytoplasm (Fig. 2.3D), along polymerized actin (phalloidin stain not shown; Krause et al. 2004) and at additional unidentified cytoplasmic sites. We note that in transfected COS-7 cells we were only able to detect cytoplasmic localized Tbx5 in the presence of Pdlim7.

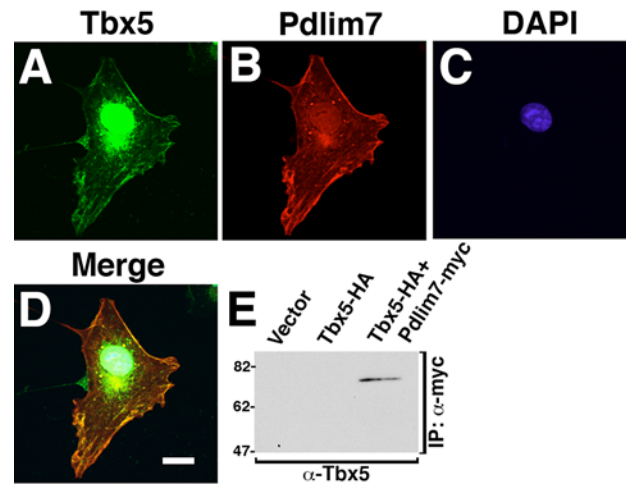


Figure 2.3: In co-transfected cells chicken Tbx5 and LMP4 interact at cytoplasmic sites. (A-D) COS-7 cells co-transfected with Tbx5-HA and Pdlim7-myc. Cells were stained with anti-HA for Tbx5 (A), anti-myc for Pdlim7 (B), and the nuclear stain DAPI (C). The merged image (D) shows co-localization of Tbx5 and Pdlim7 outside the nucleus predominantly along actin fibers. Co-immunoprecipitation of Tbx5-HA and Pdlim7-myc from COS-7 protein lysates (E). Pdlim7-myc was immunoprecipitated with myc antibodies and the Western blot processed with Tbx5-specific antibodies. Scale bar= 20 μ m. Protein molecular weight size markers in kDa are indicated on the left of the Western blot.

The co-localization of Tbx5 and Pdlim7 within the cytoplasm supports our previous *in vitro* binding studies and suggests the two proteins interact in cells (Krause et al. 2004). To confirm the interactions by independent means, we performed protein co-immunoprecipitations. Lysates of COS-7 cells co-transfected with Pdlim7-myc and Tbx5-HA were subjected to immunoprecipitation with anti-myc antibodies and Western blot analysis (Fig. 2.3E). Probing the Western blot with the Tbx5-specific antibody demonstrated that the transcription factor co-precipitated with Pdlim7 (lane 3). The vector controls and individual Tbx5-HA transfections did not result in immunoprecipitates with the anti-myc antibody (lanes 1 and 2).

Nuclear/cytoplasmic fractionation experiments of cells co-expressing Tbx5 and Pdlim7 did not reveal any evidence for nuclear localization of Pdlim7 despite the appearance of some weak staining in the nuclear area of co-transfected cells (Fig. 2.3B). The fractionation experiments also did not detect Tbx5, Pdlim7, or the Tbx5/Pdlim7 complex within the soluble fraction, indicating that they are part of additional protein complexes (data not shown). The co-immunoprecipitation of Pdlim7 and Tbx5 supports the cellular co-localization and confirms binding of the two proteins in the cell. In reciprocal co-immunoprecipitation experiments Tbx5-HA was also able to co-precipitate Pdlim7-myc (data not shown). Thus, Tbx5 localization outside the nucleus is a result of its interaction with Pdlim7.

To determine if Tbx4 was also capable of binding with Pdlim7 at cytoplasmic sites, COS-7 cells were cotransfected with Tbx4-HA and Pdlim7-myc. Cells were stained with anti-HA and anti-myc antibodies and processed for indirect confocal fluorescence (Fig. 2.4A-D). Similar to single transfections, Tbx4-HA was localized to the nucleus (Fig. 2.4A). However, Tbx4 protein was also detected at filamentous cytoplasmic sites, colocalizing with Pdlim7-myc (Fig. 2.4B and

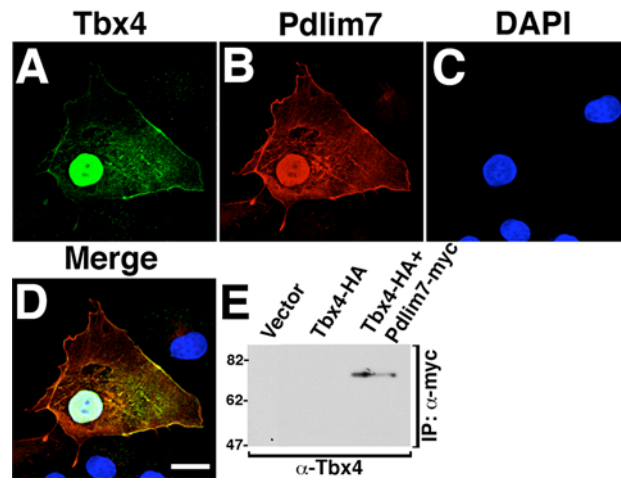


Figure 2.4: In co-transfected cells chicken Tbx4 and Pdlim7 interact at cytoplasmic sites. (A-D) COS-7 cells co-transfected with Tbx4-HA and Pdlim7-myc. Cells were stained with anti-HA for Tbx4 (A), anti-myc for Pdlim7 (B), and the nuclear stain DAPI (C). The merged image (D) shows co-localization of Tbx4 and Pdlim7 outside the nucleus predominantly along actin fibers. Co-immunoprecipitation of Tbx4-HA and Pdlim7-myc from COS-7 protein lysates (E). Pdlim7-myc was immunoprecipitated with myc antibodies and the Western blot processed with Tbx4-specific antibodies. Scale bar= 20 μ m. Protein molecular weight size markers in kDa are indicated on the left of the Western blot.

D). Similar to Tbx5, transfected COS-7 cells only displayed cytoplasmic localized Tbx4 in the presence of Pdlim7.

To confirm the Tbx4/Pdlim7 interactions, we again performed protein co-immunoprecipitations. Lysates of COS-7 cells co-transfected with Pdlim7-myc and Tbx4-HA were subjected to immunoprecipitation with anti-myc antibodies and Western blot analysis (Fig. 2.4E). Probing the Western blot with the Tbx4-specific antibody demonstrated that the transcription factor co-precipitated with Pdlim7 (lane 3). The vector controls and individual Tbx4-HA transfections did not result in immunoprecipitates with the anti-myc antibody (lanes 1 and 2). Therefore, it appears that both Tbx4 and -5 are capable of binding to Pdlim7 within a cell. Of significance is that the Tbx/Pdlim7 interaction occurs outside the nucleus along actin filaments.

Pdlim7 LIM domain 3 is required for interaction with Tbx5

Immunofluorescence combined with protein co-immunoprecipitation showed that Pdlim7 was capable of interacting with both Tbx4 and Tbx5. Both transcription factors are thought to act as positive regulators of gene transcription (Naiche et al. 2005) and we hypothesized that Pdlim7 may regulate both proteins in a similar fashion. Therefore, Tbx5 was chosen as a model to help understand the functional consequence of Tbx/Pdlim7 interactions. A first step was to understand the molecular nature of the Tbx5/Pdlim7 interaction. Previous *in vitro* GST pull-downs had suggested that the third LIM domain of Pdlim7 was necessary for interaction with Tbx5 (Krause et al. 2004). To confirm this, using full-length proteins in eukaryotic cells, a truncated form of Pdlim7 was constructed where the LIM3 domain was removed. The truncated Pdlim7 Δ LIM3-myc was transfected into COS-7 cells and processed for indirect fluorescence

(Fig. 2.5A-D). Anti-myc antibodies detected Pdlim7 Δ LIM3-myc along filamentous structures outside the nucleus (Fig. 2.5A). The localization was very similar to phalloidin stained actin (Fig. 2.5B). The merge of Pdlim7 Δ LIM3-myc and actin detection displayed significant colocalization (Fig. 2.5D). The localization of Pdlim7 Δ LIM3-myc was identical to full-length Pdlim7. Therefore, removal of the LIM3 domain did not alter the subcellular localization of the PDZ-LIM protein.

We then asked if the Pdlim7 Δ LIM3-myc protein retained its ability to bind to and sequester Tbx5 to actin filaments outside the nucleus. COS-7 cells were cotransfected and stained with anti-myc and anti-HA antibodies. In cotransfected cells, Pdlim7 Δ LIM3-myc localized along filamentous structures in the cytoplasm (Fig. 2.5E). Interestingly, Tbx5-HA remained localized strictly to the nucleus, despite the presence of the truncated form of Pdlim7 (Fig. 2.5F and H; n=40). This data supports the previous work that the third LIM domain of Pdlim7, which does not effect actin localization, is required for binding to Tbx5.

Actin destabilization does not change Tbx5/Pdlim7 binding or co-localization

Since the Tbx5/Pdlim7 complex forms at actin filaments, it was important to investigate what role an intact actin cytoskeleton would have on mediating the interaction. To determine this, Tbx5 and Pdlim7 localization was observed in COS-7 cells with destabilized actin. Twenty-four hours post-transfection of Tbx5-HA and Pdlim7-myc, cells were treated with 2 μ M latrunculin A for one hour to disrupt filamentous actin, and then processed for confocal microscopy using indirect fluorescence (Fig. 2.6). Using the anti-HA antibody, Tbx5 was detected both in the nucleus and cytoplasm of actin-disrupted cells (Fig. 2.6A). Pdlim7 was detected with the anti-myc antibody and found only in the cytoplasm of actin-disrupted cells (Fig. 2.6B). As in non-

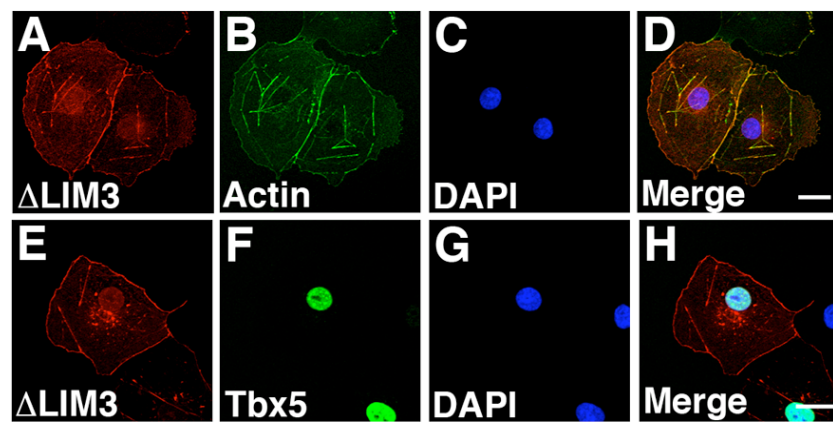


Figure 2.5: Removal of Pdlim7 LIM3 abrogates Tbx5 co-localization. (A-D) Single transfection of Pdlim7-myc with LIM3 deleted (Δ LIM3). Cells were stained with anti-myc antibodies to detect Pdlim7 Δ LIM3 (A), Phalloidin 488 to detect actin filaments (B), and DAPI to visualize the nucleus (C). (D) Merge shows colocalization of Pdlim7 Δ LIM3 with filamentous actin. (E-H) COS-7 cells co-transfected with Pdlim7 Δ LIM3 (E) and Tbx5 (F). (G) DAPI stain. (H) Merge showing Tbx5 no longer co-localizes with Pdlim7 without the LIM3 domain (n=40). Scale bar=20 μ m.

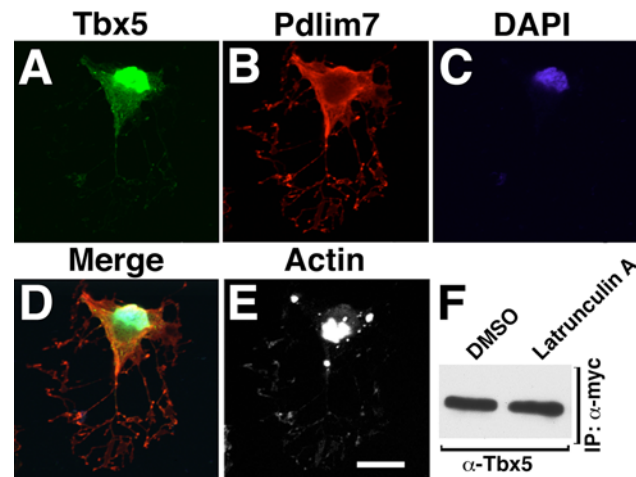


Figure 2.6: Filamentous actin is required for cytoplasmic Tbx5/Pdlim7 complex localization. (A-E) COS-7 cells co-transfected with Tbx5-HA and Pdlim7-myc. 24 hours after transfection, cells were treated with 2 μ M latrunculin A for 60 minutes to sequester actin monomers. Cells were processed with anti-HA for Tbx5 (A), anti-myc for Pdlim7 (B), the nuclear stain DAPI (C), and Alexa Fluor 633 phalloidin to detect actin (E). The merged image (D) shows that the Tbx5 and Pdlim7 complex no longer displays a filamentous pattern. For comparison, actin distribution of the cell in A-D is shown (E). Co-immunoprecipitation of Tbx5 and Pdlim7 after actin disruption (F). Tbx5-HA was co-precipitated along with Pdlim7-myc in lysates from latrunculin A and DMSO control treated COS-7 cells. Scale bar= 20 μ m.

treated cells, both Tbx5 and Pdlim7 appear to co-localize within the cytoplasm of latrunculin A treated cells (Fig. 2.6D); however, the proteins displayed no clear sub-cellular localization. Despite the lack of specific localization, Tbx5 and Pdlim7 were still able to interact as demonstrated by imaging and co-immunoprecipitation (Fig. 2.6F). Similar results were also obtained when actin was disrupted using 5 μ M cytochalasin B for 1 hour on co-transfected COS-7 cells (data not shown). It remains to be determined if an intact actin cytoskeleton is needed for initial Tbx5/Pdlim7 binding or whether it has a predominant role in proper sub-cellular localization of the protein complex. However, it appears that the interaction of both proteins is maintained despite the lack of a complete actin cytoskeleton.

Pdlim7 represses Tbx5 transcriptional activity

Tbx5 has been shown to function as a transcription factor, activating target genes in the developing limb and heart (Bruneau et al. 2001; Hiroi et al. 2001). In the mouse, the limb-specific *fibroblast growth factor 10* (*Fgf10*) and the heart-specific *atrial natriuretic factor* (*ANF*) genes have been shown to be immediate downstream targets of Tbx5 (Agarwal et al. 2003; Bruneau et al. 2001). DNA fragments containing the respective promoters were ligated to the *luciferase* gene and the resulting reporter constructs were utilized to determine Tbx5 transcriptional activity as a function of sub-cellular re-localization. COS-7 cells were transfected with constant amounts of the *luciferase* reporter and Tbx5 plasmids, and increasing amounts of Pdlim7 expression plasmids. To achieve optimal protein activities in this assay, non-tagged and small-tagged constructs were employed. Tbx5 alone revealed a robust activation of both the *Fgf10* and *ANF* reporters (Fig. 2.7), verifying that the chicken Tbx5 transcription factor can activate the respective mouse gene promoters at comparable levels to mouse Tbx5 (Agarwal et

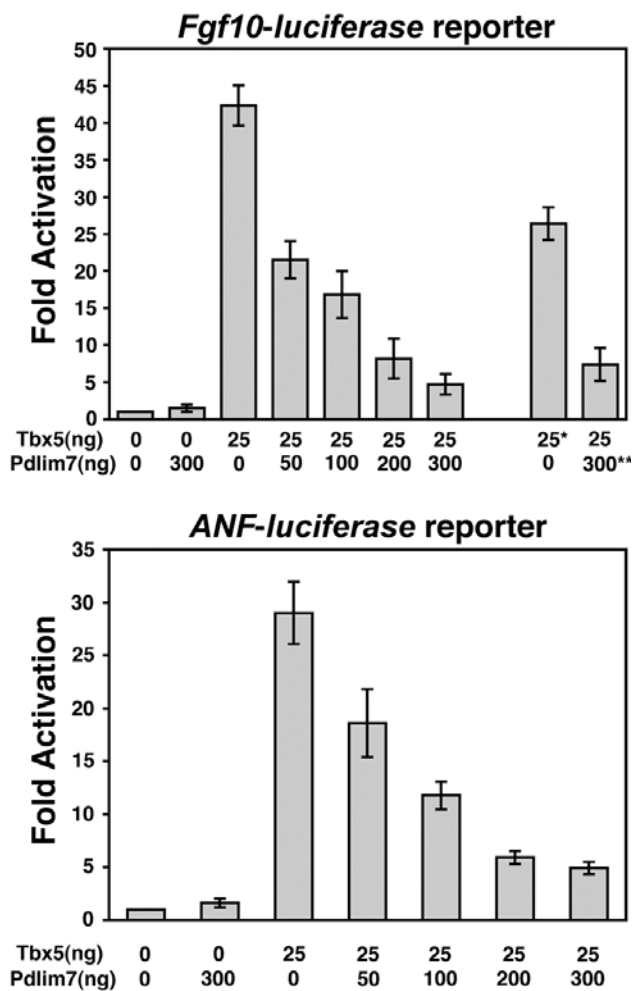


Figure 2.7: Pdlim7 represses Tbx5 transcriptional activity on the *Fgf10* and *ANF* target promoters. COS-7 cells were transfected with constant amounts of each respective reporter, Tbx5 and increasing amounts of Pdlim7 expression plasmid. Changes in *luciferase* reporter expression are indicated as fold activation. *EGFP-Tbx5 fusion protein, revealing compromised activation of the *Fgf10-luciferase* reporter construct. **Pdlim7-EYFP fusion protein, revealing compromised repression of Tbx5 activity. Data shown are from two independent experiments performed in triplicate. Data are normalized to *Renilla luciferase* to control for differences in transfection efficiency.

al. 2003; Bruneau et al. 2001). Co-transfecting Pdlim7 along with Tbx5, however, resulted in decreased Tbx5 activity on both of the reporters. The ability of Pdlim7 to repress Tbx5 transcriptional activity was dose dependent, as increasing amounts of Pdlim7 caused a linear reduction in Tbx5 activity (Fig. 2.7). The maximum amount of Pdlim7 tested (300 ng) led to a repression of Tbx5 (25 ng) of 90% and 83% employing the *Fgf10* and *ANF* promoters, respectively. Of note, our work with EGFP-Tbx5 and Pdlim7-EYFP revealed that such large fusion proteins have a significant reduction in activity. For example, transfection of COS-7 cells with 25 ng of EGFP-Tbx5 resulted in an approximately 30% reduction of transcriptional activity on the *Fgf10* promoter as compared to an equivalent amount of Tbx5-HA or non-tagged Tbx5 (Fig. 2.7). All luciferase reporter data were normalized to *Renilla* luciferase to account for variability in transfection efficiency and expression. Luciferase assays were performed in triplicate and data were collected from two independent experiments. Thus, Pdlim7 modulates Tbx5 transcriptional activity by re-localizing the transcription factor out of the nucleus.

In the presence of Pdlim7, Tbx5 shuttles dynamically between the nucleus and cytoplasm

To determine if Tbx5 re-localization and transcriptional modulation by Pdlim7 was due to shuttling of the transcription factor out of the nucleus, fluorescence recovery after photobleaching (FRAP) experiments in COS-7 cells were performed. For this series of experiments it was essential to use an EGFP-Tbx5 fusion construct in order to visualize protein in living cells. EGFP-Tbx5 revealed a reduced level of transcriptional activity compared to non-tagged or small HA-tagged Tbx5 constructs (Fig. 2.7); however, the fusion protein retained the ability to co-localize with Pdlim7 within the cytoplasm of co-transfected cells (Krause et al. 2004 and data not shown). COS-7 cells were co-transfected with EGFP-Tbx5 and Pdlim7-myc or

HcRed-Pdlim7 and grown on glass bottom culture dishes for live cell confocal microscopy. As expected, in the background of Pdlim7, EGFP-Tbx5 was detected in both nuclear and cytoplasmic compartments (Fig. 2.8). To observe shuttling of the transcription factor, the EGFP fluorescence signal in either the cytoplasm or nucleus was bleached using the 488 nm laser at maximum intensity and its recovery within the bleached compartment was observed over time. After photo-bleaching the cytoplasm, the EGFP fluorescent signal showed significant recovery over a 30 minute time window (Fig. 2.8A; see online supplemental movie 1 associated with Camarata et al. 2006). It is important to note that the fluorescence recovery in the cytoplasm occurred with concomitant decrease of fluorescence in the nucleus, indicative of active shuttling of EGFP-Tbx5 out of the nucleus to cytoplasmic sites. Quantitative data analysis for a representative cell is shown in Fig. 2.8A. Likewise, reciprocal experiments involving photo-bleaching the nucleus (Fig. 2.8B; see online supplemental movie 2 associated with Camarata et al. 2006) displayed EGFP fluorescence recovery of the nuclear compartment at the expense of the cytoplasmic signal over a similar 30 minute time frame. This result indicates movement of EGFP-Tbx5 from cytoplasmic sites into the nucleus. As a control, whole cell FRAP of co-transfected cells was performed. No EGFP recovery was observed in control cells within the same time period in this set-up, indicating that the experimental fluorescence recovery is due to protein shuttling and not to translation of additional EGFP-Tbx5 or maturation of EGFP (Fig. 2.9). Therefore, in the presence of Pdlim7, Tbx5 sub-cellular localization is dynamic and the transcription factor can shuttle between the cytoplasm and nucleus.

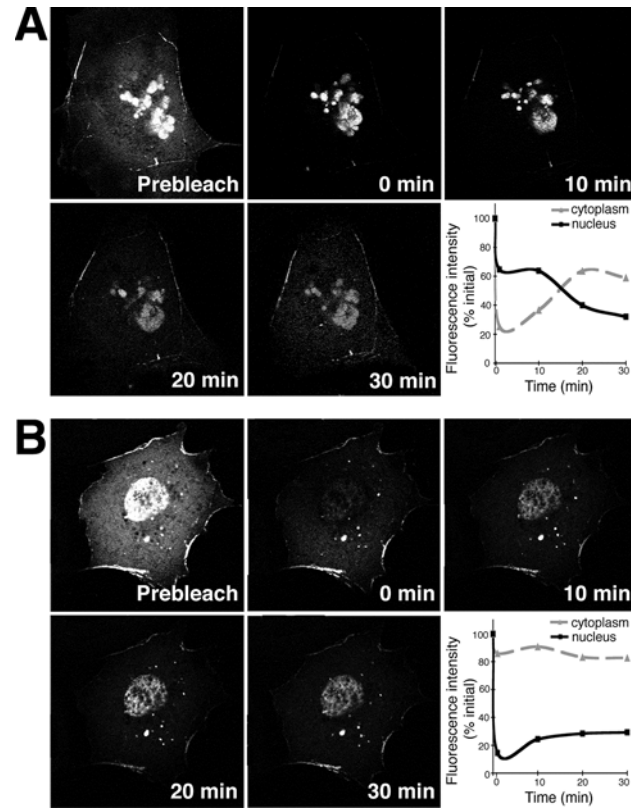


Figure 2.8: Dynamic shuttling of Tbx5 between nuclear and cytoplasmic compartments. (A-B) COS-7 cells co-transfected with EGFP-Tbx5 and Pdlm7. Photo-bleaching of cytoplasmic EGFP-Tbx5 (A). Graph displays quantitative fluorescent data for a representative cell. Photo-bleaching of nuclear EGFP-Tbx5 (B). Graph displays representative quantitative fluorescent data. Bleaching of whole cell displayed no fluorescence recovery within displayed timeframe (Fig. 2.9). All FRAP assays were performed with a minimum of three cells.

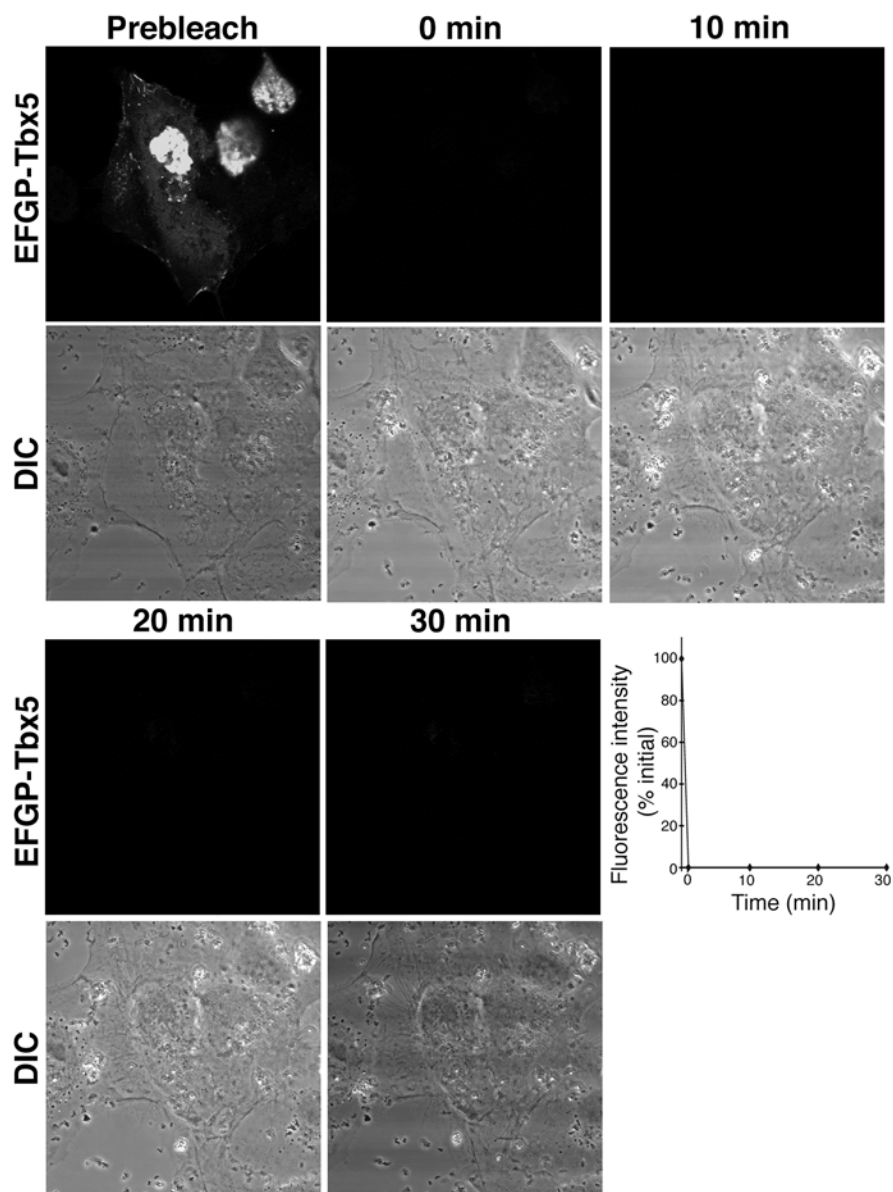


Figure 2.9: Whole cell bleach control. COS-7 cells were co-transfected with EGFP-Tbx5 and Pdlim7. One double transfected and two single transfected cells are shown. No cytoplasmic Tbx5 is observed in the single transfected cells because they are not expressing Pdlim7. EGFP fluorescence was bleached in both the cytoplasmic and nuclear compartments (top panels). No fluorescence recovery was observed during the displayed time period. Graph shows fluorescence intensity of control cell. Corresponding DIC images are shown (bottom panels).

Discussion

Tbx5 sub-cellular localization is dynamic and related to cell differentiation

We have previously hypothesized that Tbx5 transcriptional activity may be modulated by dynamic interactions between Tbx5 and Pdlim7 proteins and localization of the complex to the actin cytoskeleton (Krause et al. 2004). Here we provide evidence in support of the Tbx5/Pdlim7 regulatory model. Individually, Tbx5 and Pdlim7 localize to separate cellular compartments: the nucleus and cytoplasm, respectively. However, when expressed within the same cell Tbx5 is no longer strictly nuclear. The Tbx5 and Pdlim7 proteins bind and co-localize in the cytoplasm, predominantly in association with actin. The change in Tbx5 localization caused by Pdlim7 represses its ability to activate target promoters, as shown by *in vitro* luciferase reporter assays. The regulatory model would also imply a dynamic Tbx5/Pdlim7 complex assembly/disassembly, responding to external stimuli or signal transduction pathways and ultimately modulating Tbx5 protein activity. This notion is supported by re-localization of Tbx5 in differentiating epicardial cells and by dynamic shuttling of Tbx5 between cytoplasmic and nuclear compartments in transfected COS-7 cells, as observed by FRAP (Camarata et al. 2006). In chicken epicardial cells we observed co-expression of Tbx5 and Pdlim7; however, in contrast to COS-7 cells, Tbx5 localization was predominantly nuclear in these cells. Cytoplasmic and actin associated Tbx5 was not observed until cells were induced to differentiate. Cultured epicardial cells are well known to undergo such epithelial-to-mesenchyme transitions (EMT) when stimulated with embryonic heart conditioned medium or transforming growth factors such as TGF β (Dettman et al. 1998; Lu et al. 2001; Morabito et al. 2001; Compton et al. 2005). For the first time we have demonstrated a concomitant re-localization of Tbx5 proteins from the nucleus to the cytoplasm during this process; strongly suggesting that specific signaling

pathways, potentially involving TGF β -like factors, are involved in regulating Tbx5/Pdlim7 interactions and Tbx5 activity (Camarata et al. 2006). The data presented are in agreement with the Tbx5/Pdlim7 regulatory model and point towards a complex pathway regulating Tbx5 activity by altering its localization depending on the developmental context of the cell.

An emerging role for Pdlim7 as a signal mediator in Tbx5 regulation

The nuclear concentration of many transcription factors is a dynamic balance that is determined by competing processes of nuclear import and nuclear export; and by the presence of anchor proteins in both the nucleus and the cytoplasm. For example, NF- κ B/Rel proteins, which are involved in diverse biological processes, were initially identified as constitutive nuclear transcription factors. Subsequent analysis however revealed that, in most cells, NF- κ B is sequestered in the cytoplasm via its interaction with I κ B family proteins and only released into the nucleus in response to specific stimuli (Karin and Ben-Neriah, 2000). Additionally, the GLI-1 transcription factor has been shown not to be strictly nuclear but also cytoplasmic (Dahmane et al. 1997; Ruiz i Altaba, 1999). GLI-1 cytoplasmic localization has been shown to be due to interactions with Suppressor-of-Fused and the export of GLI-1 from the nucleus regulates its transcriptional activity (Kogerman et al. 1999). A similar novel mechanism may be emerging with Pdlim7 and Tbx5. When complexed with Pdlim7, a pool of Tbx5 is localized outside the nucleus in association with the actin cytoskeleton, thereby limiting the transcription factor's availability and activity in the nucleus. However, the specific signaling cascades that regulate the expression, localization, and function of Tbx5 have yet to be identified. Based upon our initial studies with primary chicken epicardial cultures, it appears that specific stimuli are involved in re-localization of Tbx5 during differentiation. Recently, TGF β has been shown to

induce differentiation of chicken epicardial cells into epicardial-derived cells (EPDCs; Compton et al. 2005). It will be of interest to determine if TGF β in concert with Pdlim7 is required for Tbx5 re-localization in differentiating epicardial cells or to identify the nature of other specific upstream signals.

In addition to external stimuli or signaling pathways that may modulate Tbx5 protein activity, the mechanism by which Tbx5 is shuttled out of the nucleus into the cytoplasm for interaction with Pdlim7 is not yet understood. One hypothesis would be that a small amount of Pdlim7 is – at least temporarily – present in the nucleus, and in response to a given stimulus/signal acts as a shuttling vector for Tbx5. Alternatively, it is possible that a yet unidentified transport protein shuttles Tbx5 out of the nucleus where it is then able to interact with Pdlim7. Finally, Tbx5 itself may be utilizing an intrinsic shuttling signal to translocate to the cytoplasm where Pdlim7 is waiting to localize it to actin sites. These options can be experimentally tested, and studies are under way to investigate which cellular mechanism is responsible for altering Tbx5 sub-cellular localization.

In this context it is noteworthy that PDZ-LIM proteins are thought to have diverse roles as regulators of cyto-architecture, cell motility, signal transduction, and gene expression (Bach, 2000; Kadrmas and Beckerle, 2004). Several family member proteins such as Pdlim7, Pdlim1, and the Ldb3 proteins interact via their PDZ domains with the cytoskeleton (Guy et al. 1999; Vallenius et al. 2000; Zhou et al. 1999). Consistent with these findings it is not surprising that in our studies Pdlim7 is also co-localizing with the actin cytoskeleton. Of note, Pdlim1's C-terminal LIM domain binds to and re-localizes the nuclear Clk1 kinase to actin stress fibers (Vallenius and Makela, 2002). LIM domains in general are known to mediate protein interactions, and the close Pdlim7 family member Enigma binds to the insulin receptor (Wu and

Gill, 1994), receptor tyrosine kinases (Wu et al. 1996), and PKC (Kuroda et al. 1996). Although the exact role(s) of PDZ-LIM proteins such as Pdlim7 in signaling cascades is currently speculative, the association with signal receptors and/or transducers provides an attractive link and points to an involvement in regulated signaling events eliciting a change in binding partners. The presence of Pdlim7 in epicardial cultures, which display a differentiation response to external signals along with a significant re-localization of Tbx5, also suggests involvement of this PDZ-LIM protein in a signaling cascade.

Nuclear versus cytoplasmic Tbx5 localization and its relation to development and disease

A cytoplasmic distribution for TBX5 in human lung during development has been indicated (Collavoli et al. 2003). Our observations with developing wings, primary epicardial cells as well as transfected cells reveal a previously unidentified localization of Tbx5 in both the nucleus and the cytoplasm. The actin-associated distribution of the Tbx5 transcription factor is particularly striking in the primary chicken epicardial derived cells and would suggest that an equilibrium of Tbx5 in the nucleus and cytoplasm is important for the proper maintenance of its functions within the cell, and in turn the organism. While the system may compensate for some changes in protein levels, acting as a capacitor, significant over-expression or under-expression would be expected to result in deleterious consequences. Few reports are available on *Tbx5* gain-of-function/over-expression phenotypes in higher vertebrates, but those available support our findings. For instance, retroviral over-expression of *Tbx5/4* in the respective chicken wing/leg bud resulted in limb truncations, similar to misexpression of the respective dominant-negative constructs (Rodriguez-Esteban et al. 1999). In addition, skeletal and cardiac malformations known as Holt-Oram syndrome (HOS) in humans are caused by mutations in

TBX5. The majority of *TBX5* mutations critical for disease manifestation are thought to result in early protein terminations and haploinsufficiency; however, increased TBX5 dosage, such as chromosome 12q2 duplication, has been reported to also result in HOS (Hatcher and Basson, 2001; Vaughan and Basson, 2000). These data would suggest a more generalized effect of *Tbx5* gene dosage, both under- and over-expression, in causing fairly similar if not identical phenotypes. The data presented here would also imply a change in *Tbx5* level would have direct consequences on *Tbx* protein distribution in the cell. This in turn may interfere with the differentiation program such as EMT of epicardial cells. In this context it may be of significance that epicardial cells contribute to the myocardial wall, atrio-ventricular cushions, and valves, all cardiac structures that are predominantly affected in HOS. Therefore, balanced cellular *Tbx5* levels and appropriate localization appear to be critical and *Pdlim7* may play a central role in this regulation.

Experimental data coming from many animal models have provided clear evidence for the importance of *Tbx5* in eye, limb, and heart development, and gene and RNA studies have provided some clues for the roles *Tbx5* has in the cell. However, in addition to its role as a transcription factor, our new data may also point to unknown functions of *Tbx5* outside the nucleus when associated with actin. An attractive possibility would be a direct role in regulating actin dynamics, a notion supported by the finding that *Tbx5* function is involved in cell migration in zebrafish fin development (Ahn et al. 2002). A role in migratory behavior would be quite plausible also in light of the complex phenotypes of *Tbx5* misexpression that have been observed in humans and animal models. This hypothesis can be tested, and future experiments mislocalizing *Tbx5* to distinct cellular compartments and examining the resulting functional consequences will provide new insights into this question.

Chapter 3: *Pdlim7* regulation of *Tbx5* specifies zebrafish atrio-ventricular boundary formation

Introduction

Shaping the mature vertebrate heart with separated chambers and valves requires a complex array of gene expression. Several genes have been identified to be critical for cardiac morphogenesis, however, their function as it relates to cell activities are poorly understood (Harvey, 2002). In the zebrafish, the heart forms from cells in the anterior lateral plate mesoderm aligned into two bilateral stripes of cardiac progenitors (Reviewed in Stainier, 2001). The bilateral heart fields migrate together towards the midline and form a cardiac cone, which then telescopes out to give rise to the linear heart tube; consisting of an inner endocardial cell layer and an outer myocardial layer. The zebrafish heart tube loops and constricts to morphologically and functionally delineate a single atrium and ventricle. Cells located at the constriction between the two chambers will then give rise to the mature valve (Beis et al. 2005; Scherz et al. 2008). The zebrafish heart is less-complex in design compared to avian and mammalian hearts, however, most of the developmental signaling and genetic pathways appear to be highly conserved between teleosts and higher vertebrates (Stainier, 2001).

One class of genes important for heart development and disease is the family of T-box transcription factors (Isphording et al. 2004; Stennard and Harvey 2005; Hoogaars et al. 2007). The T-box gene, *Tbx5*, is crucial for proper cardiac formation in humans (Basson et al. 1997; Li et al. 1997), mouse (Bruneau et al. 2001), and zebrafish (Garrity et al. 2002). In the zebrafish *tbx5 heartstrings (hst)* mutant the heart fails to loop and develops a string-like morphology. In addition, *hst* mutants do not develop pectoral fins (Garrity et al. 2002). In humans, similar

heart/limb problems result from mutations in *TBX5* leading to congenital birth defects characterized by a range of cardiac and forelimb malformations including septal defects and truncations of forelimb elements (Basson et al. 1997; Li et al. 1997). The function of Tbx5 during heart development appears to be sensitive to intracellular protein levels, since either haploinsufficiency or gene duplication can produce cardiac malformations (Basson et al. 1997; Vaughn and Basson 2000; Hatcher and Basson 2001). The sensitivity to dose may be due to synergistic interactions with other transcription factors in the nucleus such as Nkx2-5 (Hiroi et al. 2001) or Gata4 (Garg et al. 2003), but may similarly be a result of yet unknown functions in the cytoplasm. We have identified a PDZ-LIM protein, Pdlim7, which specifically binds Tbx5 (Krause et al. 2004) and enables the transcription factor to shuttle between the nucleus and the actin cytoskeleton (Camarata et al. 2006).

PDZ-LIM proteins are thought to act as signal mediators involved in a variety of cellular processes such as migration, signal transduction, and differentiation (Dawid et al. 1998; Bach, 2000; Kadrmas and Beckerle, 2004). During cardiogenesis PDZ-LIM proteins have crucial functional roles. Knock-out mice of *Pdlim3* develop cardiomyopathy (Pashmforoush et al. 2001). Similar cardiac defects were also detected in mutant mice (Zhou et al. 2001) and by morpholino knock-down in zebrafish (van der Meer et al. 2006) of *Ldb3*. However, in depth analysis of cardiac defects and the particular roles of PDZ-LIM proteins in heart development remain to be investigated.

The functional consequence of Tbx5/Pdlim7 interactions during cardiogenesis has not been explored. To gain insight into the significance of this protein-protein interaction we utilized the zebrafish, which can survive without a functional cardiovascular system during embryonic development (Glickman and Yelon, 2002). In this study we build upon and extend our previous

cellular work to investigate Pdlim7 function in cardiogenesis and its role in modulating Tbx5 activity.

Results

Identification of zebrafish *pdlim7*

Based on the information available from chicken *Pdlim7* and using complementary strategies of genome database searches and RT-PCR, I cloned a zebrafish cDNA with high sequence homology to the chicken gene. Of note, the zebrafish genome appears to contain a single copy of the putative *pdlim7* gene. All PDZ-LIM proteins are characterized by containing a single N-terminal PDZ domain and one or three C-terminal zinc finger LIM domains. The respective encoded chicken and zebrafish proteins had amino acid identities of 74% in the N-terminal PDZ domain and 74% to 94% between individual C-terminal LIM domains (Fig. 3.1). Phylogenetic analysis of amino acid sequences revealed that the zebrafish isolate grouped together with other known Enigma/LMP proteins, which all contain three C-terminal LIM domains, thereby confirming that it is the *Pdlim7* ortholog (Fig. 3.1).

pdlim7 is coexpressed with *tbx5* in the heart and pectoral fins

Using whole mount *in situ* hybridization, *pdlim7* mRNA could be detected in single-, two-, four- and eight-cell stage embryos revealing maternal deposition (Fig. 3.2A, B). In addition, expression was observed throughout the embryo from gastrulation up to the bud stage at 10 hours post-fertilization (hpf) (Fig. 3.2C, D). Later during development, *pdlim7* expression became restricted to developed somites and was maintained in maturing skeletal muscle (Fig. 3.2E-H). A low-level of mRNA was also observed in the head mesoderm. By 48 hpf, *pdlim7* expression displayed a distinctive chevron shape in the tail muscle (Fig. 3.2H).

Pdlim7 and *Tbx5* are interacting proteins and it was therefore of interest to assess whether there are domains of coexpression. We could detect *pdlim7* expression in the developing

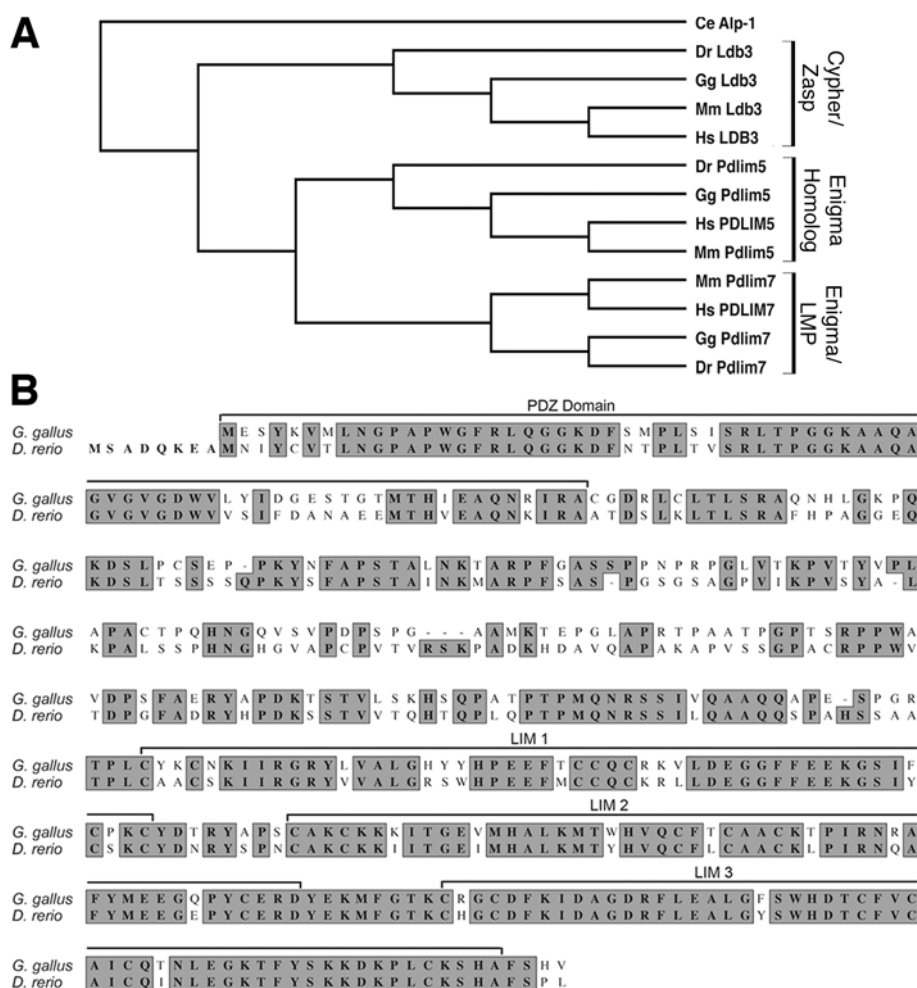


Figure 3.1: Amino acid alignment of Pdim7 proteins. (A) Phylogenetic analysis of zebrafish Pdim7. Amino acid alignments of PDZ-LIM proteins containing three LIM domains were used to create the phylogenetic tree using MacVector. *C. elegans* Alp-1 PDZ-LIM protein was used as the out-group. (B) Predicted amino acid sequences of chicken (*G. gallus*) and zebrafish (*D. rerio*) Pdim7. Identical residues are shaded and in bold. The PDZ and LIM domains are labeled. Chicken and zebrafish Pdim7 share a significant identity in the labeled functional protein interaction domains. Accession numbers for genes used to derive amino acid sequences for protein alignment: *C. elegans* alp-1, . Ldb3: *Homo sapien*, NM_007078; *Mus Musculus*, NM_011918; *Gallus gallus*, XM_421495; *Danio rerio*, DQ012157. Pdim5: *Homo sapien*, NM_006457; *Mus Musculus*, NM_019808; *Gallus gallus*, AJ851689; *Danio rerio*, BC045922. Pdim7: *Homo sapien*, NM_005451, *Mus musculus*, NM_026131; *Gallus gallus*, NM_001005345; *Danio rerio*, NM_200840.

heart and pectoral fins; both structures which have previously been shown to express *tbx5* (Begemann and Ingham 2000). Just prior to the 18-somites stage, *tbx5* is expressed in a single domain in the lateral plate mesoderm, which later separates into an anterior cardiac and posterior pectoral fin field (Fig. 3.2L; Ahn et al. 2002). At the 18-somite stage, *pdlim7* was distributed in two distinct regions in the lateral plate mesoderm that correspond to the *tbx5* expressing cardiac and pectoral fin precursors (Fig. 3.2I). Comparable to *tbx5* (Fig. 3.2M, N), cardiac expression of *pdlim7* was maintained at 24 hpf during heart tube formation and at 48 hpf during looping and chamber patterning, predominantly in the ventricle (Fig. 3.2J, K). In the developing pectoral fins, *in situ* hybridization detected *pdlim7* first in the newly induced fin buds at 32-33 hpf. During fin bud outgrowth, expression was maintained in the mesenchyme at 48 hpf until it became restricted to proximal and lateral sub-domains by 72 hpf (Fig. 3.2O-Q). The developmental time window of *pdlim7* pectoral fin expression coincides with *tbx5* fin expression (Fig. 3.2R-T; Begemann and Ingham 2000; Garrity et al. 2002). Moreover, the cardiac and limb expression domains of zebrafish *pdlim7* correspond with the gene's expression in the developing chicken, further supporting the evolutionary identity in the two species (Krause et al. 2004). In contrast to the chicken, however, eye expression for *pdlim7* was not detected in the zebrafish. *pdlim7* displays a broad and dynamic expression and revealed coexpression with *tbx5* in the heart and forelimb, supporting functional interaction of the encoded proteins in these organs.

Pdlim7 is critical for embryonic development

To test the requirement of Pdlim7 during development, we have knocked-down Pdlim7 protein expression using two non-overlapping morpholino antisense oligonucleotides (MO). MO1 was targeted to the translational start site of *pdlim7* to specifically inhibit translation while MO2 was

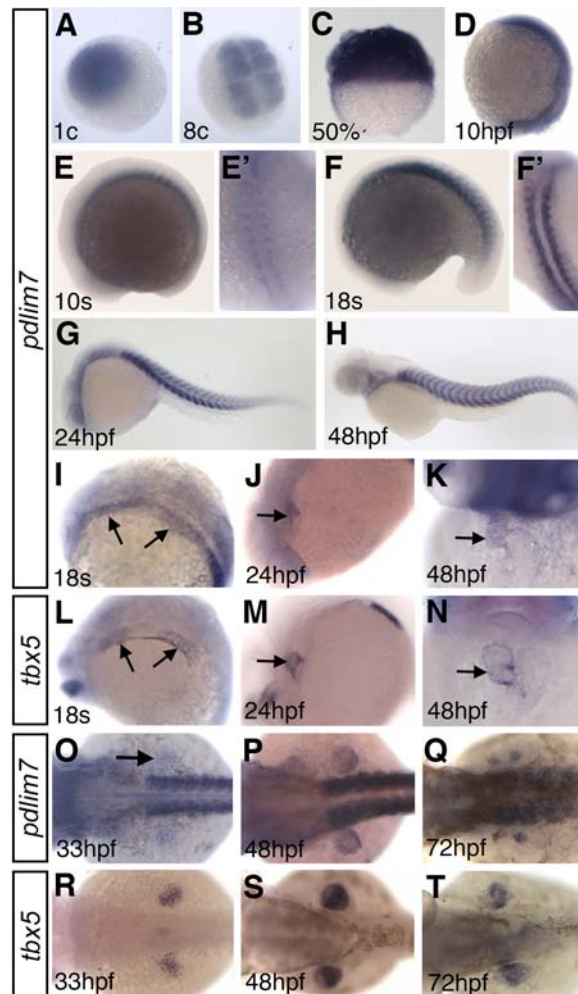


Figure 3.2: Spatial and temporal expression of zebrafish *pdlim7*. (A-H) *In situ* hybridization of *pdlim7* during the first two days of embryonic development. (A) 1-cell and (B) 8-cell stages. (C) 50% epiboly. (D) 10 hours post-fertilization (hpf). (E) 10-somites. (E') dorsal view of embryo in E. (F) 18-somites. (F') dorsal view of embryo in F. Anterior is toward the top in E' and F'. (G, H) Lateral views of 24 hpf and 48 hpf, respectively. (I-N) Comparison of *pdlim7* (I-K) and *tbx5* (L-N) cardiac expression. (I) *pdlim7* expression at 18-somites in the cardiac and pectoral fin precursors of the lateral plate mesoderm (LPM) (arrows). (J, K) Expression of *pdlim7* in the linear heart tube at 24 hpf and in the looped heart at 48hpf (arrow). (L) *tbx5* expression at 18-somites in the cardiac and pectoral fin precursors of the LPM (arrows). (M, N) *tbx5* expression in the heart at 24 hpf and 48 hpf, respectively (arrow). (O-T) Expression of *pdlim7* (O-Q) and *tbx5* (R-T) during pectoral fin development. (O-Q) *pdlim7* is expressed in the mesenchyme of the pectoral fin (arrow in O). (R-T). Expression of *tbx5* in the mesenchyme of the pectoral fin.

designed to target the splice donor site of exon 2 to interfere with mRNA splicing (Fig. 3.3 and 3.4). Injection of 2 ng of either MO into single-cell stage embryos resulted in identifiable developmental problems. By 48 hpf, morphant embryos displayed overall growth and tail defects compared to wild-type siblings (Fig. 3.5A-B). MO knock-down of *pdlim7* caused significant disorganization of the muscle fibers in the tail which could be detected by 24 hpf and embryos did not display the typical touch response by two days of development. However, protein markers for muscle differentiation were still expressed in the *pdlim7* morphants. (Fig. 3.6). The tail muscle defects following *pdlim7* MO injection could be suppressed by coinjecting 25 pg of chicken *pdlim7* (Fig. 3.5C). Approximately 38% of coinjected embryos (n=70) had longer and more organized trunks. Muscle disorganization has also been observed after knock-down of the related PDZ-LIM gene, *cypher* (van der Meer et al. 2006). It appears that *pdlim7*, like other PDZ-LIM genes, plays a critical role in muscle formation and function.

Along with the muscle defects, knock-down of Pdlim7 protein using either MO1 or MO2 resulted in specific heart and pectoral fin defects. The injected embryos developed pericardial edema due to the developmental heart defects. In Pdlim7 depleted embryos the heart failed to loop and further differentiation was arrested (Fig. 3.5). The severity of the cardiac phenotype did not increase with higher doses of injected MO. However, the percentage of embryos displaying looping defects was dose dependent. Injection of different concentrations of either MO1 or MO2 led to an increased percentage of embryos with heart looping defects (Fig. 3.3 and 3.4). The complex *pdlim7* morphant phenotype could not be rescued by mRNA injection, however, coinjection of MO1 and MO2 at subcritical concentrations resulted in a synergistic interaction (Fig. 3.7). Coinjection of MO1 and MO2, at 1ng and 1.5ng respectively, produced embryos displaying looping defects in 95% of cases. In contrast, injection of each MO individually at the

pdlim7 ATG MO1 controls

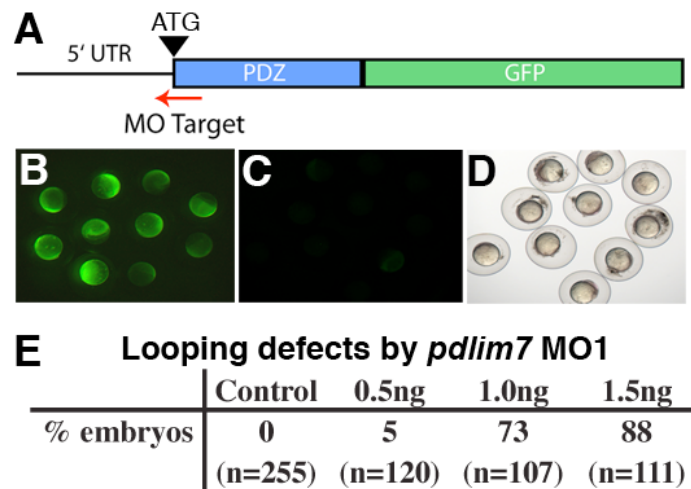


Figure 3.3: *pdlim7* translational start site morpholino causes heart-looping defects. (A) Schematic of control construct used to *in vitro* synthesize mRNA to test the specificity of the protein initiation morpholino (MO1). Red arrow denotes MO1 target sequence. (B) Embryos were injected with mRNA synthesized from the construct in A and GFP expression was detected at 50% epiboly. (C) Embryos were co-injected with the GFP expression construct mRNA along with MO1. No GFP expression was detected at 50% epiboly. (D) Brightfield microscopy of embryos in C. (E) Quantification of heart-looping defects in MO1 injected embryos stained with *cmhc2*. n, number of embryos scored.

pdlim7 Splice MO2 controls

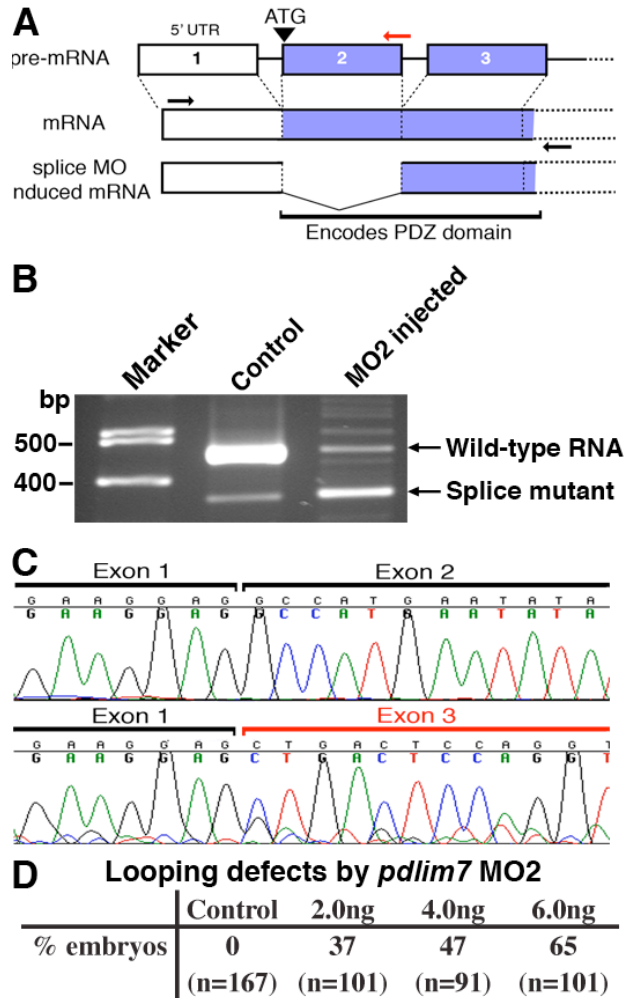


Figure 3.4: *pdlim7* splice-site targeted morpholino causes heart-looping defects in zebrafish. (A) Schematic of *pdlim7* splice morpholino (MO2) function. Red arrow denotes MO2 target sequence at exon 2 donor site. Exon 2 contains the translation initiation sequence. (B) RT-PCR assay to detect improper splicing of *pdlim7* mRNA after injection of MO2. Black arrows in A show position of primers used for PCR. (C) Sequencing of wild-type (top) and splice mutant (bottom) PCR product to confirm improper splicing. (D) Quantification of heart looping-defects in MO2 injected embryos stained with *cmcl2*. n, number of embryos scored.

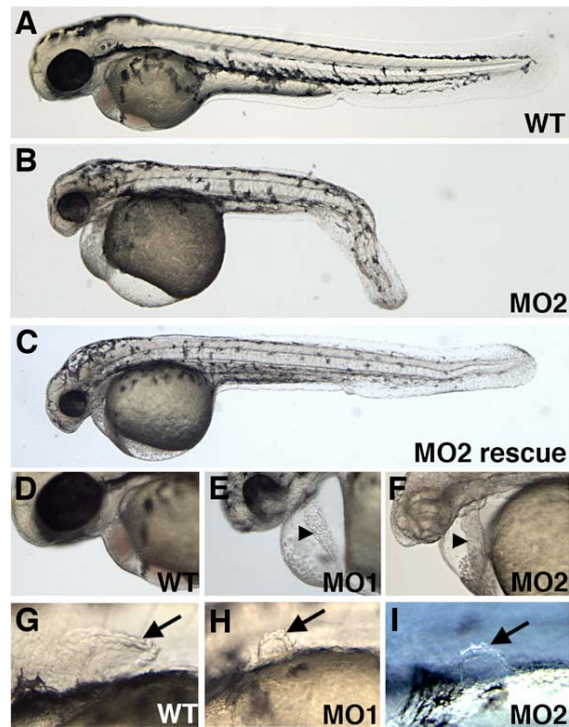


Figure 3.5: Knock-down of *pdlim7* perturbs heart and pectoral fin development. (A-C) Lateral view of wild-type (A), MO2, (B) and rescued MO2 (C) injected embryos at 48 hpf. (D-F) Magnification of hearts of wild-type (D), MO1 (E), and MO2 (F) injected embryo at 48 hpf. Arrowhead in E and F indicates string-like heart. Embryo in F treated with 0.0045% PTU to inhibit pigmentation over the heart. (G-I) Magnification of pectoral fins of wild-type (G), MO1 (H), and MO2 (I) morphants at 48 hpf (arrows). The head is to the left. (G) Wild-type pectoral fin. (H) MO1 morphant pectoral fin. (I) MO2 morphant pectoral fin.

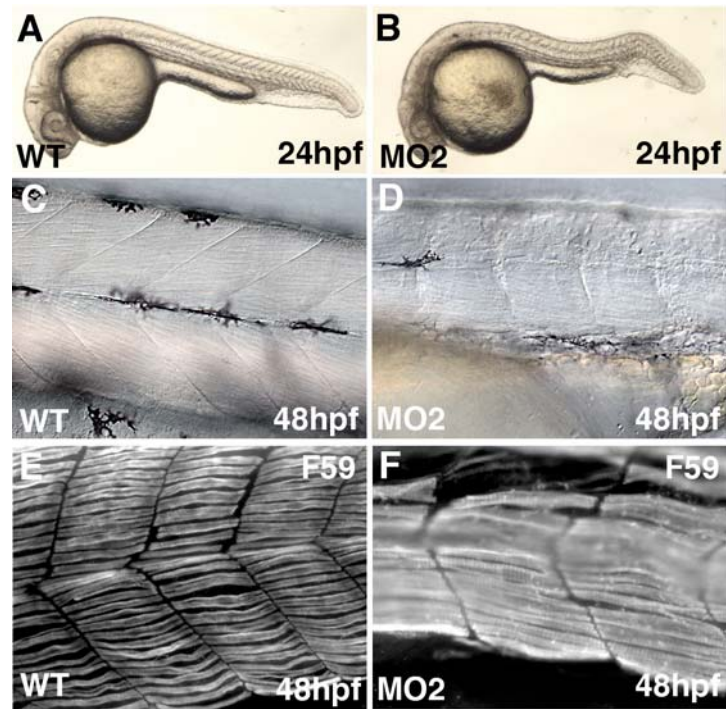


Figure 3.6: Pdlm7 is required for proper muscle development. (A) Lateral view of wild-type embryo at 24 hpf. (B) Lateral view of embryo injected with 2 ng of MO2 at 24 hpf. (C) Magnification of tail muscle of wild-type embryo at 48 hpf. (D) Tail muscle of 48 hpf embryo injected with 2ng MO2. (E) Immunofluorescence of wild-type embryo stained at 48 hpf with F59 fast muscle marker. (F) MO2 injected embryo stained at 48 hpf with F59 antibodies.

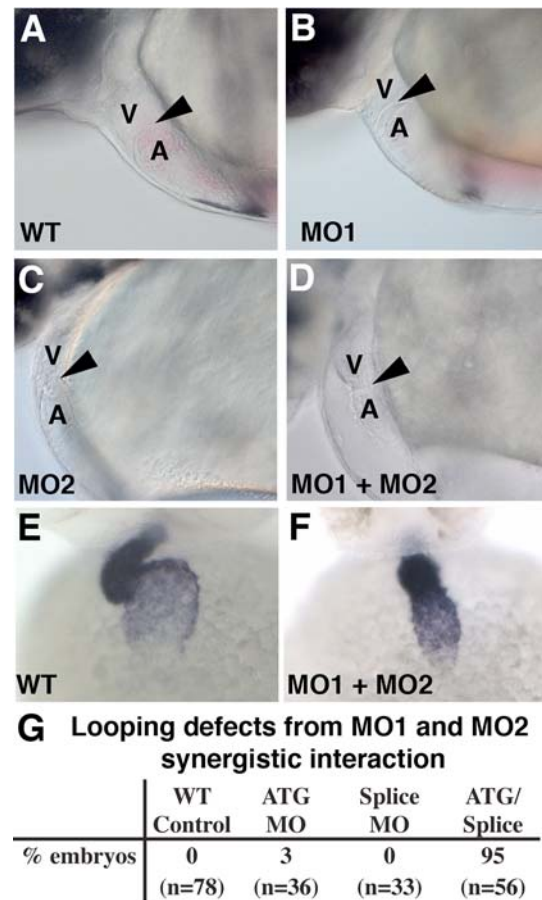


Figure 3.7: Synergistic activity of *pdlim7* initiation and splice morpholinos. (A-D) Lateral view of the heart in live embryos 48 hpf. (A) Wild-type control. (B) Initiation MO1 injected, 1ng. (C) Splice MO2 injected, 1.5ng. Atrium is in focus in A-C and ventricle is out of focus due to normal heart looping. Position of looping denoted by arrowhead. (D) Co-injected embryo with MO1 and MO2, 1ng/1.5ng respectively. Both atrium and ventricle are in the same focal plane and no looping observed (arrowhead). (E-F) Ventral view of *in situ* hybridization showing *cmlc2* expression in 48 hpf embryos. (E) Wild-type control. (F) *pdlim7* MO co-injected embryo. (G) Quantification of embryos with cardiac looping defects. n, number of embryos scored. V, ventricle. A, atrium.

same concentrations did not cause observable cardiac defects. The synergism of MO1 and MO2 indicates specificity of the two MOs for the same target gene, *pdlim7*. Of note, the cardiac phenotype of *Pdlim7* morphants resembled that observed for *tbx5 heartstrings (hst)* embryos, further suggesting the two genes may cooperate during heart development (Fig. 3.5D-F and data not shown; Garrity et al. 2002).

Loss of *Tbx5* activity in *hst* mutants or *tbx5* MO-treated embryos also leads to the lack of pectoral fins (Ahn et al. 2002; Garrity et al. 2002). Close inspection of the *pdlim7* MO-treated zebrafish demonstrated that pectoral fin development was perturbed. By 48 hpf, pectoral fins in morphant embryos were significantly smaller in size than those of wild-type embryos (Fig. 3.5G-H). While the defect of pectoral fin development in *pdlim7* MO embryos appears to be less severe than in the *tbx5* mutants or morphants, it nevertheless suggests that forelimb outgrowth may require *Pdlim7* function.

pdlim7 and *tbx5* functionally interact during heart development

The coexpression of *pdlim7* and *tbx5* along with similar cardiac phenotypes suggests the two genes function together during formation of the zebrafish heart. To further investigate this, we utilized the *hst* genetic mutant zebrafish line to determine if misexpression of *pdlim7* could enhance the string-like heart phenotype. The mutant *hst* allele causes a premature stop codon in *tbx5* resulting in a protein truncation at the C-terminal end, shortly after the T-domain (Fig. 3.8A; Garrity et al. 2002). We have previously shown that *Pdlim7* binds to the transactivation domain of chicken *Tbx5* (Krause et al. 2004). Because of its shorter size, the *Tbx5 hst* form is not expected to bind *Pdlim7*. To confirm this notion and to determine that the zebrafish proteins behave identical to their chicken orthologs (Krause et al. 2004; Camarata et al. 2006), we

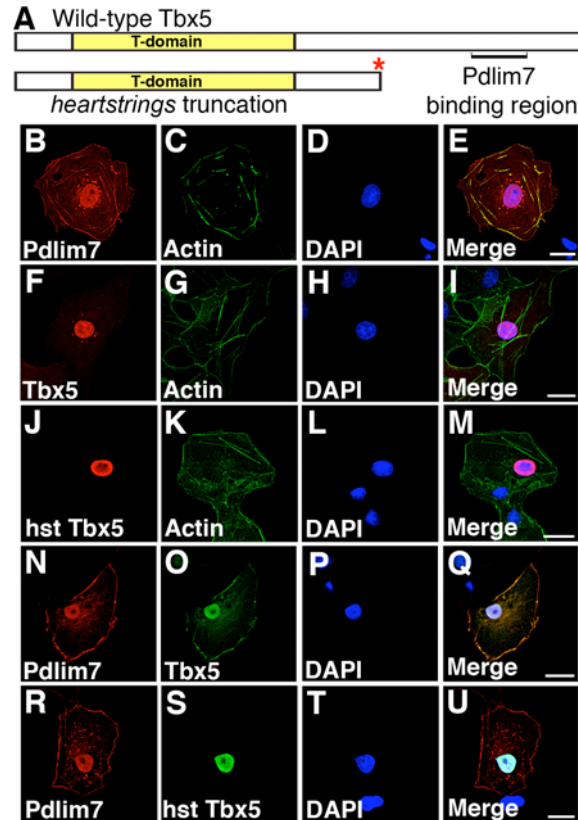


Figure 3.8: Pdlim7 colocalizes with full-length Tbx5 but not the *heartstrings* truncated form. (A) Schematic of wild-type and *heartstrings* (*hst*) truncated Tbx5 protein. Pdlim7 binding region is denoted in wild-type Tbx5. Red asterisk highlights the truncation of the *hst* encoded protein caused by a premature stop codon (Garrity et al. 2002). (B-E) Single transfection of myc-Pdlim7 in COS-7 cells. Cells were stained with anti-myc antibodies (B), Alexa-488 phalloidin to stain filamentous actin (C), and DAPI to visualize the nucleus (D). (E) Merged image of B-D. 3-dimensional analysis of confocal z-stacks demonstrated Pdlim7 to have perinuclear localization (Supplemental movie 1). (F-I) Single transfection of full-length HA-Tbx5. Cells were stained with anti-HA antibodies (F), Alexa-488 phalloidin (G), and DAPI (H). (I) Merged image of F-H. (J-M) Individual transfection of truncated HA-Tbx5 resembling the encoded *hst* allele. Cells were stained for Tbx5 (J), actin (K), and the nucleus (L). (M) Merged image of J-L. (N-Q) Cotransfected COS-7 cells stained for Pdlim7 (N), full-length Tbx5 (O), and the nucleus (P). (Q) Merged image of N-P. (R-U) Cotransfected cells stained for Pdlim7 (R), truncated Tbx5 (S), and the nucleus (T). (U) Merged image of R-T. Scale bar, 20 μ m.

expressed recombinant proteins in cultured cells. COS-7 cells were transfected and confocal immunofluorescence was used to detect the subcellular localization of epitope tagged Pdlim7 and full-length or a truncated forms of Tbx5 (Fig. 3.8). Similar to chicken Pdlim7, in single transfected cells zebrafish myc-Pdlim7 colocalized with filamentous actin (Fig. 3.8B-E). Occasionally, Pdlim7 antibody staining suggested nuclear distribution of the protein, however, repeated analysis of confocal virtual stacks has demonstrated that Pdlim7 is never in the nucleus but can display a perinuclear localization (data not shown). On the other hand, cells transfected with only HA-Tbx5 revealed the transcription factor strictly in the nucleus (Fig. 3.8F-I). A truncated form of Tbx5 constructed to resemble the *hst* allele product also localized to the nucleus (Fig. 3.8J-M). Next, cells were cotransfected with both full-length myc-Pdlim7 and the different HA-Tbx5 forms and processed for confocal immunodetection. As expected, comparable to the chicken protein, Tbx5 was detected within the nucleus but also in the cytoplasm colocalized with Pdlim7 along the actin cytoskeleton (Fig. 3.8N-Q). In contrast, in cotransfections with the truncated *hst* form of HA-Tbx5, no colocalization was detected (Fig. 3.8R-U). The *hst* Tbx5 protein remained strictly nuclear, despite the presence of Pdlim7. Therefore, similar to the chicken orthologs, zebrafish Pdlim7 and Tbx5 can interact in the cell along the actin cytoskeleton. However, providing the first evidence in eukaryotic cells for the importance of the C-terminus of Tbx5 for protein binding, the truncated *hst* mutant protein cannot bind to Pdlim7 nor localize to actin filaments.

Knowing that Pdlim7 regulates Tbx5 transcriptional activity by shuttling the transcription factor out of the nucleus and localizing it to actin filaments (Fig. 3.8; Krause et al. 2004; Camarata et al. 2006; Kulisz and Simon 2008), we hypothesized that *hst*/+ heterozygotes are more sensitive to moderate overexpression of *pdlim7*. Increased Pdlim7 levels in the cell should

relocalize wild-type Tbx5 to actin filaments while decreasing nuclear Tbx5 levels. We note that, embryos heterozygous for the *hst* mutation (*hst/+*) develop normal hearts despite a 50% reduction in wild-type Tbx5 (Fig. 3.9C; Garrity et al. 2002). However, mouse and humans are characterized by a higher Tbx5 sensitivity and similar reduced protein levels lead to severe cardiac defects (Bruneau et al. 2001; Li et al. 1997; Basson et al. 1997).

To determine if forced elevated Pdlim7 levels would cause heart looping-defects, wild-type and *hst/+* mutant embryos were injected with 75 pg of *in vitro* synthesized mRNA of *pdlim7* and stained at 48 hpf with *cmlc2* (Yelon et al. 1999) to outline the heart. Wild-type zebrafish embryos tolerated the increased *pdlim7* level well and only rarely revealed heart problems as compared to uninjected siblings (Fig. 3.9A, B). At the same time, *hst* heterozygotes were very sensitive to *pdlim7* mRNA injection (Fig. 3.9C, D). More than 30% of the embryos obtained from a wild-type and *hst* heterozygote parental cross failed to undergo cardiac looping and developed a string-like heart (Fig. 3.9E). To determine if the overexpression cardiac phenotype correlates with the *hst* heterozygosity, individual embryos were genotyped after *in situ* hybridization. The genotyping revealed that the injected embryos displaying a string-like heart phenotype were heterozygous for *hst* (n=21). Therefore, misexpression of *pdlim7* in the *hst/+* genetic background enhances the string-like heart phenotype, demonstrating a functional interaction of the two genes *in vivo*, supporting our previous mechanistic data (Camarata et al. 2006).

Cardiac differentiation and chamber identity is not altered after loss of Pdlim7

Next, we wondered whether the cardiac looping defect of *pdlim7* morphants was the result of a heart patterning problem. Genetic knock-out or misexpression of Tbx5 in the mouse resulted in

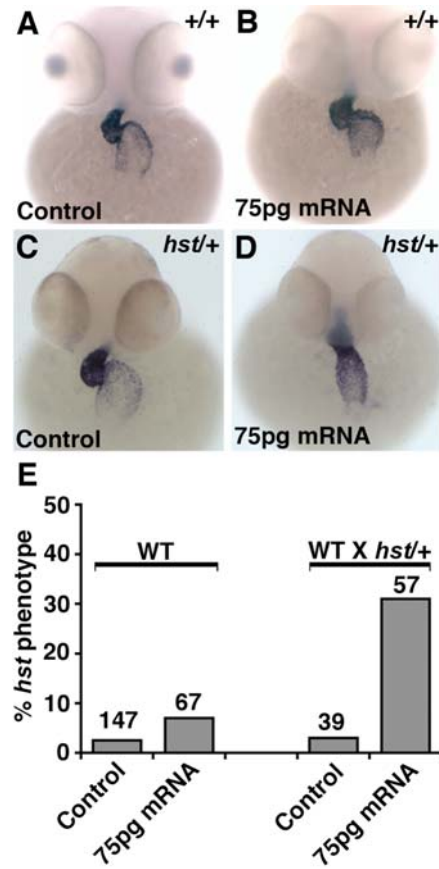


Figure 3.9: *pdlim7* and *tbx5* genetically interact during heart development. (A-D) *In situ* hybridization of 48 hpf embryos with *cmhc2*. (A) Uninjected wild-type control. (B) Wild-type embryo injected with 75 pg of *pdlim7* mRNA. (C) Uninjected *hst/+* embryo. (D) *hst/+* embryo injected with 75 pg *pdlim7* mRNA. (E) Quantification of uninjected and injected embryos with a string-like heart.

alterations of cardiac gene expression, especially within the ventricle (Liberatore et al. 2000; Bruneau et al. 2001). We wished to establish if similar changes in cardiac gene expression could be detected in *pdim7*-compromised hearts. Wild-type embryos were injected with 2ng of MO1 or MO2, fixed, and processed for *in situ* hybridization with cardiac markers. At 24 hpf the zebrafish heart is shaped as a tube, jogged to the left of the embryo, and can be visualized using the cardiomyocyte marker *cmlc2* (Fig. 3.10A; Stainier 2001). Embryos injected with either *pdlim7* MOs expressed *cmlc2*, however at 24 hpf, the heart tube appeared more compact and less extended compared to wild-type embryos (Fig. 3.10B, C). By 48 hpf, heart looping had neared completion, bringing the ventricle and atrium into a characteristic S-shape with *cmlc2* being expressed throughout the heart with stronger expression in the ventricle (Fig. 3.10D; Yelon et al. 1999). In *pdlim7* morphants, the heart fails to loop and progressively deteriorates as observed in live embryos (Fig. 3.5). Nevertheless, *cmlc2* remained expressed throughout the string-like heart (Fig. 3.10E, F). To gain a more precise view when heart morphology was perturbed by the down-regulation of *pdlim7*, *cmlc2* expression was assessed at the cardiac cone stage (22 hpf). At this early heart-forming stage, no changes in heart morphology and *cmlc2* distribution could be observed suggesting the problems occurred after this developmental time point. It therefore appears that myocardial specification occurs normally in the absence of Pdlim7 protein.

To determine if cardiac chamber identity was altered after *pdlim7* knock-down, morphant embryos were stained for *ventricular myosin heavy chain (vmhc)* and *atrial myosin heavy chain (amhc)* to specifically visualize the two heart chambers. At both time points, 24 hpf and 48 hpf, *vmhc* was detected in the ventricle of the developing heart (Fig. 3.10G, J). In MO injected embryos the ventricular marker was also detected at 24 hpf (Fig. 3.10H, I) and 48 hpf (Fig. 3.10K, L). The expression domain of *vmhc* in MO2 morphants at 24 hpf did not appear

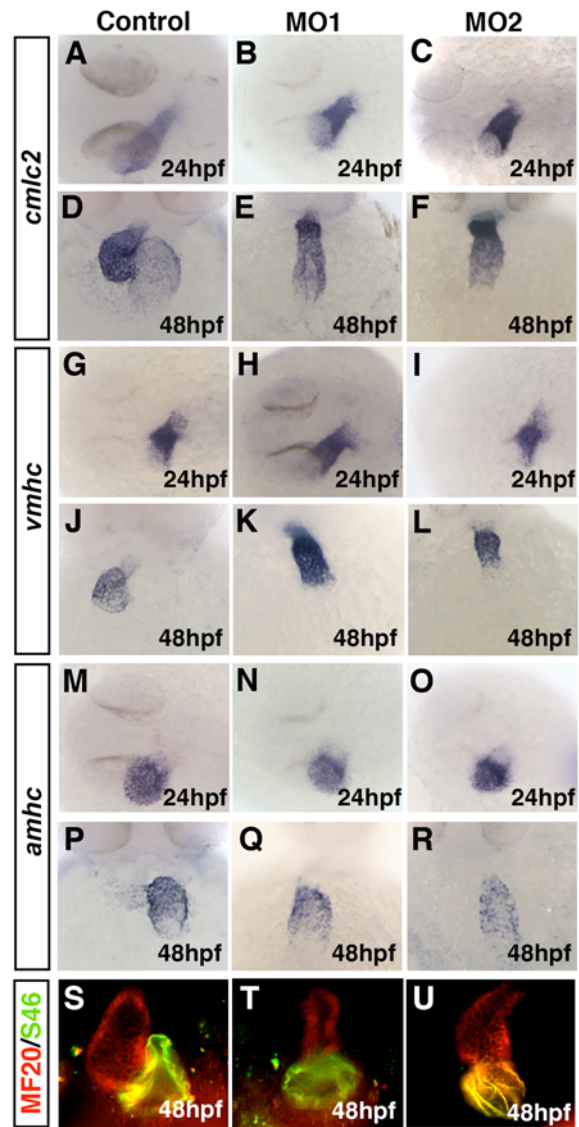


Figure 3.10: Knock-down of *pdlim7* does not alter cardiomyocyte or chamber patterning. (A-F) *In situ* hybridization of *cmhc2* at 24 hpf (A-C) and 48 hpf (D-F) in wild-type (A, D), MO1 (B, E), and MO2 (C, F) injected embryos. (G-L) Expression of the ventricular marker *vmhc* at 24 hpf (G-I) and 48 hpf (J-L) in wild-type (G, J), MO1 (H, K), and MO2 (I, L) injected embryos. (M-S) Expression of the atrial marker *amhc* at 24 hpf (M-O) and 48 hpf (P-R) in wild-type (M, P), MO1 (N, Q), and MO2 (O, R) injected embryos. (S-U) Frontal view 48 hpf embryos stained with MF20 and S46 antibodies to detect the ventricle (red) and atrium (yellow). (S) Wild-type control. (T, U) MO1 and MO2 injected embryos, respectively.

significantly different than in wild-type embryos. However, in MO1 injected embryos the ventricle appeared somewhat more extended (Fig. 3.10H). The extended expression domain for *vmhc* was maintained at 48 hpf in MO1 morphants as compared to the MO2 injected embryos. The atrial-specific marker *amhc* identified, as expected, the developing atrium at the two chosen time points (Fig. 3.10M, P). *amhc* was also detected in the morphant embryos. At 24 hpf the atrial domain, however, appeared more compact in MO1 and MO2 injected embryos as compared to wild-type controls (Fig. 3.10M-O). By 48 hpf, the *pdlim7* MO injected embryos expressed *amhc* in the appropriate posterior domain, which is located below the ventricle due to the position of the heart on the yolk, despite the defect in chamber morphology (Fig. 3.10Q, R).

Cardiac chamber specification was also determined at the protein level using MF20 and S46 antibodies. MF20 detects myosin heavy chain proteins within the entire heart while S46 recognizes a myosin heavy chain epitope specifically in the atrium (Stainier and Fishman 1992). Co-staining wild-type zebrafish hearts at 48 hpf clearly characterized the ventricle (red) and atrium (yellow) in the looped heart (Fig. 3.10S). MF20/S46 staining was not perturbed in *pdlim7* morphant embryos at 48 hpf but heart looping defects were observed (Fig. 3.10T, U). Based upon gene and protein markers, cardiomyocyte differentiation and chamber identity appeared to be unaffected in *pdlim7* morphant embryos. Apparently the heart forms and functions normally through the early heart tube stages, however, further differentiation into a looped heart is arrested. As in *pdlim7* morphants, *tbx5 hst* mutants did not show changes in the expression of *cmlc2*, *vmhc*, or S46 detection (Garrity et al. 2002). Therefore in zebrafish cardiac patterning, *pdlim7* and *tbx5* do not appear to be essential. Both genes, on the other hand, are required for proper heart morphology, with *pdlim7* playing an earlier role at or slightly before 24 hpf and both *pdlim7* and *tbx5* being essential at 48 hpf for heart-looping.

Pdlim7 and Tbx5 are required for atrio-ventricular boundary formation

The most dramatic change in gene expression observed in *hst* mutant embryos was detected for *versican* and *bmp4*, which are both markers for the boundary between the atrium and ventricle (Garrity et al. 2002). Since we proposed that Pdlim7 regulates Tbx5 function, we next investigated whether the expression of *versican*, *bmp4*, as well as the cardiac expression of *tbx5* was perturbed in *pdlim7* morphant embryos (Fig. 3.11). Early in zebrafish cardiac development, when the heart is assembled as a tube, *tbx5* is expressed in myocardial cells with enhanced expression in the atrium (Fig. 3.11A; Begemann and Ingham 2000). By 48 hpf, *tbx5* expression shifts and is predominantly detected in the ventricle (Fig. 3.11D; Garrity et al. 2002). Upon closer inspection, we could also detect *tbx5* concentrated in the region of the atrio-ventricular (A/V) boundary, the future site of valve formation. A/V valve expression for *Tbx5* has also been noted in the mouse and chicken (Bruneau et al. 1999). Injection of MO1 or MO2 did not change the atrial-enhanced expression domain of *tbx5* in the heart tube at 24 hpf (Fig. 3.11B, C). Interestingly, at 48 hpf the expression of *tbx5* at the A/V boundary was lost after injection of MO1 or MO2 (Fig. 3.11E, F). Instead, *tbx5* appeared to be upregulated throughout the heart with a stronger expression in the ventricle. The misexpression of *tbx5* after MO injection further supports a role for Pdlim7 in the regulation of the Tbx5 transcription factor.

Along with *tbx5*, the A/V boundary markers *versican* and *bmp4* were similarly affected after *pdlim7* MO injection. At the linear heart tube stage expression of *versican* and *bmp4* in wild-type and *pdlim7* morphant embryos was comparable (data not shown). However, we could detect changes in *versican* after MO injection by 48 hpf. At this later stage in wild-type controls, *versican* defined the A/V boundary (Fig. 3.11G; Hurlstone et al. 2003). Injection of *pdlim7* MO1 or MO2, however, resulted in an expansion of expression into both chambers (Fig. 3.11H, I).

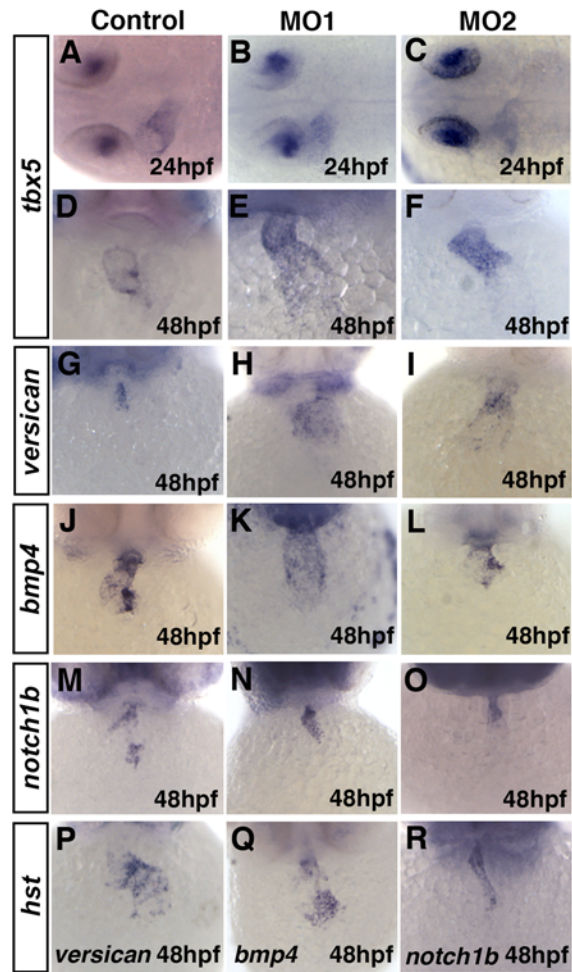


Figure 3.11: *Pdlim7* is required for AV boundary specification. (A-F) *In situ* hybridization of *tbx5* at 24 hpf (A-C) and 48 hpf (D-F) in wild-type (A, D), MO1 (B, E), and MO2 (C, F) injected embryos. (G-O) Expression of the AV boundary markers at 48 hpf, *versican* (G-I), *bmp4* (J-L) and *notch1b* (M-O). (P-R) Expression of AV boundary markers in *hst* homozygous embryos at 48 hpf.

Like *versican*, *bmp4* was expressed at the A/V boundary in looped hearts (Fig. 3.11J; Wash and Stainier, 2001). However, the normal retraction of *bmp4* expression to the A/V boundary by 48 hpf did not occur after *pdlim7* knock-down (Fig. 3.11K, L). Furthermore, the A/V boundary gene, *notch1b*, was also misexpressed compared to wild-type in *pdlim7* MO injected embryos (Fig. 3.11M-O; Wash and Stainier, 2001). Thus, the defect in the *pdlim7* morphants appears to be that a normal A/V boundary is not formed and further heart development, including heart looping, is arrested. In this context we note that loss of A/V boundary restriction of *versican*, *bmp4*, and *notch1b* was also detected in *hst* mutants (Fig. 3.11P-R; Garrity et al. 2002). The similarity in cardiac phenotypes and gene misexpression suggests that Tbx5 and Pdlim7 together participate in proper heart morphogenesis and the Tbx5/Pdlim7 interaction is critical for A/V boundary specification.

Tbx5 and Pdlim7 regulate *tbx2b* atrio-ventricular expression

In the present study, we demonstrate that Tbx5 and Pdlim7 are required for appropriate restriction of gene expression at the AV boundary. Recent work by Chi et al. (2008) has identified a putative Tbx5 binding element in the promoter of the AV boundary gene *tbx2b*. We therefore wished to determine if *tbx2b* expression in the heart was dependent upon Tbx5. We initially assessed the expression of *tbx2b* in wild-type, *hst/+*, or *hst/hst* embryos (Fig. 3.12A-C). In wild-type embryos, we found *tbx2b* expressed in the heart at 48 hpf specifically at the AV boundary (Fig. 3.12A). In *hst/+* embryos, we detected reduced levels of expression while in *hst/hst* embryos *tbx2b* was completely absent (Fig. 3.12B, C). The presence of a Tbx5-binding-element in the promoter of *tbx2b* along with the reduction of expression in *hst* heterozygous

mutants and complete loss in homozygotes reveals that Tbx5 regulates *tbx2b* at the AV boundary.

Next, we examined whether Pdlim7 could regulate *tbx2b* expression via its interaction with Tbx5. Since in previous experiments both *pdlim7* MOs yielded comparable phenotypes, we concentrated on the splice-inhibiting MO2 for injection into wild-type embryos. Similar to the AV boundary genes tested, at 48 hpf, *tbx2b* expression was expanded in *pdlim7* morphants (31%, n=42) (Fig. 3.12D). The expansion of *tbx2b* expression in the heart suggested that Pdlim7 could regulate Tbx5 transcriptional activity *in vivo*. To gain further insight into Pdlim7 regulation of Tbx5, we took advantage of the reduced *tbx2b* AV boundary expression in *hst/+* embryos. According to our model, Pdlim7 could regulate *tbx2b* expression via complex formation with Tbx5 (Fig 3.12H). Knock-down of Pdlim7 would, therefore, result in higher nuclear Tbx5 levels and consequently increased *tbx2b* expression (Fig. 3.12I). To test this prediction, uninjected or MO2 injected embryos from a parental cross with wild-type and *hst/+* adults were analyzed for *tbx2b* expression. As expected, in controls, half of the embryos displayed a reduced level of *tbx2b* expression at the AV boundary (50%, n=94) and genotyping confirmed the presence of the *hst* allele (15/20) (Fig. 3.12G). MO2 injected embryos from the *hst/+* parental-cross yielded three *tbx2b* AV boundary expression classes, normal (47%), reduced (31.5%), and expanded (21.5%) (n=70; Fig. 3.12G). Injected embryos with reduced *tbx2b* expression contained the *hst* allele (19/22; see Table 1), however, compared to controls, the overall number of this expression class was reduced. Based upon Pdlim7/Tbx5 interactions it could be expected that after *pdlim7* knock-down wild-type embryos would be more sensitive to expansion of *tbx2b* AV boundary expression (Fig 3.12H, I). Genotyping revealed the majority of embryos with expanded *tbx2b* expression were in fact wild-type (10/14). Additionally, our Pdlim7/Tbx5 interaction model

would predict that lower *Pdlim7* levels could rescue the reduced *tbx2b* expression in *hst* heterozygotes. This notion is supported by the observation of fewer than expected embryos with low levels of *tbx2b* AV boundary expression (Fig. 3.12G). Interestingly, injected embryos displaying a normal level of *tbx2b* were disproportionately *hst*/+ (13/24) (Fig. 3.12E). Therefore, it appears that the reduced AV boundary expression of *tbx2b* in *hst* heterozygotes could be rescued to a level that resembles expression detected in wild-type embryos.

Contrary to knock-down of *Pdlim7*, overexpression is expected to shift Tbx5 out of the nucleus causing a reduction in *tbx2b* gene activation (Fig. 3.12J). To test this prediction, 75 pg of *pdlim7* mRNA was injected into wild-type embryos. Expression analysis of *tbx2b* at 48 hpf yielded three expression classes, normal (57%), reduced (41%), and a novel class with absent *tbx2b* expression (2%) (n=91). The significant number of embryos with reduced *tbx2b* AV boundary expression strongly suggested that overexpression of *Pdlim7* can misregulate Tbx5 transcriptional activity. Interestingly, 2% of injected embryos displayed no *tbx2b* expression in the heart, similar to *hst* homozygous embryos. To determine if the number of embryos with no *tbx2b* expression could be increased, we crossed wild-type adults to *hst*/+ heterozygotes and injected the resulting embryos with *pdlim7* mRNA. Again, detection of *tbx2b* at 48 hpf yielded three classes, normal (27%), reduced (59%), and absent (14%) (n=92; Fig. 3.12G). The overall number of *pdlim7* mRNA injected embryos with normal *tbx2b* AV boundary expression was less than predicted (Fig. 3.12G) and genotyping revealed embryos in this class were predominantly wild-type (18/25). Overexpression of *Pdlim7* is expected to increase the amount of actin-associated Tbx5 and thus result in reduced *tbx2b* expression (Fig. 3.12J). Following this prediction, wild-type embryos should display a lower level of *tbx2b* expression, resembling *hst* heterozygotes. Analysis of embryos with such reduced expression revealed that close to half

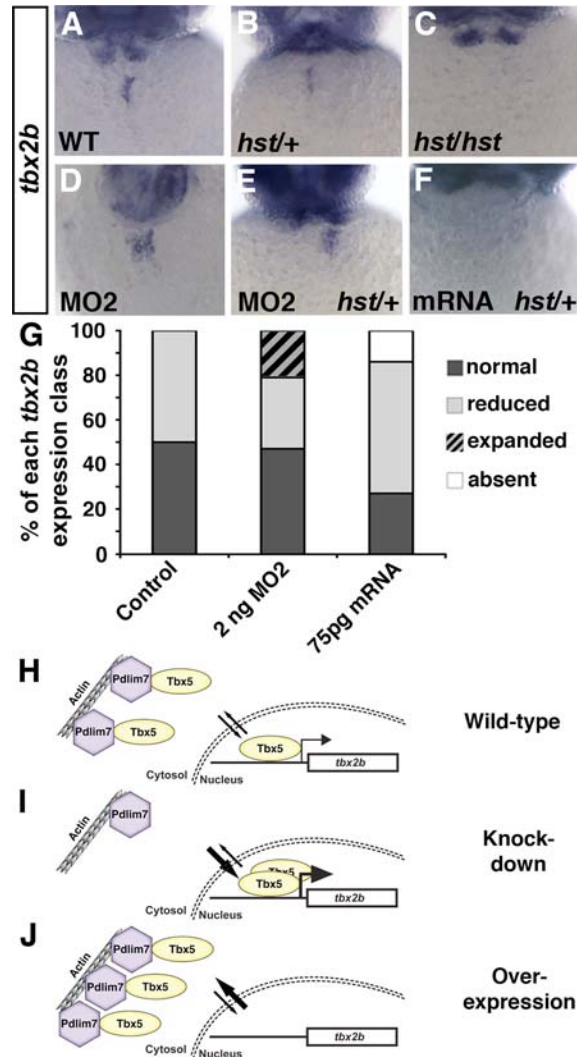


Figure 3.12: Pdlim7 and Tbx5 directly regulate *tbx2b* AV expression. (A) *In situ* hybridization of *tbx2b* in wild-type embryos at 48 hpf at the AV boundary. (B, C) Expression of *tbx2b* in *hst/+* and *hst/hst* embryos, respectively. (D) AV boundary expansion of *tbx2b* in MO2 morphant. (E) *tbx2b* expression in *hst/+* embryo injected with 2ng MO2 or (F) injected with 75 pg *pdlim7* mRNA. (G) Quantification of *tbx2b* expression levels in uninjected controls (n, 70), 2ng MO2 (n, 70), and 75 pg mRNA (n, 46). (H-J) Schematics illustrating the effect on the Tbx5 target gene *tbx2b* in wild-type (H), Pdlim7 MO (I), or *pdlim7* mRNA (J) injected embryos.

were in fact wild-type (22/51). Furthermore, our model predicts that *hst*/*+* embryos would be more sensitive to a loss of *tbx2b* expression as a result of Tbx5 relocalization (Fig. 3.12J). This notion was supported by the increased appearance of phenotypically *hst* homozygous embryos, with no *tbx2b* AV boundary expression (Fig. 3.12F). Genotyping revealed that most of these embryos were, however, heterozygous for the *hst* allele (7/11). Thus, overexpression of Pdlim7 in both wild-type and *hst*/*+* genetic backgrounds can effectively reduce *tbx2b* expression at the AV boundary to a degree that mRNA can no longer be detected by in situ hybridization. These results with protein overexpression along with the corresponding knock-down studies reveal a novel mechanism for the regulation of *tbx2b* gene expression via dynamic Pdlim7/Tbx5 protein complex formation at the boundary between the ventricle and atrium during zebrafish cardiac development.

Genotyping of *pdlim7* MO2 or mRNA injected embryos

<i>tbx2b</i> expression class	+/+	<i>hst</i> +/-
MO2 injection		
Normal	11/24	13/24
Reduced	3/22	19/22
Expanded	10/14	4/14
mRNA injection		
Normal	18/25	7/25
Reduced	22/51	29/51
Absent	4/11	7/11

Table 3.1

Discussion

Pdlim7 is required for cardiac morphogenesis

Morpholino knock-down of *Pdlim7* resulted in cardiac morphology defects which were first apparent at the heart tube stage. The heart tube displayed a more compact presumptive atrium, which then failed to loop, and further differentiation was arrested. We could not detect changes in the expression of early patterning and chamber identity genes, suggesting other causes for the string-like heart. It is well known that several activities must be orchestrated in a coordinated manner during heart morphogenesis including cell proliferation, differentiation, and migration (Harvey, 2002). Central to these physiological processes is actin remodeling, and misregulation of the actin cytoskeleton in *pdlim7* morphants may explain the improper heart shape. PDZ-LIM proteins, including *Pdlim7*, localize to actin filaments and alter actin dynamics (Guy et al. 1999; Vallenius et al. 2000; Nakagawa et al. 2000; Pashmforoush et al. 2001; Torrado et al. 2004; Krause et al. 2004; Camarata et al. 2006). Recent studies have shown that cell shape is also regulated during zebrafish heart development and contribute to the final shape and function of the organ (Beis et al. 2005; Auman et al. 2007; Rohr et al. 2008). For instance, atrial cells of the linear heart tube adopt an elongated shape, which is different from the more compact shape of cells within the ventricular domain (Rohr et al. 2008). *Pdlim7* is expressed in the heart tube predominantly in the presumptive atrium and in *pdlim7* morphants the atrial expression of *amhc* is more compact (Fig. 3.2 and 3.10). Therefore, it is conceivable that *Pdlim7* is regulating cell shape via its interaction with the actin cytoskeleton in atrial cells. Cell shape is also involved in the morphogenesis of heart looping and the constriction between the atrium and ventricle during boundary formation (Beis et al. 2005; Auman et al. 2007). Garrity et al. (2002) have shown that cardiac looping is disrupted in *hst* mutants and our data with *pdlim7* morphants reveal similar

outcomes (Fig. 3.5). The resemblance in looping defects between *pdlim7* and *tbx5* compromised zebrafish suggests that Tbx5 may also be involved in heart morphogenesis through regulation of the actin cytoskeleton. Indeed, gene expression analysis to identify Tbx5 target genes has uncovered cytoskeletal components as candidates, suggesting Tbx5 may indirectly regulate actin dynamics through a transcriptional mechanism (Mori et al. 2006; Plageman and Yutzey, 2006). However, direct regulation of the cytoskeleton is also conceivable since Tbx5 is localized to actin filaments in a complex with Pdlim7 (Camarata et al. 2006). The examination of Tbx5 forms engineered to localize exclusively to the nucleus or cytoplasm will help determine by what mechanism the protein may regulate cell shape during cardiogenesis.

Tbx5 and Pdlim7 specify atrio-ventricular identity

Specification of cells at the AV boundary begins around 36 hpf both morphologically and molecularly (Beis et al. 2005). Cells at this boundary adopt a cuboidal shape and express genes such as *versican*, *bmp4*, *notch1b*, and *tbx2b* (Walsh and Stanier, 2001; Chi et al. 2008). Our work has also demonstrated a high level of *tbx5* expression at the zebrafish heart AV boundary. MO knock-down of *pdlim7* resulted in misexpression of AV boundary genes including *tbx5*. Most genes were no longer restricted to the boundary in morphant embryos and appeared misregulated throughout the ventricle, similar to what has been observed in *tbx5 hst* mutant embryos (Fig. 3.11; Garrity et al. 2002). However, in contrast to a complete loss in *hst* embryos, *tbx2b* expression was expanded after *pdlim7* knock-down. This data along with the presence of a putative Tbx5 binding site in the promoter of *tbx2b* identified by Chi et al. (2008) strongly argues that this gene is a direct target of Tbx5. Our *in vitro* reporter assays had indicated that Pdlim7 represses Tbx5 nuclear function by sequestering the transcription factor to polymerized

actin (Camarata et al. 2006). The expansion of *tbx2b* expression in embryos with reduced *Pdlim7* supports these previous cell culture findings and would suggest that Tbx5 and *Pdlim7* proteins interact in AV boundary cells.

In the developing chicken heart, we have detected Tbx5/*Pdlim7* complexes colocalized along actin filaments at comparable locations, namely the atrio-ventricular cushion (AVC), but not in the chamber myocardium (Bimber et al. 2007). The AVC in avians and mammals, similar to the AV boundary in zebrafish, will give rise to chamber valves, contribute to the septum, and conduction system (Christoffels et al. 2004; Eisenberg and Markwald, 1995; Markwald et al. 1996; Bies et al. 2005; Scherz et al. 2008; De la Cruz et al. 1983; Davis et al. 2001; Rentschler et al. 2001). In this context it is of interest that *Tbx5*^{del/+} mice display ventricular myocardial but also septal and conduction system defects (Bruneau et al. 2001; Moskowitz et al. 2004). Furthermore, *Tbx5*^{del/del} animals fail to develop an AVC (Bruneau et al. 2001). The myocardial and AVC associated phenotypes in *Tbx5* mutant mice may be therefore due to separate nuclear and non-nuclear Tbx5 functions depending on *Pdlim7* interactions. Further analysis using genetically engineered mice with altered *pdlim7* levels will help to understand the role of Tbx5/*Pdlim7* interactions in cushion and valve development and these investigations are currently ongoing in our laboratory.

TBX5 regulation in congenital heart disease

In the present study we have provided evidence that both zebrafish Tbx5 and *Pdlim7* operate in one pathway and that their direct interaction is critical for AV boundary specification possibly by regulating the expression of *tbx2b* at the boundary. Our previous work in the chicken has shown that Tbx5 and *Pdlim7* colocalize outside the nucleus (Bimber et al. 2007). During development

Tbx5 can take on different subcellular distribution patterns, for instance in cells of the AVC. In relation to this, it is important to note that in mutant mouse models of *Tbx5* and *Pdlim7* AVC associated phenotypes have been observed (Bruneau et al. 2001; Krcmery and Simon, unpublished observations). In humans, mutations in *TBX5* cause Holt-Oram syndrome (HOS), a dominant congenital condition associated with a range of forelimb and cardiac malformations (Basson et al. 1997; Li et al. 1997). The varying cardiac phenotypes of HOS include conduction system abnormalities and mitral or tricuspid valve defects (Basson et al. 1997; Li et al. 1997; Bruneau 1999; Reamon-Buettner and Borlak, 2004; Borozdin et al. 2006). The valves are derived almost entirely from endocardial cushion cells located at the AV boundary (de Lange et al. 2004; Lincoln et al. 2004). The cushions are composed of extracellular matrix (ECM) including Versican and it has been shown that this ECM molecule is critical for cushion function and required for proper valve development (Henderson and Copp, 1998; Mjaatvedt et al. 1998). Following development, the valves undergo extensive remodeling to form a fully functioning mature valve at which point Versican becomes highly restricted in its expression (Kruithof et al. 2007). In the zebrafish, we find *versican* expression significantly misregulated in *pdlim7* morphant and *tbx5 hst* embryos suggesting that Versican function may be regulated by Pdlim7/Tbx5 interactions (Fig. 3.11; Garrity et al. 2002). Thus, the cushion and valve related phenotypes in HOS may not be exclusively due to *TBX5* haploinsufficiency, a 50% reduction in transcriptional activity, but may result from reduced Pdlim7 binding and actin cytoskeletal interaction. Forced misexpression of Tbx5 forms that cannot bind to Pdlim7 will clarify this point.

Along with Tbx5, additional T-box proteins, are expressed in and required for the development of the heart (Harvey, 2002; Isphording et al. 2004). The work presented here on

Tbx5 may serve as an initial model for understanding the functional role of Tbx protein nuclear/cytoplasmic shuttling in cardiac and more generally in vertebrate development and disease. The presence of an evolutionarily conserved nuclear export sequence and the detection of family members Tbx4, Brachyury, and T-brain outside the nucleus support this idea (unpublished observations; Kulisz and Simon, 2008; Krause et al. 2004; Inman and Downs, 2006; Hong and Hsueh, 2007). Here we present the first *in vivo* functional evidence that Tbx nuclear/cytoplasmic shuttling is required for organ formation and future work will determine if this mechanism is a common theme for T-box transcription factors that is critical for controlling function.

Chapter 4: Conclusions

Model of Pdim7/Tbx5 interactions

Tbx5 nuclear/cytoplasmic localization is dynamic

In vitro GST pulldown studies suggested the actin associated Pdim7 interacted with the transcription factor Tbx5 (Krause et al. 2004). I performed immunolocalization and co-immunoprecipitation assays using cultured cells and confirmed that Pdim7 binds to Tbx5 (Krause et al. 2004; Camarata et al. 2006). Of significance is that the interaction between Pdim7 and Tbx5 occurs outside of the nucleus. In a complex with Pdim7, Tbx5 is sequestered to filamentous actin and this change in localization can inhibit the ability of Tbx5 to activate reporter genes in cell culture and *in vivo* (Camarata et al. 2006; Camarata et al. 2008). I also performed FRAP assays and determined that the Pdim7/Tbx5 interaction is dynamic, which suggests that binding is regulated (Camarata et al. 2006).

Further evidence showing the dynamics of Pdim7/Tbx5 interaction has come from primary chicken epicardial explant cells. Epicardial explant cells from a stage 25HH chicken heart cultured on fibronectin can be maintained in culture in low serum conditions as an undifferentiated epithelial-like sheet. After the addition of serum, the explant cells can then be triggered to differentiate into epicardial-derived cells (EPDC) and express smooth muscle markers such as *calponin* (Dettman et al 1998; Lu et al. 2001; Morabito et al 2001). Both Pdim7 and Tbx5 are natively expressed in both undifferentiated epicardial cells and EPDCs (Camarata et al. 2006). Pdim7 localization is maintained along filamentous actin regardless of the differentiation state of the primary chicken epicardial explant cells. Tbx5 on the other hand, changes its localization when cells are triggered to differentiate. In the epithelial-like explant

cells, Tbx5 is predominantly localized to the nucleus. After the cells are triggered to differentiate into EPDCs, Tbx5 changes its localization to both nuclear and actin associated, where it complexes with Pdlim7 (Camarata et al. 2006). Therefore, Pdlim7/Tbx5 binding is controlled by extrinsic signals, despite the presence of both proteins within the same cell.

Differential localization for Tbx5 has also been observed in the developing chicken heart. Immunohistochemical studies has detected Tbx5 protein, similar to mRNA detection by *in situ* hybridization, in the developing left ventricle, left and right atrium, and atrioventricular cushion (AVC) (Bimber et al. 2007; Bruneau et al. 1999). Tbx5 is localized in the nucleus in the left ventricle and both atria. However, in the AVC, where Tbx5 protein is first detected at stage 29HH, it is localized both in the nucleus and cytoplasm (Bimber et al. 2007). Pdlim7 is also expressed in the AVC at this developmental time point and colocalizes with Tbx5 along actin filaments. By stage 33HH Tbx5 protein is downregulated while Pdlim7 expression is maintained. The brief window of expression of Tbx5 in the AVC and its interaction with Pdlim7 suggests strict regulation.

Regulation of Tbx5 shuttling and Pdlim7 interaction

How Tbx5 nuclear/cytoplasmic shuttling is regulated remains an unanswered question. The Simon laboratory has identified a functional nuclear export sequence in the T-domain of Tbx5 (Kulisz and Simon, 2008). The transcription factor utilizes this export sequence to interact with the CRM1 dependent nuclear export machinery. However, what triggers Tbx5 to interact with CRM1 or become exported is unclear. One possible mechanism that may regulate Tbx5 activity and subcellular localization is posttranslational modification, for example phosphorylation. The Tbx5 binding partner, Pdlim7, interacts with protein kinases, such as PKC

(Kuroda et al. 1996). Behaving as a scaffold, Pdlm7 binds to Tbx5 bringing it into close proximity with kinases that could then phosphorylate Tbx5 and modify its cellular behavior. Currently, no studies have been done to address this issue. Another posttranslational modification model is suggested by recent experimental evidence in the *C. elegans* pharynx, an organ that shares functional and molecular similarities with cardiac muscle of other species. The nematode genome contains a single *tbx-2* subfamily member, which is expressed in the pharynx and is required for its development (Miyahara et al. 2004; Roy Chowdhuri et al. 2006; Smith and Mango, 2007). Of significance, TBX-2 protein displays a filamentous localization in the cytoplasm of pharyngeal muscle cells (Smith and Mango, 2007). Furthermore, TBX-2 is sumoylated in the pharynx and the addition of SUMO groups is required for TBX-2 function (Roy Chowdhuri et al. 2006). In this context, it is interesting to note that protein sumoylation has an important impact on protein structure and function (reviewed in Geiss-Friedlander and Melchior, 2007). The addition of SUMO groups has been shown to control nuclear/cytoplasmic shuttling of other proteins (Salinas et al. 2004; Kindsmuller et al. 2007). Two consensus sites for sumoylation have been identified in *C. elegans* TBX-2 and they are present in chicken Tbx5 (Kulisz and Simon, unpublished observations). Chicken Tbx5 isolated from transfected cells and detected by Western blot, migrates at a higher molecular weight (75-80 kDa) compared to its predicted size (58 kDa) (Camarata et al. 2006; Camarata and Simon, unpublished observations). The difference between the predicted and actual size is close to the addition of two, 10 kDa SUMO proteins. Therefore, it is reasonable to consider the idea that Tbx5 is sumoylated and that the posttranslational modification regulates nuclear/cytoplasmic shuttling. Mutagenesis of the putative SUMO sites in Tbx5 and testing its ability to colocalize with Pdlm7 will determine if sumoylation in fact controls Tbx5 nuclear/cytoplasmic shuttling.

Posttranslational modifications may play a direct role on Tbx5 subcellular localization and activity. Another level of regulation may be more indirect and involve modifications or interactions with the binding partner, Pdlim7. Human PDLIM7 was first identified in a yeast two-hybrid screen as an interactor with the endocytic code of the insulin receptor (Insr) (Wu and Gill, 1994). Similar to the human protein, chicken Pdlim7 binds to the Insr in an insulin dependent manner (see Appendix B). Pdlim7 fails to bind to the Insr in the absence of insulin, however, after the addition of insulin the Insr becomes activated and interacts with Pdlim7. This fits with the concept that Pdlim7 interacts with the endocytic code of the Insr, which is thought to become accessible after ligand binding (Chang et al. 1993). *In vitro* GST pull-down analysis has shown that the Insr binds to the LIM3 domain of Pdlim7, the same domain that interacts with Tbx5. Competition assays of *E. coli* expressed recombinant protein shows that Tbx5 and the Insr cannot bind to LIM3 of Pdlim7 simultaneously (see Appendix B). Based upon this data, it is possible that insulin signaling may regulate the Pdlim7/Tbx5 interaction. In the presence of insulin, the Insr binds to Pdlim7, releasing Tbx5, which then can relocate to the nucleus.

Another intriguing mechanism of regulating Pdlim7/Tbx5 interactions is through mechanotransduction. Cells are greatly influenced by the stresses found in their environment and by their own contractile machinery (see review Bershadsky et al. 2003). One tissue in particular that is placed under tremendous stress during development is the beating heart (see reviews Bartman and Hove, 2005; Omens et al. 2007). In fact, fluid force and cardiomyocyte contraction is required for appropriate formation of the heart (Hove et al. 2003; Berduougo et al. 2003; Huang et al. 2003; Bartman et al. 2004). Forces are sensed by cells through sites of cell adhesion to either neighboring cells or the extracellular matrix (ECM). Contact with the ECM usually is through focal adhesions, which connects the cytoskeleton with the ECM and contains a

number of proteins such as integrins and α -actinin. It is at sites such as focal adhesions that cellular forces can be relayed into signal transduction pathways (Want et al. 1993; Juliano and Haskill 1993). Several PDZ-LIM proteins bind to α -actinin, for example Pdlim3, and are localized to focal adhesions (Faulkner et al. 1999; Zhou et al. 1999; Passier et al. 2000; Pashmforoush et al. 2001). Genetic knock-out of *Pdlim3* or the related family member *Ldb3* in the mouse leads to cardiomyopathy (Pashmforoush et al. 2001; Zhou et al. 2001). Furthermore, in *Ldb3* mutant mice, stressing the muscle results in progressive defects of muscle architecture (Zhou et al. 2001). It is possible that PDZ-LIM proteins participate in the signal transduction of forces generated by cell contacts or changes in the cytoskeleton. Both *Ldb3* and *Pdlim7* bind to PKC, a signaling molecule which has been shown to have increased activity due to mechanical stress (Kumuro et al. 1991; Sadoshima and Izumo, 1993). In relation to *Tbx5* function, it could be hypothesized that *Tbx5* is localized to focal adhesions via *Pdlim7* binding. The protein complex at the focal adhesion could interpret changes in mechanical force on the cell and initiate a signaling cascade, possibly involving PKC. Activated PKC could then phosphorylate *Tbx5*, *Pdlim7*, or both and thereby alter the binding of the two proteins. Such a mechanism would allow a fast response to changes in cell shape by allowing *Tbx5* to 'sense' the cellular environment and activate appropriate target genes. Interestingly, *ANF* and *connexin-43*, both targets of *Tbx5* (Bruneau et al. 2001), are upregulated by differential external loads in cultured cardiomyocytes (Gopalan et al. 2003). Therefore, the presence of *Tbx5* along actin filaments via *Pdlim7* may not just simply be a passive mechanism to regulate gene transcription, but a more active pathway of responding to extracellular stimuli.

Taking all of the data together, a comprehensive novel regulatory model of *Pdlim7/Tbx5* interaction can be proposed (Figure 4.1). *Tbx5* can dynamically shuttle in and out of the nucleus

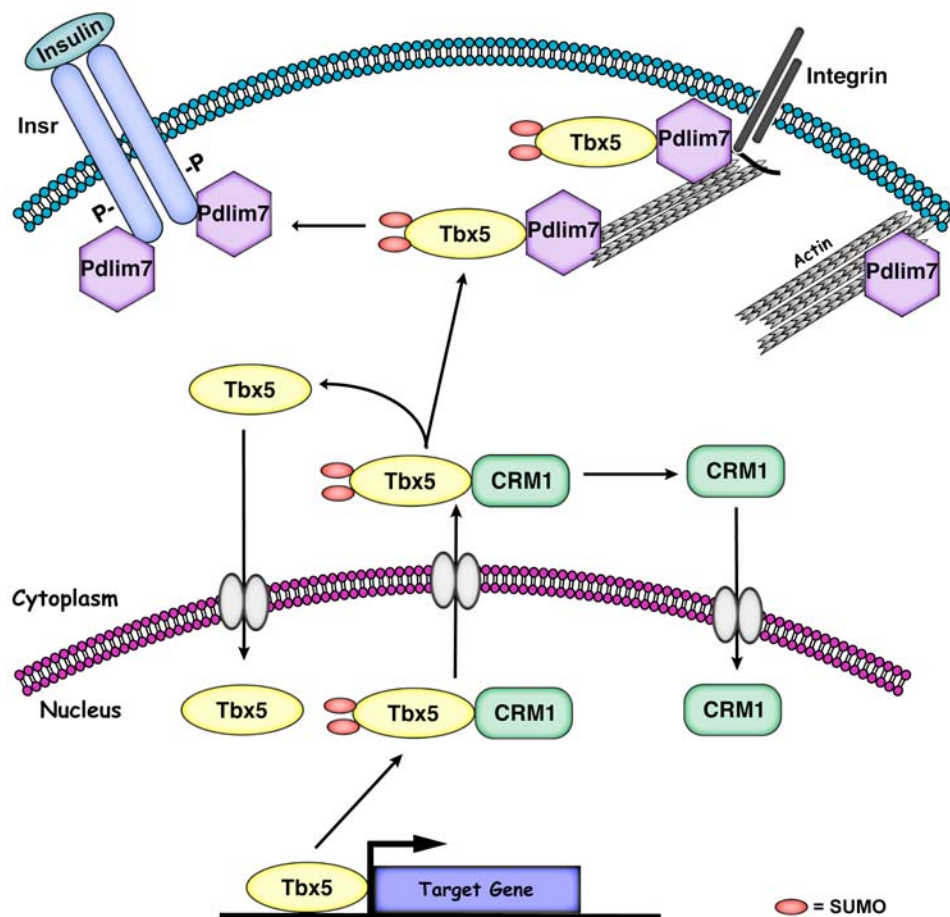


Figure 4.1: Comprehensive model of Pdlim7/Tbx5 interaction and regulation. Tbx5 dynamically shuttles between the nucleus and Pdlim7 along actin filaments. Export of Tbx5 from the nucleus is dependent on binding to the CRM1 export protein. Sumoylation may provide a signal to allow Tbx5 export. Once outside the nucleus, Tbx5 can then bind to Pdlim7. However, the Pdlim7/Tbx5 interaction may be regulated by the availability of the LIM3 domain of Pdlim7. Pdlim7 can interact with the insulin receptor (Insr) via LIM3 once the receptor has bound ligand. Both Tbx5 and Insr cannot bind to Pdlim7 simultaneously, providing a mechanism for release and nuclear localization of Tbx5. In addition, the localization of Pdlim7/Tbx5 complex to focal adhesions could allow Tbx5 to respond to changes in the cytoskeleton depending on cellular behavior, including migration or differentiation. Adapted from Kulisz and Simon, 2008.

utilizing the CRM1 export pathway. The activation of Tbx5 to shuttle may be dependent on posttranslational modifications, for example, sumoylation. Once outside the nucleus, Tbx5 can interact with Pdlim7. However, Pdlim7 must be available for interaction, which is dependent on signaling events such as activated Insr. In addition, Tbx5 cytoplasmic localization and activity may be controlled by mechanotransduction mechanisms, especially within the developing heart. It will be intriguing to further link upstream signaling events, like insulin signaling or ECM interactions, with downstream Tbx5 function.

T-box proteins are nuclear/cytoplasmic shuttling proteins

Tbx5 is a member of the T-box transcription factor family, which is thought to have strict functional roles within the nucleus. Supporting this idea, Tbx5 contains two functional nuclear localization sequences (NLS) (Collavoli et al. 2003; Zaragoza et al. 2004). However, the discovery that Tbx5 binds to Pdlim7 and relocalizes outside the nucleus along actin filaments, both in cell culture and *in vivo*, prompted a new question (Krause et al. 2004; Camarata et al. 2006; Bimber et al. 2007). How might Tbx5 exit the nucleus? Analysis of the Tbx5 amino acid sequence detected a consensus CRM1 dependent nuclear export sequence (NES) in the T-domain (Kulisz and Simon, 2008). The NES motif in Tbx5 is required for binding to the export shuttling protein CRM1 and interaction in the cytoplasm with Pdlim7. Therefore, the nuclear/cytoplasmic shuttling of Tbx5 requires both NLS and NES motifs.

The highly related T-box protein, Tbx4, also colocalizes with Pdlim7 along actin filaments and contains an identical NES motif that is found in Tbx5 (Krause et al. 2004; Kulisz and Simon, 2008). Tbx5 and Tbx4 are part of the Tbx2/3/4/5 subfamily of T-box genes, which evolved from a single primordial gene that underwent unequal crossing-over and gene

duplication events (Agulnik et al. 1996; Simon, 1999). Analysis of the related Tbx2 and Tbx3 protein sequences revealed that these members also contain a CRM1 pathway consensus NES (Kulisz and Simon, 2008). The presence of the NES motif is not only limited to the Tbx2/3/4/5 subfamily but is found in all T-box proteins in mouse, chicken, and human. In fact, diverged NES motifs can be identified within the T-domain of all T-box proteins from human all the way down to the simplest metazoan, the sponge. It appears, then, that the ability to shuttle in and out of the nucleus is a function adopted at the earliest stage of T-box evolution and retained in all T-box proteins found in animals. Evidence supporting the idea that all T-box proteins are shuttling proteins comes from reports of cytoplasmic localized family members (see Table 4.1).

Cytoplasmic localization has been observed for mouse Brachyury (Inman and Downs, 2006) and Tbr-1 (Hong and Hsueh, 2007), zebrafish Eomesodermin (Bruce et al. 2003), *C. elegans* Tbx-2 (Miyahara et al. 2004; Smith and Mango, 2007), and Brachyury in the sponge (Adell and Muller 2005). Further study of T-box protein family members will undoubtedly identify additional examples of cytoplasmic localization.

PDZ-LIM proteins facilitate cytoplasmic retention of nuclear factors

Several members of the PDZ-LIM family are expressed in muscle cells and are involved in cellular cytoarchitecture (Kadrmas and Beckerle, 2004). For example, Ldb3 associates with the actin cytoskeleton and its function is required for maintenance of the Z-line in striated muscle (Faulkner et al. 1999; Zhou et al. 1999; Passier et al. 2000). However, several PDZ-LIM genes are also expressed in non-muscle tissues. *Pdlim5*, in both human and rat, is expressed in the brain, lung, liver, and kidney (Kuroda et al. 1996; Ueki et al. 1999). Chicken *Pdlim7*, in addition to skeletal and cardiac muscle expression, is detected in endocardial-derived tissue and in the

Reported cytoplasmic T-box proteins	
In cell culture	<i>In vivo</i>
Tbx4, chicken ¹	Brachyury, mouse ⁴ , sponge ⁵
Tbx5, chicken ¹	Tbx5, chicken ⁶
Tbx5a, zebrafish ²	Eomesodermin, zebrafish ⁷
Tbx5b, zebrafish ³	Tbr-1, mouse ⁸ , sea urchin ⁹
	Tbx-2, <i>C. elegans</i> ^{10,11}

1, Krause et al. 2004

2, Camarata et al. 2008

3, Camarata and Simon unpublished observations

4, Inman and Downs 2006

5, Adell and Muller 2005

6, Bimber et al. 2007

7, Bruce et al. 2003

8, Hong and Hsueh 2007

9, Fuchikami et al. 2002

10, Miyahara et al. 2004

11, Smith and Mango 2007

Table 4.1

lung (Bimber et al. 2007; Camarata and Simon, unpublished observations). Furthermore, mouse *Pdlim7* is expressed in developing bone (Boden et al. 1998). The wide range of cell types that express PDZ-LIM proteins suggests they have other functions besides muscle associated actin regulation.

One additional function, which appears common to several PDZ-LIM proteins, is localizing nuclear factors to the cytoplasm. The single LIM domain containing *Pdlim1*, from mouse, interacts with *Clik1* kinase via its LIM domain (Vallenius and Makela, 2002). When transfected alone, *Clik1* kinase localizes strictly to the nucleus. However, in the presence of *Pdlim1*, *Clik1* localizes to the nucleus, but is also targeted to actin stress fibers where it colocalizes with *Pdlim1* (Vallenius and Makela, 2002). Similarly, human PDLIM5 interacts with the basic helix-loop-helix repressor *Id2* via LIM domain 1 (Lasorella and Lavarone, 2006). *Id2* is a member of the *Id* protein family, which act as inhibitors of differentiation and normally reside in the nucleus (Norton et al. 1998; Norton, 2000). When PDLIM5 and *Id2* are coexpressed in transfected cells or in neuroblastoma cells that natively express both factors, *Id2* is relocalized to the cytoplasm (Lasorella and Lavarone, 2006). The removal of *Id2* from the nucleus by PDLIM5 relieves the transcriptional inhibition of *Id2*. The mechanism of regulating *Id2* subcellular localization appears to play a role in cell proliferation and cell cycle progression.

I have identified a similar function for chicken and zebrafish *Pdlim7*. *Pdlim7* relocalizes both *Tbx5* and *Tbx4* to actin filaments (Krause et al. 2004; Camarata et al. 2006). In the case of *Tbx5*, relocalization outside the nucleus by *Pdlim7* effects gene activation both in reporter assays and in the developing zebrafish heart (Camarata et al. 2006; Camarata et al. 2008). Altering the level of *Tbx5* in the nucleus also has a significant effect on the morphology of the developing heart in zebrafish (Camarata et al. 2008).

Combining the notion that all T-box proteins are shuttling factors and that PDZ-LIM proteins can sequester nuclear proteins outside the nucleus, an exciting question can be raised. Is there a stronger connection between two seemingly unrelated gene families? The interaction between PDZ-LIM and T-box proteins may not be limited to *Pdlim7* and *Tbx4* or *Tbx5*. For example, *C. elegans* *Tbx-2* is expressed in a filamentous pattern in pharyngeal muscle cells, a cell type that also expresses the primordial PDZ-LIM gene *Alp-1* (Smith and Mango, 2007; McKeown et al. 2006). T-box genes are also expressed in a wide variety of tissues and are found in the earliest metazoans (Naiche et al. 2005). PDZ-LIM genes are expressed in several of the same tissue as T-box genes and while the combination of the PDZ and LIM domain appear to be a vertebrate invention, the LIM domain is found in all eukaryotes (Kadrmas and Beckerle, 2004). Therefore, the potential exists that these two gene families and interactions between respective encoded proteins co-evolved from single cell eukaryotes to multi-organ mammals. Identification of additional interactions between T-box and PDZ-LIM proteins will help solidify the structural and functional relationship between these previously unrelated gene families.

References

- Adell, T. and Muller, W. E.** (2005). Expression pattern of the Brachyury and Tbx2 homologues from the sponge *Suberites domuncula*. *Biol Cell* **97**, 641-50.
- Agarwal, P., Wylie, J. N., Galceran, J., Arkhitko, O., Li, C., Deng, C., Grosschedl, R. and Bruneau, B. G.** (2003). Tbx5 is essential for forelimb bud initiation following patterning of the limb field in the mouse embryo. *Development* **130**, 623-33.
- Agulnik, S. I., Garvey, N., Hancock, S., Ruvinsky, I., Chapman, D. L., Agulnik, I., Bollag, R., Papaioannou, V. and Silver, L. M.** (1996). Evolution of mouse T-box genes by tandem duplication and cluster dispersion. *Genetics* **144**, 249-54.
- Ahn, D. G., Kourakis, M. J., Rohde, L. A., Silver, L. M. and Ho, R. K.** (2002). T-box gene *tbx5* is essential for formation of the pectoral limb bud. *Nature* **417**, 754-8.
- Auman, H. J., Coleman, H., Riley, H. E., Olale, F., Tsai, H. J. and Yelon, D.** (2007). Functional modulation of cardiac form through regionally confined cell shape changes. *PLoS Biol* **5**, e53.
- Bach, I.** (2000). The LIM domain: regulation by association. *Mech Dev* **91**, 5-17.
- Barres, R., Gremeaux, T., Gual, P., Gonzalez, T., Gugenheim, J., Tran, A., Le Marchand-Brustel, Y. and Tanti, J. F.** (2006). Enigma interacts with adaptor protein with PH and SH2 domains to control insulin-induced actin cytoskeleton remodeling and glucose transporter 4 translocation. *Mol Endocrinol* **20**, 2864-75.
- Bartman, T. and Hove, J.** (2005). Mechanics and function in heart morphogenesis. *Dev Dyn* **233**, 373-81.
- Bartman, T., Walsh, E. C., Wen, K. K., McKane, M., Ren, J., Alexander, J., Rubenstein, P. A. and Stainier, D. Y.** (2004). Early myocardial function affects endocardial cushion development in zebrafish. *PLoS Biol* **2**, E129.
- Basson, C. T., Bachinsky, D. R., Lin, R. C., Levi, T., Elkins, J. A., Soultz, J., Grayzel, D., Kroumpouzou, E., Traill, T. A., Leblanc-Straceski, J. et al.** (1997). Mutations in human TBX5 [corrected] cause limb and cardiac malformation in Holt-Oram syndrome. *Nat Genet* **15**, 30-5.
- Begemann, G. and Ingham, P. W.** (2000). Developmental regulation of Tbx5 in zebrafish embryogenesis. *Mech Dev* **90**, 299-304.
- Beis, D., Bartman, T., Jin, S. W., Scott, I. C., D'Amico, L. A., Ober, E. A., Verkade, H., Frantsve, J., Field, H. A., Wehman, A. et al.** (2005). Genetic and cellular analyses of zebrafish

atrioventricular cushion and valve development. *Development* **132**, 4193-204.

Berdougo, E., Coleman, H., Lee, D. H., Stainier, D. Y. and Yelon, D. (2003). Mutation of weak atrium/atrial myosin heavy chain disrupts atrial function and influences ventricular morphogenesis in zebrafish. *Development* **130**, 6121-9.

Bershadsky, A. D., Balaban, N. Q. and Geiger, B. (2003). Adhesion-dependent cell mechanosensitivity. *Annu Rev Cell Dev Biol* **19**, 677-95.

Bimber, B., Dettman, R. W. and Simon, H. G. (2007). Differential regulation of Tbx5 protein expression and sub-cellular localization during heart development. *Dev Biol* **302**, 230-42.

Boden, S. D., Liu, Y., Hair, G. A., Helms, J. A., Hu, D., Racine, M., Nanes, M. S. and Titus, L. (1998). LMP-1, a LIM-domain protein, mediates BMP-6 effects on bone formation. *Endocrinology* **139**, 5125-34.

Bongers, E. M., Duijf, P. H., van Beersum, S. E., Schoots, J., Van Kampen, A., Burckhardt, A., Hamel, B. C., Losan, F., Hoefsloot, L. H., Yntema, H. G. et al. (2004). Mutations in the human TBX4 gene cause small patella syndrome. *Am J Hum Genet* **74**, 1239-48.

Borozdin, W., Bravo Ferrer Acosta, A. M., Bamshad, M. J., Botzenhart, E. M., Froster, U. G., Lemke, J., Schinzel, A., Spranger, S., McGaughan, J., Wand, D. et al. (2006). Expanding the spectrum of TBX5 mutations in Holt-Oram syndrome: detection of two intragenic deletions by quantitative real time PCR, and report of eight novel point mutations. *Hum Mutat* **27**, 975-6.

Bruce, A. E., Howley, C., Zhou, Y., Vickers, S. L., Silver, L. M., King, M. L. and Ho, R. K. (2003). The maternally expressed zebrafish T-box gene eomesodermin regulates organizer formation. *Development* **130**, 5503-17.

Bruneau, B. G., Logan, M., Davis, N., Levi, T., Tabin, C. J., Seidman, J. G. and Seidman, C. E. (1999). Chamber-specific cardiac expression of Tbx5 and heart defects in Holt-Oram syndrome. *Dev Biol* **211**, 100-8.

Bruneau, B. G., Nemer, G., Schmitt, J. P., Charron, F., Robitaille, L., Caron, S., Conner, D. A., Gessler, M., Nemer, M., Seidman, C. E. et al. (2001). A murine model of Holt-Oram syndrome defines roles of the T-box transcription factor Tbx5 in cardiogenesis and disease. *Cell* **106**, 709-21.

Cai, C. L., Zhou, W., Yang, L., Bu, L., Qyang, Y., Zhang, X., Li, X., Rosenfeld, M. G., Chen, J. and Evans, S. (2005). T-box genes coordinate regional rates of proliferation and regional specification during cardiogenesis. *Development* **132**, 2475-87.

Camarata, T., Bimber, B., Kulisz, A., Chew, T. L., Yeung, J. and Simon, H. G. (2006). LMP4 regulates Tbx5 protein subcellular localization and activity. *J Cell Biol* **174**, 339-48.

- Camarata, T., Topczewski, J. and Simon, H. G.** (2008). Pdlim7 (LMP4) regulation of Tbx5 specifies zebrafish atrio-ventricular boundary formation.
- Chang, C. P., Lazar, C. S., Walsh, B. J., Komuro, M., Collawn, J. F., Kuhn, L. A., Tainer, J. A., Trowbridge, I. S., Farquhar, M. G., Rosenfeld, M. G. et al.** (1993). Ligand-induced internalization of the epidermal growth factor receptor is mediated by multiple endocytic codes analogous to the tyrosine motif found in constitutively internalized receptors. *J Biol Chem* **268**, 19312-20.
- Chapman, D. L., Garvey, N., Hancock, S., Alexiou, M., Agulnik, S. I., Gibson-Brown, J. J., Cebra-Thomas, J., Bollag, R. J., Silver, L. M. and Papaioannou, V. E.** (1996). Expression of the T-box family genes, Tbx1-Tbx5, during early mouse development. *Dev Dyn* **206**, 379-90.
- Chen, J. N. and Fishman, M. C.** (1996). Zebrafish tinman homolog demarcates the heart field and initiates myocardial differentiation. *Development* **122**, 3809-16.
- Chi, N. C., Shaw, R. M., De Val, S., Kang, G., Jan, L. Y., Black, B. L. and Stainier, D. Y.** (2008). Foxn4 directly regulates tbx2b expression and atrioventricular canal formation. *Genes Dev* **22**, 734-9.
- Christoffels, V. M., Burch, J. B. and Moorman, A. F.** (2004). Architectural plan for the heart: early patterning and delineation of the chambers and the nodes. *Trends Cardiovasc Med* **14**, 301-7.
- Collavoli, A., Hatcher, C. J., He, J., Okin, D., Deo, R. and Basson, C. T.** (2003). TBX5 nuclear localization is mediated by dual cooperative intramolecular signals. *J Mol Cell Cardiol* **35**, 1191-5.
- Compton, L. A., Potash, D. A., Mundell, N. A. and Barnett, J. V.** (2006). Transforming growth factor-beta induces loss of epithelial character and smooth muscle cell differentiation in epicardial cells. *Dev Dyn* **235**, 82-93.
- Dahmane, N., Lee, J., Robins, P., Heller, P. and Ruiz i Altaba, A.** (1997). Activation of the transcription factor Gli1 and the Sonic hedgehog signalling pathway in skin tumours. *Nature* **389**, 876-81.
- Davis, D. L., Edwards, A. V., Juraszek, A. L., Phelps, A., Wessels, A. and Burch, J. B.** (2001). A GATA-6 gene heart-region-specific enhancer provides a novel means to mark and probe a discrete component of the mouse cardiac conduction system. *Mech Dev* **108**, 105-19.
- Dawid, I. B., Breen, J. J. and Toyama, R.** (1998). LIM domains: multiple roles as adapters and functional modifiers in protein interactions. *Trends Genet* **14**, 156-62.
- De la Cruz, M. V., Gimenez-Ribotta, M., Saravalli, O. and Cayre, R.** (1983). The contribution of the inferior endocardial cushion of the atrioventricular canal to cardiac septation

and to the development of the atrioventricular valves: study in the chick embryo. *Am J Anat* **166**, 63-72.

de Lange, F. J., Moorman, A. F., Anderson, R. H., Manner, J., Soufan, A. T., de Gier-de Vries, C., Schneider, M. D., Webb, S., van den Hoff, M. J. and Christoffels, V. M. (2004). Lineage and morphogenetic analysis of the cardiac valves. *Circ Res* **95**, 645-54.

Dettman, R. W., Denetclaw, W., Jr., Ordahl, C. P. and Bristow, J. (1998). Common epicardial origin of coronary vascular smooth muscle, perivascular fibroblasts, and intermyocardial fibroblasts in the avian heart. *Dev Biol* **193**, 169-81.

DiGeorge, A. M. and Harley, R. D. (1965). The association of aniridia, Wilms's tumor, and genital abnormalities. *Trans Am Ophthalmol Soc* **63**, 64-9.

Durick, K., Gill, G. N. and Taylor, S. S. (1998). Shc and Enigma are both required for mitogenic signaling by Ret/ptc2. *Mol Cell Biol* **18**, 2298-308.

Durick, K., Wu, R. Y., Gill, G. N. and Taylor, S. S. (1996). Mitogenic signaling by Ret/ptc2 requires association with enigma via a LIM domain. *J Biol Chem* **271**, 12691-4.

Eisenberg, L. M. and Markwald, R. R. (1995). Molecular regulation of atrioventricular valvuloseptal morphogenesis. *Circ Res* **77**, 1-6.

Fanning, A. S. and Anderson, J. M. (1999). PDZ domains: fundamental building blocks in the organization of protein complexes at the plasma membrane. *J Clin Invest* **103**, 767-72.

Faulkner, G., Pallavicini, A., Formentin, E., Comelli, A., Ievolella, C., Trevisan, S., Bortoletto, G., Scannapieco, P., Salamon, M., Mouly, V. et al. (1999). ZASP: a new Z-band alternatively spliced PDZ-motif protein. *J Cell Biol* **146**, 465-75.

Franco, D., Lamers, W. H. and Moorman, A. F. (1998). Patterns of expression in the developing myocardium: towards a morphologically integrated transcriptional model. *Cardiovasc Res* **38**, 25-53.

Fuchikami, T., Mitsunaga-Nakatsubo, K., Amemiya, S., Hosomi, T., Watanabe, T., Kurokawa, D., Kataoka, M., Harada, Y., Satoh, N., Kusunoki, S. et al. (2002). T-brain homologue (HpTb) is involved in the archenteron induction signals of micromere descendant cells in the sea urchin embryo. *Development* **129**, 5205-16.

Garg, V., Kathiriya, I. S., Barnes, R., Schluterman, M. K., King, I. N., Butler, C. A., Rothrock, C. R., Eapen, R. S., Hirayama-Yamada, K., Joo, K. et al. (2003). GATA4 mutations cause human congenital heart defects and reveal an interaction with TBX5. *Nature* **424**, 443-7.

Garrity, D. M., Childs, S. and Fishman, M. C. (2002). The heartstrings mutation in zebrafish

causes heart/fin Tbx5 deficiency syndrome. *Development* **129**, 4635-45.

Geiss-Friedlander, R. and Melchior, F. (2007). Concepts in sumoylation: a decade on. *Nat Rev Mol Cell Biol* **8**, 947-56.

Gibson-Brown, J. J., Agulnik, S. I., Chapman, D. L., Alexiou, M., Garvey, N., Silver, L. M. and Papaioannou, V. E. (1996). Evidence of a role for T-box genes in the evolution of limb morphogenesis and the specification of forelimb/hindlimb identity. *Mech Dev* **56**, 93-101.

Gibson-Brown, J. J., Agulnik, S. I., Silver, L. M., Niswander, L. and Papaioannou, V. E. (1998). Involvement of T-box genes Tbx2-Tbx5 in vertebrate limb specification and development. *Development* **125**, 2499-509.

Glickman, N. S. and Yelon, D. (2002). Cardiac development in zebrafish: coordination of form and function. *Semin Cell Dev Biol* **13**, 507-13.

Goldberg, R., Motzkin, B., Marion, R., Scambler, P. J. and Shprintzen, R. J. (1993). Velo-cardio-facial syndrome: a review of 120 patients. *Am J Med Genet* **45**, 313-9.

Gong, W., Gottlieb, S., Collins, J., Blescia, A., Dietz, H., Goldmuntz, E., McDonald-McGinn, D. M., Zackai, E. H., Emanuel, B. S., Driscoll, D. A. et al. (2001). Mutation analysis of TBX1 in non-deleted patients with features of DGS/VCFS or isolated cardiovascular defects. *J Med Genet* **38**, E45.

Gopalan, S. M., Flaim, C., Bhatia, S. N., Hoshijima, M., Knoell, R., Chien, K. R., Omens, J. H. and McCulloch, A. D. (2003). Anisotropic stretch-induced hypertrophy in neonatal ventricular myocytes micropatterned on deformable elastomers. *Biotechnol Bioeng* **81**, 578-87.

Guy, P. M., Kenny, D. A. and Gill, G. N. (1999). The PDZ domain of the LIM protein enigma binds to beta-tropomyosin. *Mol Biol Cell* **10**, 1973-84.

Hamburger, V. and Hamilton, H. L. (1951). A series of normal stages in the development of the chick embryo. *Journal of Morphology* **88**, 49-92.

Harrelson, Z., Kelly, R. G., Goldin, S. N., Gibson-Brown, J. J., Bollag, R. J., Silver, L. M. and Papaioannou, V. E. (2004). Tbx2 is essential for patterning the atrioventricular canal and for morphogenesis of the outflow tract during heart development. *Development* **131**, 5041-52.

Harris, B. Z. and Lim, W. A. (2001). Mechanism and role of PDZ domains in signaling complex assembly. *J Cell Sci* **114**, 3219-31.

Harvey, R. P. (2002). Patterning the vertebrate heart. *Nat Rev Genet* **3**, 544-56.

Hasson, P., Del Buono, J. and Logan, M. P. (2007). Tbx5 is dispensable for forelimb outgrowth. *Development* **134**, 85-92.

- Hatcher, C. J. and Basson, C. T.** (2001). Getting the T-box dose right. *Nat Med* **7**, 1185-6.
- Hatcher, C. J., Kim, M. S., Mah, C. S., Goldstein, M. M., Wong, B., Mikawa, T. and Basson, C. T.** (2001). TBX5 transcription factor regulates cell proliferation during cardiogenesis. *Dev Biol* **230**, 177-88.
- Henderson, D. J. and Copp, A. J.** (1998). Versican expression is associated with chamber specification, septation, and valvulogenesis in the developing mouse heart. *Circ Res* **83**, 523-32.
- Herrmann, B. G., Labeit, S., Poustka, A., King, T. R. and Lehrach, H.** (1990). Cloning of the T gene required in mesoderm formation in the mouse. *Nature* **343**, 617-22.
- Hiroi, Y., Kudoh, S., Monzen, K., Ikeda, Y., Yazaki, Y., Nagai, R. and Komuro, I.** (2001). Tbx5 associates with Nkx2-5 and synergistically promotes cardiomyocyte differentiation. *Nat Genet* **28**, 276-80.
- Hong, C. J. and Hsueh, Y. P.** (2007). Cytoplasmic distribution of T-box transcription factor Tbr-1 in adult rodent brain. *J Chem Neuroanat* **33**, 124-30.
- Hoogaars, W. M., Barnett, P., Moorman, A. F. and Christoffels, V. M.** (2007). T-box factors determine cardiac design. *Cell Mol Life Sci* **64**, 646-60.
- Hove, J. R., Koster, R. W., Forouhar, A. S., Acevedo-Bolton, G., Fraser, S. E. and Gharib, M.** (2003). Intracardiac fluid forces are an essential epigenetic factor for embryonic cardiogenesis. *Nature* **421**, 172-7.
- Hurlstone, A. F., Haramis, A. P., Wienholds, E., Begthel, H., Korving, J., Van Eeden, F., Cuppen, E., Zivkovic, D., Plasterk, R. H. and Clevers, H.** (2003). The Wnt/beta-catenin pathway regulates cardiac valve formation. *Nature* **425**, 633-7.
- Hyatt, T. M. and Ekker, S. C.** (1999). Vectors and techniques for ectopic gene expression in zebrafish. *Methods Cell Biol* **59**, 117-26.
- Inman, K. E. and Downs, K. M.** (2006). Localization of Brachyury (T) in embryonic and extraembryonic tissues during mouse gastrulation. *Gene Expr Patterns* **6**, 783-93.
- Isaac, A., Rodriguez-Esteban, C., Ryan, A., Altabef, M., Tsukui, T., Patel, K., Tickle, C. and Izpisua-Belmonte, J. C.** (1998). Tbx genes and limb identity in chick embryo development. *Development* **125**, 1867-75.
- Isphording, D., Leylek, A. M., Yeung, J., Mischel, A. and Simon, H. G.** (2004). T-box genes and congenital heart/limb malformations. *Clin Genet* **66**, 253-64.
- Juliano, R. L. and Haskill, S.** (1993). Signal transduction from the extracellular matrix. *J Cell*

Biol **120**, 577-85.

Kadmas, J. L. and Beckerle, M. C. (2004). The LIM domain: from the cytoskeleton to the nucleus. *Nat Rev Mol Cell Biol* **5**, 920-31.

Karin, M. and Ben-Neriah, Y. (2000). Phosphorylation meets ubiquitination: the control of NF- κ B activity. *Annu Rev Immunol* **18**, 621-63.

Khan, P., Linkhart, B. and Simon, H. G. (2002). Different regulation of T-box genes Tbx4 and Tbx5 during limb development and limb regeneration. *Dev Biol* **250**, 383-92.

Kimmel, C. B., Ballard, W. W., Kimmel, S. R., Ullmann, B. and Schilling, T. F. (1995). Stages of embryonic development of the zebrafish. *Dev Dyn* **203**, 253-310.

Kirby, M. (2007). Cardiac Development. Oxford: Oxford University Press.

Kispert, A. and Hermann, B. G. (1993). The Brachyury gene encodes a novel DNA binding protein. *EMBO J* **12**, 4898-9.

Kogerman, P., Grimm, T., Kogerman, L., Krause, D., Uden, A. B., Sandstedt, B., Toftgard, R. and Zaphiropoulos, P. G. (1999). Mammalian suppressor-of-fused modulates nuclear-cytoplasmic shuttling of Gli-1. *Nat Cell Biol* **1**, 312-9.

Komuro, I., Katoh, Y., Kaida, T., Shibasaki, Y., Kurabayashi, M., Hoh, E., Takaku, F. and Yazaki, Y. (1991). Mechanical loading stimulates cell hypertrophy and specific gene expression in cultured rat cardiac myocytes. Possible role of protein kinase C activation. *J Biol Chem* **266**, 1265-8.

Krause, A., Zacharias, W., Camarata, T., Linkhart, B., Law, E., Lischke, A., Miljan, E. and Simon, H. G. (2004). Tbx5 and Tbx4 transcription factors interact with a new chicken PDZ-LIM protein in limb and heart development. *Dev Biol* **273**, 106-20.

Kruithof, B. P., Krawitz, S. A. and Gaussin, V. (2007). Atrioventricular valve development during late embryonic and postnatal stages involves condensation and extracellular matrix remodeling. *Dev Biol* **302**, 208-17.

Kulisz, A. and Simon, H. G. (2008). An evolutionarily conserved nuclear export signal facilitates cytoplasmic localization of the Tbx5 transcription factor. *Mol Cell Biol* **28**, 1553-64.

Kuroda, S., Tokunaga, C., Kiyohara, Y., Higuchi, O., Konishi, H., Mizuno, K., Gill, G. N. and Kikkawa, U. (1996). Protein-protein interaction of zinc finger LIM domains with protein kinase C. *J Biol Chem* **271**, 31029-32.

Lasorella, A. and Iavarone, A. (2006). The protein ENH is a cytoplasmic sequestration factor for Id2 in normal and tumor cells from the nervous system. *Proc Natl Acad Sci U S A* **103**, 4976-

81.

Levin, M. (2005). Left-right asymmetry in embryonic development: a comprehensive review. *Mech Dev* **122**, 3-25.

Li, Q. Y., Newbury-Ecob, R. A., Terrett, J. A., Wilson, D. I., Curtis, A. R., Yi, C. H., Gebuhr, T., Bullen, P. J., Robson, S. C., Strachan, T. et al. (1997). Holt-Oram syndrome is caused by mutations in TBX5, a member of the Brachyury (T) gene family. *Nat Genet* **15**, 21-9.

Liberatore, C. M., Searcy-Schrick, R. D. and Yutzey, K. E. (2000). Ventricular expression of *tbx5* inhibits normal heart chamber development. *Dev Biol* **223**, 169-80.

Lincoln, J., Alfieri, C. M. and Yutzey, K. E. (2004). Development of heart valve leaflets and supporting apparatus in chicken and mouse embryos. *Dev Dyn* **230**, 239-50.

Lindsay, E. A., Vitelli, F., Su, H., Morishima, M., Huynh, T., Pramparo, T., Jurecic, V., Ogunrinu, G., Sutherland, H. F., Scambler, P. J. et al. (2001). *Tbx1* haploinsufficiency in the DiGeorge syndrome region causes aortic arch defects in mice. *Nature* **410**, 97-101.

Lints, T. J., Parsons, L. M., Hartley, L., Lyons, I. and Harvey, R. P. (1993). *Nkx-2.5*: a novel murine homeobox gene expressed in early heart progenitor cells and their myogenic descendants. *Development* **119**, 969.

Logan, M., Simon, H. G. and Tabin, C. (1998). Differential regulation of T-box and homeobox transcription factors suggests roles in controlling chick limb-type identity. *Development* **125**, 2825-35.

Logan, M. and Tabin, C. (1998). Targeted gene misexpression in chick limb buds using avian replication-competent retroviruses. *Methods* **14**, 407-20.

Lu, J., Landerholm, T. E., Wei, J. S., Dong, X. R., Wu, S. P., Liu, X., Nagata, K., Inagaki, M. and Majesky, M. W. (2001). Coronary smooth muscle differentiation from proepicardial cells requires rhoA-mediated actin reorganization and p160 rho-kinase activity. *Dev Biol* **240**, 404-18.

Markwald, R., Eisenberg, C., Eisenberg, L., Trusk, T. and Sugi, Y. (1996). Epithelial-mesenchymal transformations in early avian heart development. *Acta Anat (Basel)* **156**, 173-86.

McKeown, C. R., Han, H. F. and Beckerle, M. C. (2006). Molecular characterization of the *Caenorhabditis elegans* ALP/Enigma gene *alp-1*. *Dev Dyn* **235**, 530-8.

Merscher, S., Funke, B., Epstein, J. A., Heyer, J., Puech, A., Lu, M. M., Xavier, R. J., Demay, M. B., Russell, R. G., Factor, S. et al. (2001). TBX1 is responsible for cardiovascular defects in velo-cardio-facial/DiGeorge syndrome. *Cell* **104**, 619-29.

- Minguillon, C., Del Buono, J. and Logan, M. P.** (2005). Tbx5 and Tbx4 are not sufficient to determine limb-specific morphologies but have common roles in initiating limb outgrowth. *Dev Cell* **8**, 75-84.
- Miyahara, K., Suzuki, N., Ishihara, T., Tsuchiya, E. and Katsura, I.** (2004). TBX2/TBX3 transcriptional factor homologue controls olfactory adaptation in *Caenorhabditis elegans*. *J Neurobiol* **58**, 392-402.
- Mjaatvedt, C. H., Yamamura, H., Capehart, A. A., Turner, D. and Markwald, R. R.** (1998). The *Cspg2* gene, disrupted in the *hdf* mutant, is required for right cardiac chamber and endocardial cushion formation. *Dev Biol* **202**, 56-66.
- Morabito, C. J., Dettman, R. W., Kattan, J., Collier, J. M. and Bristow, J.** (2001). Positive and negative regulation of epicardial-mesenchymal transformation during avian heart development. *Dev Biol* **234**, 204-15.
- Mori, A. D., Zhu, Y., Vahora, I., Nieman, B., Koshiba-Takeuchi, K., Davidson, L., Pizard, A., Seidman, J. G., Seidman, C. E., Chen, X. J. et al.** (2006). Tbx5-dependent rheostatic control of cardiac gene expression and morphogenesis. *Dev Biol* **297**, 566-86.
- Moskowitz, I. P., Pizard, A., Patel, V. V., Bruneau, B. G., Kim, J. B., Kupersmidt, S., Roden, D., Berul, C. I., Seidman, C. E. and Seidman, J. G.** (2004). The T-Box transcription factor Tbx5 is required for the patterning and maturation of the murine cardiac conduction system. *Development* **131**, 4107-16.
- Naiche, L. A., Harrelson, Z., Kelly, R. G. and Papaioannou, V. E.** (2005). T-box genes in vertebrate development. *Annu Rev Genet* **39**, 219-39.
- Naiche, L. A. and Papaioannou, V. E.** (2003). Loss of Tbx4 blocks hindlimb development and affects vascularization and fusion of the allantois. *Development* **130**, 2681-93.
- Naiche, L. A. and Papaioannou, V. E.** (2007). Tbx4 is not required for hindlimb identity or post-bud hindlimb outgrowth. *Development* **134**, 93-103.
- Nakagawa, N., Hoshijima, M., Oyasu, M., Saito, N., Tanizawa, K. and Kuroda, S.** (2000). ENH, containing PDZ and LIM domains, heart/skeletal muscle-specific protein, associates with cytoskeletal proteins through the PDZ domain. *Biochem Biophys Res Commun* **272**, 505-12.
- Ng, J. K., Kawakami, Y., Buscher, D., Raya, A., Itoh, T., Koth, C. M., Rodriguez Esteban, C., Rodriguez-Leon, J., Garrity, D. M., Fishman, M. C. et al.** (2002). The limb identity gene Tbx5 promotes limb initiation by interacting with Wnt2b and Fgf10. *Development* **129**, 5161-70.
- Norton, J. D.** (2000). ID helix-loop-helix proteins in cell growth, differentiation and tumorigenesis. *J Cell Sci* **113** (Pt 22), 3897-905.

- Norton, J. D., Deed, R. W., Craggs, G. and Sablitzky, F.** (1998). Id helix-loop-helix proteins in cell growth and differentiation. *Trends Cell Biol* **8**, 58-65.
- Ohuchi, H., Takeuchi, J., Yoshioka, H., Ishimaru, Y., Ogura, K., Takahashi, N., Ogura, T. and Noji, S.** (1998). Correlation of wing-leg identity in ectopic FGF-induced chimeric limbs with the differential expression of chick Tbx5 and Tbx4. *Development* **125**, 51-60.
- Omens, J. H., McCulloch, A. D. and Lorenzen-Schmidt, I.** (2007). Mechanotransduction in Cardiac Remodeling and Heart Failure. In *Cardiac Mechanotransduction*, (ed. M. Weckstrom and P. Tavi), pp. 78-92. New York: Springer.
- Pashmforoush, M., Pomies, P., Peterson, K. L., Kubalak, S., Ross, J., Jr., Hefti, A., Aebi, U., Beckerle, M. C. and Chien, K. R.** (2001). Adult mice deficient in actinin-associated LIM-domain protein reveal a developmental pathway for right ventricular cardiomyopathy. *Nat Med* **7**, 591-7.
- Passier, R., Richardson, J. A. and Olson, E. N.** (2000). Oracle, a novel PDZ-LIM domain protein expressed in heart and skeletal muscle. *Mech Dev* **92**, 277-84.
- Plageman, T. F., Jr. and Yutzey, K. E.** (2006). Microarray analysis of Tbx5-induced genes expressed in the developing heart. *Dev Dyn* **235**, 2868-80.
- Pomies, P., Macalma, T. and Beckerle, M. C.** (1999). Purification and characterization of an alpha-actinin-binding PDZ-LIM protein that is up-regulated during muscle differentiation. *J Biol Chem* **274**, 29242-50.
- Ponting, C. P., Phillips, C., Davies, K. E. and Blake, D. J.** (1997). PDZ domains: targeting signalling molecules to sub-membranous sites. *Bioessays* **19**, 469-79.
- Rallis, C., Bruneau, B. G., Del Buono, J., Seidman, C. E., Seidman, J. G., Nissim, S., Tabin, C. J. and Logan, M. P.** (2003). Tbx5 is required for forelimb bud formation and continued outgrowth. *Development* **130**, 2741-51.
- Reamon-Buettner, S. M. and Borlak, J.** (2004). TBX5 mutations in non-Holt-Oram syndrome (HOS) malformed hearts. *Hum Mutat* **24**, 104.
- Reiter, J. F., Alexander, J., Rodaway, A., Yelon, D., Patient, R., Holder, N. and Stainier, D. Y.** (1999). Gata5 is required for the development of the heart and endoderm in zebrafish. *Genes Dev* **13**, 2983-95.
- Rentschler, S., Vaidya, D. M., Tamaddon, H., Degenhardt, K., Sassoon, D., Morley, G. E., Jalife, J. and Fishman, G. I.** (2001). Visualization and functional characterization of the developing murine cardiac conduction system. *Development* **128**, 1785-92.
- Rodriguez-Esteban, C., Tsukui, T., Yonei, S., Magallon, J., Tamura, K. and Izpisua**

Belmonte, J. C. (1999). The T-box genes Tbx4 and Tbx5 regulate limb outgrowth and identity. *Nature* **398**, 814-8.

Rohr, S., Otten, C. and Abdelilah-Seyfried, S. (2008). Asymmetric involution of the myocardial field drives heart tube formation in zebrafish. *Circ Res* **102**, e12-9.

Roy Chowdhuri, S., Crum, T., Woollard, A., Aslam, S. and Okkema, P. G. (2006). The T-box factor TBX-2 and the SUMO conjugating enzyme UBC-9 are required for ABA-derived pharyngeal muscle in *C. elegans*. *Dev Biol* **295**, 664-77.

Ruiz i Altaba, A. (1999). Gli proteins encode context-dependent positive and negative functions: implications for development and disease. *Development* **126**, 3205-16.

Sadoshima, J. and Izumo, S. (1993). Mechanical stretch rapidly activates multiple signal transduction pathways in cardiac myocytes: potential involvement of an autocrine/paracrine mechanism. *EMBO J* **12**, 1681-92.

Salinas, S., Briancon-Marjollet, A., Bossis, G., Lopez, M. A., Piechaczyk, M., Jariel-Encontre, I., Debant, A. and Hipkind, R. A. (2004). SUMOylation regulates nucleocytoplasmic shuttling of Elk-1. *J Cell Biol* **165**, 767-73.

Salinas, S., Briancon-Marjollet, A., Bossis, G., Lopez, M. A., Piechaczyk, M., Jariel-Encontre, I., Debant, A. and Hipkind, R. A. (2004). SUMOylation regulates nucleocytoplasmic shuttling of Elk-1. *J Cell Biol* **165**, 767-73.

Sangadala, S., Boden, S. D., Viggswarapu, M., Liu, Y. and Titus, L. (2006). LIM mineralization protein-1 potentiates bone morphogenetic protein responsiveness via a novel interaction with Smurf1 resulting in decreased ubiquitination of Smads. *J Biol Chem* **281**, 17212-9.

Scherz, P. J., Huisken, J., Sahai-Hernandez, P. and Stainier, D. Y. (2008). High-speed imaging of developing heart valves reveals interplay of morphogenesis and function. *Development* **135**, 1179-87.

Schmeichel, K. L. and Beckerle, M. C. (1994). The LIM domain is a modular protein-binding interface. *Cell* **79**, 211-9.

Schultheiss, T. M., Xydas, S. and Lassar, A. B. (1995). Induction of avian cardiac myogenesis by anterior endoderm. *Development* **121**, 4203-14.

Shprintzen, R. J., Goldberg, R. B., Lewin, M. L., Sidoti, E. J., Berkman, M. D., Argamaso, R. V. and Young, D. (1978). A new syndrome involving cleft palate, cardiac anomalies, typical facies, and learning disabilities: velo-cardio-facial syndrome. *Cleft Palate J* **15**, 56-62.

Simon, H. (1999). T-box genes and the formation of vertebrate forelimb- and hindlimb specific

pattern. *Cell Tissue Res* **296**, 57-66.

Smith, P. A. and Mango, S. E. (2007). Role of T-box gene *tbx-2* for anterior foregut muscle development in *C. elegans*. *Dev Biol* **302**, 25-39.

Stainier, D. Y. (2001). Zebrafish genetics and vertebrate heart formation. *Nat Rev Genet* **2**, 39-48.

Stainier, D. Y. and Fishman, M. C. (1992). Patterning the zebrafish heart tube: acquisition of anteroposterior polarity. *Dev Biol* **153**, 91-101.

Stennard, F. A. and Harvey, R. P. (2005). T-box transcription factors and their roles in regulatory hierarchies in the developing heart. *Development* **132**, 4897-910.

Takeuchi, J. K., Koshiba-Takeuchi, K., Matsumoto, K., Vogel-Hopker, A., Naitoh-Matsuo, M., Ogura, K., Takahashi, N., Yasuda, K. and Ogura, T. (1999). *Tbx5* and *Tbx4* genes determine the wing/leg identity of limb buds. *Nature* **398**, 810-4.

Takeuchi, J. K., Koshiba-Takeuchi, K., Suzuki, T., Kamimura, M., Ogura, K. and Ogura, T. (2003). *Tbx5* and *Tbx4* trigger limb initiation through activation of the Wnt/Fgf signaling cascade. *Development* **130**, 2729-39.

Thisse, C. and Thisse, B. (1999). Antivin, a novel and divergent member of the TGFbeta superfamily, negatively regulates mesoderm induction. *Development* **126**, 229-40.

Thisse, C., Thisse, B., Schilling, T. F. and Postlethwait, J. H. (1993). Structure of the zebrafish *snail1* gene and its expression in wild-type, spadetail and no tail mutant embryos. *Development* **119**, 1203-15.

Torrado, M., Senatorov, V. V., Trivedi, R., Fariss, R. N. and Tomarev, S. I. (2004). Pdlim2, a novel PDZ-LIM domain protein, interacts with alpha-actinins and filamin A. *Invest Ophthalmol Vis Sci* **45**, 3955-63.

Towbin, H., Staehelin, T. and Gordon, J. (1979). Electrophoretic transfer of proteins from polyacrylamide gels to nitrocellulose sheets: procedure and some applications. *Proc Natl Acad Sci U S A* **76**, 4350-4.

Ueki, N., Seki, N., Yano, K., Masuho, Y., Saito, T. and Muramatsu, M. (1999). Isolation, tissue expression, and chromosomal assignment of a human LIM protein gene, showing homology to rat enigma homologue (ENH). *J Hum Genet* **44**, 256-60.

Vallenius, T., Luukko, K. and Makela, T. P. (2000). CLP-36 PDZ-LIM protein associates with nonmuscle alpha-actinin-1 and alpha-actinin-4. *J Biol Chem* **275**, 11100-5.

Vallenius, T. and Makela, T. P. (2002). Clik1: a novel kinase targeted to actin stress fibers by

the CLP-36 PDZ-LIM protein. *J Cell Sci* **115**, 2067-73.

van der Meer, D. L., Marques, I. J., Leito, J. T., Besser, J., Bakkers, J., Schoonheere, E. and Bagowski, C. P. (2006). Zebrafish cypher is important for somite formation and heart development. *Dev Biol* **299**, 356-72.

Vatta, M., Mohapatra, B., Jimenez, S., Sanchez, X., Faulkner, G., Perles, Z., Sinagra, G., Lin, J. H., Vu, T. M., Zhou, Q. et al. (2003). Mutations in Cypher/ZASP in patients with dilated cardiomyopathy and left ventricular non-compaction. *J Am Coll Cardiol* **42**, 2014-27.

Vaughan, C. J. and Basson, C. T. (2000). Molecular determinants of atrial and ventricular septal defects and patent ductus arteriosus. *Am J Med Genet* **97**, 304-9.

Walsh, E. C. and Stainier, D. Y. (2001). UDP-glucose dehydrogenase required for cardiac valve formation in zebrafish. *Science* **293**, 1670-3.

Wang, N., Butler, J. P. and Ingber, D. E. (1993). Mechanotransduction across the cell surface and through the cytoskeleton. *Science* **260**, 1124-7.

Westin, J. and Lardelli, M. (1997). Three novel Notch genes in zebrafish: implications for vertebrate Notch gene evolution and function. *Development Genes and Evolution* **207**, 51-63.

Wu, R., Durick, K., Songyang, Z., Cantley, L. C., Taylor, S. S. and Gill, G. N. (1996). Specificity of LIM domain interactions with receptor tyrosine kinases. *J Biol Chem* **271**, 15934-41.

Wu, R. Y. and Gill, G. N. (1994). LIM domain recognition of a tyrosine-containing tight turn. *J Biol Chem* **269**, 25085-90.

Xia, H., Winokur, S. T., Kuo, W. L., Altherr, M. R. and Brecht, D. S. (1997). Actinin-associated LIM protein: identification of a domain interaction between PDZ and spectrin-like repeat motifs. *J Cell Biol* **139**, 507-15.

Yelon, D., Horne, S. A. and Stainier, D. Y. (1999). Restricted expression of cardiac myosin genes reveals regulated aspects of heart tube assembly in zebrafish. *Dev Biol* **214**, 23-37.

Zaragoza, M. V., Lewis, L. E., Sun, G., Wang, E., Li, L., Said-Salman, I., Feucht, L. and Huang, T. (2004). Identification of the TBX5 transactivating domain and the nuclear localization signal. *Gene* **330**, 9-18.

Zhou, Q., Chu, P. H., Huang, C., Cheng, C. F., Martone, M. E., Knoll, G., Shelton, G. D., Evans, S. and Chen, J. (2001). Ablation of Cypher, a PDZ-LIM domain Z-line protein, causes a severe form of congenital myopathy. *J Cell Biol* **155**, 605-12.

Zhou, Q., Ruiz-Lozano, P., Martone, M. E. and Chen, J. (1999). Cypher, a striated muscle-

restricted PDZ and LIM domain-containing protein, binds to alpha-actinin-2 and protein kinase
C. J Biol Chem **274**, 19807-13.

Appendix A: Materials and Methods

Pdlim7 antibody design

To identify a region in chicken Pdlim7 suitable for specific antibody production, a multi-protein sequence alignment (MacVector 7.0 software) was conducted to compare two closely related subclasses of PDZ-LIM proteins: Pdlim7 and Pdlim5 proteins. Pdlim7 protein sequences from human (Wu and Gill, 1994), rat (Boden et al. 1998), and chicken (Krause et al. 2004) were compared to Pdlim5 sequences from human (Ueki et al. 1999), mouse (Nakagawa et al. 2000) and rat (Kuroda et al. 1996). From this alignment a 17-amino acid peptide (DPAFAERYAPDKTSTVL) was identified that was conserved in Pdlim7 proteins but not in Pdlim5 proteins. In addition, based on its predicted antigenicity and hydrophobicity the peptide was suitable to elicit a good immune response. Peptide synthesis and rabbit immunization was performed by Invitrogen custom antibody services. The final rabbit antiserum was affinity purified on antigen peptide conjugated columns and tested for specificity (see Fig. 2.1).

Cell culture, transfection and reporter assays

COS-7 cells were grown in DMEM supplemented with 10% FBS, 1% L-glutamine, and penicillin/streptomycin. Cells were transfected using Lipofectamine 2000 according to manufacturer's instructions (Invitrogen). For reporter assays, COS-7 cells were grown in 12-well culture dishes and transfected with 300ng of reporter plasmid, 10ng of *Renilla* luciferase plasmid, and expression plasmids as described. The total amount of DNA transfected was held constant at 1 μ g. Transfected cells were cultured for 36 hours before lysis. Luciferase activity was measured using the Dual-Luciferase assay system (Promega) and samples were read on a

Lumat LB 9501 (Berthold). All reporter assays were carried out in triplicate and the collected data from two independent experiments was normalized to the *Renilla* luciferase activity.

For zebrafish expression constructs, COS-7 cells were transfected by electroporation with 4 μ g of each expression construct along with 12 μ g of sheered salmon sperm DNA and 0.1M HEPES buffer using a Bio-Rad Gene Pulsar set to 960 μ FD, 200 Ohms, and 0.25 volts. Cells were allowed to recover for 24 hours before fixation and immunofluorescence detection.

Immunofluorescence and imaging

COS-7 cells were fixed in 4% paraformaldehyde (PFA) followed by 1% Triton X-100 extraction and sequential incubation with primary and secondary antibodies in 1% BSA. Affinity purified rabbit polyclonal anti-Pdlim7 (Fig. 2.1) and anti-Tbx5 (Khan et al., 2002) were used at a 1:500 dilution. Anti-HA (HA-7; Sigma), anti-myc (9E10; Sigma), and anti-calponin (CP-93; Sigma) were diluted 1:500. Primary antibodies were detected using Alexa 488 and Alexa 546 conjugated secondary antibodies at 1:500 dilutions (Molecular Probes). Filamentous actin was detected using Alexa Fluor 488 Phalloidin or Alexa Fluor 633 Phalloidin (Molecular Probes). Nuclei were stained using DAPI (Roche). For double staining experiments, LMP4 antibodies were directly coupled to rhodamine using the EZ-Label protein labeling kit (Pierce Biotechnology). Confocal microscopy was performed using a Zeiss 510 META system (Zeiss, Inc) equipped with a Plan Apochromat 63x/1.4 Oil DIC lens. Images were processed in Adobe Photoshop CS2.

Zebrafish embryos were stained as described by Yelon et al., (1999). Briefly, embryos were fixed for one hour at room temperature in 1% paraformaldehyde followed by incubation for one hour in blocking buffer (10% sheep serum, 2mg/ml BSA, 0.2% saponin, in PBS). Embryos

were next incubated with MF20 (developed by D. A. Fischman), S46 (developed by F. E. Stockdale) or F59 (developed by F. E. Stockdale) monoclonal antibodies, which were obtained from the Developmental Studies Hybridoma Bank (University of Iowa). Primary antibodies were diluted in 0.2% saponin/PBS and embryos incubated for one hour. Following a brief wash in 0.2% saponin/PBS, primary antibodies were detected using AlexaFluor 568 IgG_{2b} and AlexaFluor 488 IgG₁ (Invitrogen). Stained embryos were imaged on a Leica DMI 6000 inverted microscope (Leica Microsystems Inc.) using ImagePro software (Media Cybernetics).

FRAP

Cells were transfected with EGFP-Tbx5 and either LMP4-myc or HcRed-LMP4. Cells were grown on uncoated No. 1.0 glass bottom 35mm culture dishes (MatTek Corporation) containing DMEM/10%FBS and equilibrated on a 37°C heated stage fitted on Zeiss LSM 510 laser scanning microscope. EGFP photobleaching was performed using the 488nm laser line at 100% intensity. Changes in pixel intensity were analyzed using OpenLab 4.0 (Improvision). Whole cell bleaching of a co-transfected cell was performed to determine onset of EGFP protein synthesis and maturation.

Co-immunoprecipitation

For co-immunoprecipitation, COS-7 cells were grown to 80-90% confluency in 10cm culture dishes and transfected with 10µg of Tbx5-HA and 14µg of Pdlim7-myc. After 24 hours cells were lysed in lysis buffer (25mM Tris-HCl, 100mM NaF, 10mM EGTA, 5mM EDTA, 250mM NaCl, 1% NP-40, 50mM Na₄P₂O₇·H₂O, 0.5% DOC, and 10mM ATP) containing protease inhibitors (P8340, Sigma). Lysates were incubated on ice for 20 min. followed by centrifugation

at 52,000 rpm for 10 min. The supernatant was incubated with anti-myc conjugated Protein A sepharose beads (Amersham Biosciences) overnight at 4°C. The sepharose beads were washed in lysis buffer and the bound protein was eluted with SDS buffer and boiling, then analyzed by immunoblotting with the indicated antibodies. Protein lysates were subjected SDS-PAGE (Laemmli, 1970) and immunoblot analysis (Towbin et al. 1979) with the indicated antibodies.

Actin disruption

COS-7 cells were treated with 2 μ M latrunculin A (Sigma) or 5 μ M cytochalasin D (Sigma) for 60 minutes at 37°C. Parallel cultures were treated with the vehicle DMSO as a control. After treatment, the cells were immediately prepared for cell imaging or biochemical analysis.

Expression constructs

Full-length chicken Tbx5 was cloned into a pcDNA3.1 expression vector containing a HA tetramer tag. Tbx5 was additionally placed as an N-terminal fusion into a modified pEGFP-C1 vector suitable for the Gateway recombination system (Invitrogen). Full-length chicken Pdlim7 was cloned into pcDNA3.1 containing a myc C-terminal tag. Chicken Pdlim7 was also recombined as an N-terminal fusion into a modified HcRed-C1 expression vector suitable for the Gateway recombination system (Invitrogen). Mouse Pdlim5 (Genbank Accession: DQ177283) fragments were cloned from mouse brain cDNA into the pGEX-6P-2 prokaryotic expression vector to create an N-terminal GST fusion protein (Amersham Biosciences). The PDZ/proline-rich fragment covers amino acids 1-414 and was amplified using forward primer 5'ACGCGTCGACCATGAGCAACTACAGTGTGTCATTG-3' and reverse primer 5'-ATAGTTTAGCGGCCGCTCACATGGGGGTCCGCTTGCCCG-3'. The Pdlim5 LIM 1/2/3

fragment covers amino acids 412-593 and was amplified using forward primer 5'-ACGCGTCGACCATGTGTGCCCACTGCAACCA-3' and reverse primer 5'-ATAGTTTAGCGGCCGCTGATTTTCAAAAATTCACAGAATGAG-3'. Recombinant mouse Pdlim5 peptides were expressed in BL21 *E. coli* as described (Krause et al. 2004).

Zebrafish

Wild-type (TU and EK/TU) and *heartstrings*^{m21} (*hst*, Garrity et al. 2002) stocks were maintained at 28.5°C. Embryos were cultured in 0.0045% phenyl thiourea in Danieau buffer to inhibit pigmentation and were staged according to Kimmel et al. (1995).

Identification of zebrafish pdlim7

For the identification of zebrafish *pdlim7*, BLAST searches were performed using the chicken LMP4/Pdlim7 amino acid sequence as a query (Krause et al. 2004). An I.M.A.G.E. Consortium clone was identified (6788497 LLAM) and obtained from Open Biosystems. In parallel, *pdlim7* cDNA was directly isolated by RT-PCR from 48-hour embryos using forward primer 5' CACGGATCCAAGGAGGCCATGAATATATATTGTGTA 3' containing a 5' BamHI site and reverse primer 5' CACCTCGAGTCACAGCGGGGAGAACGCATGG 3' containing a 3' XhoI site. The *pdlim7* PCR fragment was cloned into pBluescriptII KS+ (Stratagene) and sequenced. Using MacVector software (MacVector Inc.) the predicted amino acid sequence of the zebrafish Pdlim7 was used to compile a phylogenetic tree with other PDZ-LIM family proteins from various species (see Fig. 3.1).

In situ hybridization

Whole mount *in situ* hybridization was performed as previously described (Thisse et al. 1993) using an Insitu Pro VSi robot (Intavis). *tbx5* cDNA was isolated by RT-PCR from 24-hour embryos using forward primer 5' ACGAATTCCTAGTGCTGGAAGTTGATACGAGC 3' containing a 5' EcoRI site and reverse primer 5'

CACCTCGAGGCATGTTAGCTGGCTTCGTTCA 3' containing a 3' XhoI site. The *tbx5* cDNA was subsequently cloned into pBluescriptII KS+ for antisense probe production.

Additional probes used were *cmlc2*, *vmhc*, (Yelon et al. 1999), *amhc* (Berdougo et al. 2003), *tbx2b* (Chi et al. 2008), *bmp4* (Walsh and Stainier 2001), *versican* (Thisse and Thisse 1999), and *notch1b* (Westin and Lardelli 1997). Embryos were imaged on a Leica MZ16 stereomicroscope fitted with a Leica DFC490 color camera using ImagePro MC (MediaCybernetics) software. Images were processed using Photoshop CS2 (Adobe Systems, Inc.).

Morpholino and RNA injection

Antisense morpholino (MO) oligonucleotides were obtained from Gene Tools (Gene Tools, LLC). Two MOs, MO1 and MO2, were designed against *pdlim7*. MO1 ATATTCATGGCCTCCTTCTGGTCGG was targeted to inhibit translation, while MO2 CCAAAATGGAGGACACTTACCCTGG was targeted to the splice donor site of exon 2 (see Figs. 3.3 and 3.4). MOs were resuspended in sterile water and the concentration determined according to manufacturer's instructions. Embryos were injected at the one-cell stage and fixed at appropriate time points.

mRNA was synthesized using the mMessage mMachine kit (Ambion). To test the specificity of MO1, the 5' UTR and PDZ domain of *Pdlim7* was cloned into a Gateway

(Invitrogen) compatible pCS2 vector with a membrane localized GFP C-terminal fusion tag. For *pdlim7* overexpression, the entire open reading frame was cloned into a Gateway compatible pT3TS vector (Hyatt and Ekker, 1999).

Genotyping

Single embryos were genotyped after *in situ* hybridization by extracting genomic DNA using a NucleoSpin Tissue kit (Clontech) following manufacturer's instructions. A 322 bp genomic fragment surrounding the *hst*^{m21} mutation site was PCR amplified using forward primer 5' TGGAGCCATAAGCTCACAGTATTCC 3' and reverse primer 5' AGTGTGTGGTTTAGAGGCACACC 3'. PCR fragments were sequenced for detection of the *hst* mutation (Garrity et al. 2002).

Online supplemental material

Representative time-lapse video of cytoplasmic FRAP (Fig. 2.8A) and nuclear FRAP (Fig. 2.8B) are provided online in supplemental Movie 1 and Movie 2, respectively; available at <http://www.jcb.org/cgi/content/full/jcb.200511109/DC1>.

Appendix B: Pdlim7 interacts with the Insulin receptor

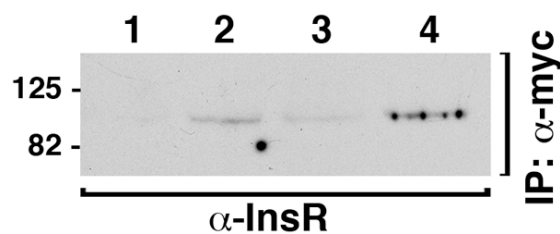


Figure Appendix B.1: Pdlim7 binds to the active form of Insulin receptor. HEK293 cells were transfected chicken myc-Pdlim7 and human insulin receptor (Insr) (lanes 3 and 4). Cells were grown overnight in low serum conditions (0.5%). 24 hours after transfection cells were treated with low serum media or media containing 100 nM insulin for 10 min. The cells were then lysated and the lysates were immunoprecipitated with the anti-myc antibody. The resulting immunoprecipitates were analyzed by Western blot using an Insr specific antibody. Lanes 1-2: cells transfected only with myc-Pdlim7 without (lane 1) or with (lane 2) insulin stimulation. A weak band is detected in lane 2 showing the natively expressed Insr can be precipitated with Pdlim7. Lanes 3-4: cells transfected with both myc-Pdlim7 and the Insr without (lane 3) or with (lane 4) insulin stimulation. A strong band is detected in lane 4 showing the interaction between Pdlim7 and the Insr. No significant interaction is observed in lanes 1 or 3 suggesting insulin binding to the receptor is necessary for Pdlim7/Insr interactions.

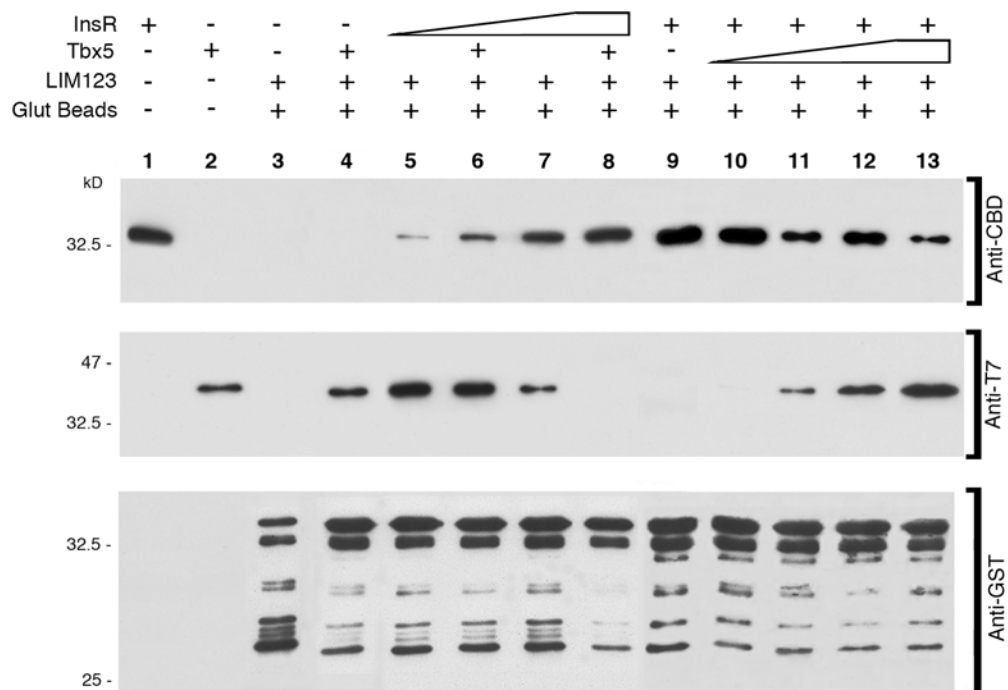


Figure Appendix B.2: Tbx5 and InsR compete for binding chicken Pdlim7. For co-precipitations, *E. coli* lysates containing CBD-tagged InsR, T7/His₆-tagged Tbx5, and GST-LIM123 proteins were used. Lanes 1-3 are CBD-InsR, T7/His₆-Tbx5, and GST-LIM123 positive controls, respectively. Lanes 4 and 9 are Tbx5 and InsR, respectively, incubated alone with GST-LIM123. Lanes 5-8 contain constant input of GST-LIM123 and T7/His₆-Tbx5 with CBD-InsR titrated in at 1:50, 1:20, 1:10, and 1:5 ratios, respectively. Lanes 10-13 contain constant input of GST-LIM123 and CBD-InsR with T7/His₆-Tbx5 titrated in at 1:50, 1:20, 1:10, and 1:5 ratios, respectively. Anti-T7 antibodies were used to detect T7/His₆-Tbx5, anti-CBD antibodies to detect CBD-InsR, and anti-GST antibodies were used to detect GST-LIM123. Cloning of Pdlim7 GST-LIM123 and T7/His₆-Tbx5 described in Krause et al. 2004. The endocytic code of human insulin receptor is described in Wu and Gill 1994. This work was done in collaboration with Pauli Undessor.

Appendix C: Pdim7 Δ LIM3 behaves as a dominant-negative

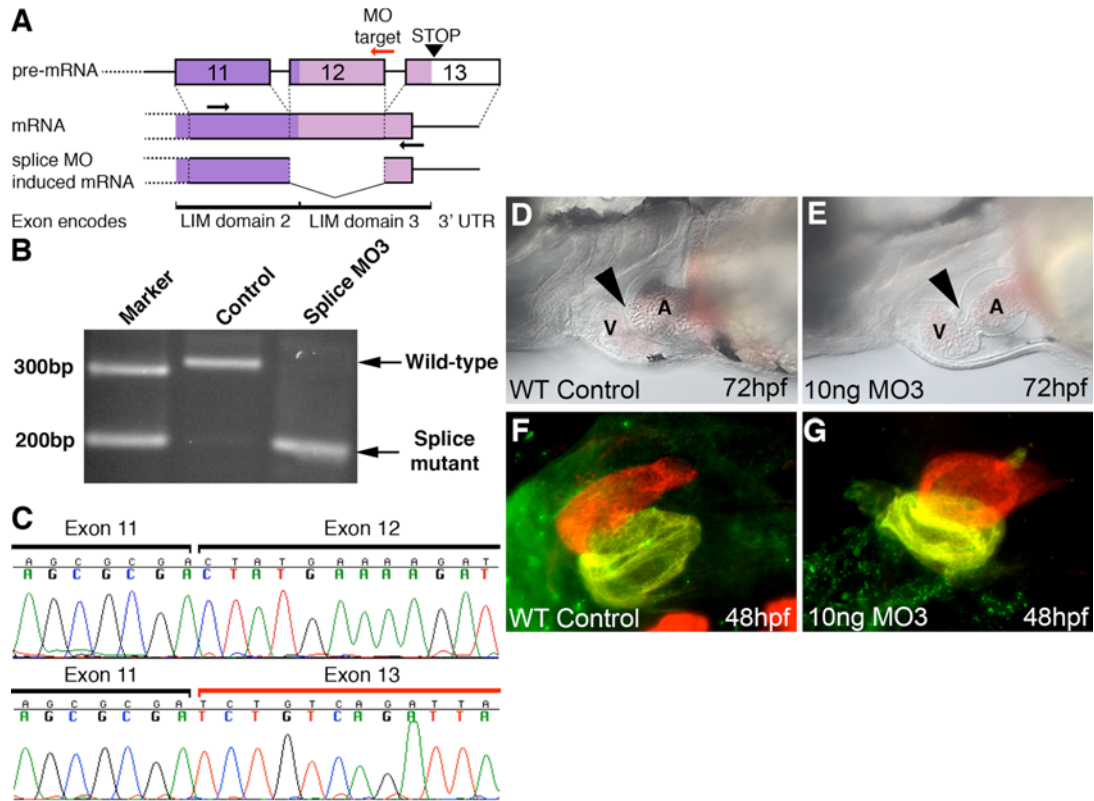


Figure Appendix C.1: *pdlim7* splice morpholino targeting the Tbx5 binding LIM3 domain causes heart looping defects in zebrafish. (A) Schematic of *pdlim7* LIM3 splice morpholino (MO3) function. (B) RT-PCR detecting improper splicing of *pdlim7* mRNA after injection of the splice targeted MO3. (C) Sequencing of the splice mutant PCR product to confirm improper splicing. (D-E) Brightfield lateral images of control and splice MO3 injected embryos at 72hpf. (F-G) Control and splice MO3 injected embryos stained at 48hpf with MF20 (red) and S46 (green) antibodies to detect chambers. Ventral view in D-E. Red=ventricle, yellow=atrium. v=ventricle, a=atrium. Arrowhead points to the atrium/ventricle boundary.

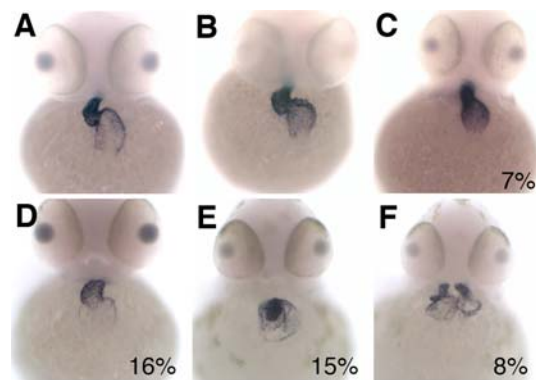


Figure Appendix C.2: Dominant-negative effects of *Pdlim7* Δ LIM3. (A-C) Injection of 75 pg of wild-type *pdlim7* mRNA. Injected embryos were fixed at 48 hpf and stained for *cmlc2* to outline the heart. Wild-type *Pdlim7* did not cause significant cardiac defects. (D-F) The Tbx5 binding domain, LIM3, was removed from *Pdlim7* and 75 pg of mRNA was injected into single-cell wild-type embryos. Expression of this construct resulted in significant cardiac defects ranging from a non-looped heart (D), compressed cardiac chambers (E), or cardia bifida (F). These defects do not relate to Tbx5 mutant phenotypes and are a result of dominant-negative action of *Pdlim7* Δ LIM3. The percentages relate to the percentage of embryos of each phenotypic class. (A-C) n=57. (D-F) n=100.